Soft Radiation Theorems at All Loop Order in Quantum Field Theory

A Dissertation presented

by

Hualong Gervais

to

The Graduate School

in Partial Fulfillment of the

Requirements

for the Degree of

Doctor of Philosophy

in

Physics

Stony Brook University

August 2017

Stony Brook University

The Graduate School

Hualong Gervais

We, the dissertation committe for the above candidate for the

Doctor of Philosophy degree, hereby recommend

acceptance of this dissertation

George Sterman
Distinguished Professor, Physics and Astronomy

Peter van Nieuwenhuizen
Distinguished Professor, Physics and Astronomy

Dmitri Tsybychev
Associate Professor, Physics and Astronomy

Amarjit Soni
Professor, Brookhaven National Lab

This dissertation is accepted by the Graduate School

Charles Taber
Dean of the Graduate School

Abstract of the Dissertation

Soft Radiation Theorems at All Loop Order in Quantum Field Theory

by

Hualong Gervais

Doctor of Philosophy

in

Physics

Stony Brook University

2017

We study the emission of soft photons and soft gravitons coupling to high energy fixed angle scattering processes at first order in the electromagnetic coupling and in Newton's constant, respectively, but to all loop orders in a class of theories without soft divergences, including massive and massless Yukawa and scalar theories. We adapt a method introduced by del Duca for quantum electrodynamics to show that subleading corrections to the soft photon and soft graviton theorems are sensitive to the structure of nonleading external jets of collinear lines. Our techniques are based on a power counting analysis of loop integrals, an application of jet Ward identities, and hard-soft-collinear factorization. We also apply Grammer and Yennie's decomposition to isolate separately gauge invariant contributions to the soft expansion. These are interpreted as infrared sensitive matrix elements coupling to a field strength tensor in the case of photons, and to the linearized Riemann curvature tensor in the case of gravitons.

Dedication Page

To Gérard Gervais, my father, who encouraged me to pursue higher studies in physics.

Contents

List of Figures

List of Tables

Acknowledgements

I wish to thank my advisor, George Sterman, for his insights and guidance throughout the completion of the research that this dissertation is based on.

I thank my wife, Bing Wang, for relentlessly encouraging me, especially during the most demanding times.

I also wish to thank the Fond du Québec de recherche en sciences de la nature et technologies for the financial support through their doctoral research fellowship.

1 Introduction to Soft Theorems

1.1 Introduction

The subject of the emission of soft particles in quantum field theory has a long history dating back to the classic theorems of Low, Burnett and Kroll, and Weinberg [1–3]. The leading term in the soft particle energy, q^0, universally behaves as $1/q^0$ and comes from dressing an external line with a tree level vertex. The form of a soft theorem is strongly influenced by the underlying symmetries of the theory. In QED, Low's classic result shows that the next to leading term is fixed by gauge invariance, implemented through the use of Ward identities. More recently, it has been shown that soft graviton theorems can be realized as the Ward identities of a symmetry of the gravitational S-matrix [4, 5]. This observation is part of a renewed interest in soft theorems in both gauge and gravitational theories. In particular, Ref. [6] has used the BCFW relation [7, 8] to not only derive Weinberg's leading term for soft graviton emission but also determine the next and next to next to leading terms at tree level. While it was later confirmed that these higher order terms in the soft graviton theorem can be understood from the gravitational Ward identity [9] following a treatment similar to Low's analysis [10, 11], the role of loop corrections, especially in the high-energy and massless limits has received a lot of further study [12–18].

In the case of gauge theories, the resummation of logarithms associated with soft and collinear gluon emissions has been applied to numerous collider observables [19–27] and loop corrections to the subleading term in soft theorems are important for applications to precision studies of the Standard Model [28–30].

Soft theorems in gravity and gauge theories have also been studied from several other viewpoints, including scattering equations [31–33], string theory techniques [34–37], the one particle irreducible effective action [38,39], path integral and diagrammatic methods [40–47], and effective field theory [18]. In particular, Ref. [18] stresses the importance of matrix elements involving higher dimension operators, which we will derive from an independent point of view.

In this dissertation, we focus on loop corrections to the soft photon and soft graviton theorems, specifically for the emission of a single soft photon or graviton from scalar and Yukawa theories in four dimensions. In particular, we will consider how loop corrections alter proofs of soft radiation theorems based on Low's analysis. Our final forms of the soft photon and graviton theorems consider the case where all external hard particles are outgoing fermions or antifermions. The extension of our results to the cases where the scalars are charged and allowed to appear as external particles is straightforward but involves more terms in our final formulas.

We couple the electromagnetic field to massive fermions interacting with massless scalars

through Yukawa interactions in four dimensions. The scalars are allowed to interact via a quartic potential but will be kept neutral for simplicity. Our results will hold to first order in the electric charge but to all orders in the Yukawa and ϕ^4 couplings.

Gravitons are coupled to fermions and scalars through the stress tensor operator. The full dynamics of the graviton field is given by the Einstein-Hilbert action. We will, however, not consider graviton loops in this work. Yukawa and ϕ^4 theories provide a nontrivial testing ground for our ideas, which are also applicable to soft quanta emission from gauge theories and gravity. It will be convenient to use the term *elastic* here and below to refer only to the absence of energy loss to the electromagnetic and gravitational fields.

We are primarily interested in the high energy limit, studied by Del Duca [14] in the context of soft photon emission in the wide-angle scattering of charged particles, although we will also briefly consider low energies. Ref. [14] pointed out that the original form of Low's theorem holds only for photon energies below the scale m^2/E, with m the mass scale of virtual lines and E the typical center-of-mass energy of the nonradiative amplitude. Del Duca showed that for $E_\gamma > m^2/E$, corrections to Low's theorem appear in the first power correction, and that they can be interpreted in terms of infrared-sensitive matrix elements involving the field strength, associated with the collinear singularities in the massless limit. These contributions are not determined directly by the Ward identities. They remain universal, however, depending only on the charge, spin, and momentum of the external lines. This universality is a generalization and variant of the factorization theorems that play such a large role in applications of gauge invariance in perturbative quantum chromodynamics [28, 48]. In the case of gravity, we will find analogous corrections where the role of Del Duca's field strength is played by the Riemann tensor of linearized gravity, both at high and low energies – see Eq. (161) below.[1]

Our approach to loop corrections at high energies is based on Refs. [12,13], which revisit the problem of photon and graviton emission at high energies. Ref. [12] focuses on photon emission in Yukawa and scalar theories in the regime where the soft momentum q is of the order $O(m^2/E)$. Ref. [13] treats soft graviton emission at both high and low energies.

In Ref [12], it was pointed out that in the result of loop integration over regions neighboring pinch surfaces, there arise contributions with branch cuts within $O(m^2/E)$ of the point $q = 0$. Following Ref. [12], we will refer to such contributions as nonanalytic. Branch cuts of nonanalytic contributions are associated with particle production thresholds and make an expansion of the nonradiative amplitude (henceforth referred to as the "elastic" amplitude) to a fixed power of q inaccurate when $q = O(m^2/E)$. This phenomenon can be traced back to invariants involving q being of the same order as terms not involving q in denominators of the loop integrand [12,14]. Expanding the elastic amplitude, however, is a key step in Low's

[1] After this work was completed, Ref. [39] appeared, which also derives corrections that we identify as the linearized Riemann tensor.

original analysis – see [1, 10] for details.

A solution to this problem is to factorize the elastic amplitude into jet functions, a soft cloud, and a hard part. The jet functions gather all collinear lines of the diagram, the soft cloud gathers all the soft lines, and the hard part includes all hard, short distance, exchanges. Such a factorization is reminiscent of the soft collinear effective theory approach to soft radiation [18]. The hard part is analogous to the matching coefficients of SCET and the jet functions correspond to the higher dimension operators of the effective theory. Refs. [12, 13] applied power counting techniques to provide a systematic way of classifying factorized contributions to the radiative amplitude according to their order of magnitude. This allowed for a complete list of all nonleading loop corrections to the soft photon and soft graviton theorems, carefully taking into account the analytic structure of the loop integrals in all regions. Further, we will also provide a decomposition of the radiative jet functions inspired from Grammer and Yennie's decomposition [49], and find that loop corrections sensitive to the collinear region couple to the photon through a field strength tensor, and to the graviton through a linearized Riemann tensor, both at high and low energies.

In the remainder of this introduction, we will review the soft theorems of Low, Burnett and Kroll, and Cachazo and Strominger. For each theorem, we will emphasize their original formulation and derivation, while paying close attention to their region of validity. We will also take this opportunity to introduce the importance of a careful treatment of the analytic structure of loop integrals.

1.2 Review of Low, Burnett, and Kroll's theorem

In the high energy regime where $q \sim m^2/E$ and $E \gg m$, we will see that a complete treatment of Low's theorem requires a study of the analytic structure of loop integrals. To introduce the need for this analysis, we begin by reviewing Low's classic approach to soft photon radiation in this section. The original treatment of Low appears in [1] and his analysis was also adapted to non-Abelian gauge theory and gravity in [10]. While reviewing Low's theorem, we will discuss the issue of retaining momentum conservation when transitioning between the kinematics with and without an external photon. This point is often neglected in the literature, but we believe it is relevant if one is to apply Low's theorem to realistic scenarios.

Low's theorem is traditionally stated as the expansion of a radiative amplitude $M(q)$ in powers of q up to order q^0,

$$M(q) = \frac{1}{q}\sigma_{-2} + \sigma_0 \,, \tag{1}$$

where the coefficients σ_{-2} and σ_0 are built from the quantities at hand in the problem, such as m and E. However, since we are considering the region where $q \sim m^2/E$, the soft

momentum q is no longer the only "small" quantity in the problem. For example, a quantity scaling as qE/m^2 would be of the same order as the first subleading term σ_0.

To get a complete soft photon expansion, it is important to identify carefully all contributions to the radiative amplitude that are of the same order of magnitude as the leading and subleading terms in Eq. (1). This requires us to define a common "small" scale in terms of which all orders of magnitude will be expressed. With that objective in mind, we treat the total center of mass energy E as the scale of hard processes. We are interested in the high energy regime where the dimensionless parameter $\lambda \equiv \frac{m}{E}$ is much less than 1, and use it to quantify what we mean by "small". Using this notation, we then have that $q \sim \lambda^2 E$ and $m \sim \lambda E$. Further, given an arbitrary quantity a, the notation $a = O(\lambda^\gamma)$ will mean that there exists some constant A such that $|a| \leq A\lambda^\gamma$. The constant A can be constructed with the appropriate power of E to have the same dimension as a but may not depend on q or m. For instance, we have $q = O(\lambda^2)$ and $m = O(\lambda)$. Low's theorem is then an expansion going from $O(\lambda^{-2})$ to $O(\lambda^0)$. With these definitions established, we proceed to reviewing Low's theorem.

It is enough to consider Low's original case of scalar Compton scattering to illustrate our points on the importance of the infrared behavior of loop integrals. Therefore, consider a radiative Compton scattering process

$$f(p_1) + s(k_1) \to f(p_2) + s(k_2) + \gamma(q)\,, \tag{2}$$

where a charged fermion and a neutral scalar of respective momenta p_1 and k_1 scatter into a fermion and scalar of momenta p_2 and k_2 while a soft photon of momentum q is emitted. As defined above, the corresponding elastic amplitude is the same process without the emission of the soft photon. Naturally, the momenta p_1, p_2, k_1, and k_2 are all on-shell and

$$p_1 + k_1 = p_2 + k_2 + q\,, \tag{3}$$

as required by momentum conservation.

The Feynman diagrams contributing to the radiative amplitude are generated by attaching an external soft photon line to the diagrams contributing to the elastic amplitude. We distinguish between two types of radiative emission amplitudes. Those where the soft photon is attached to an external fermion line are called "external" radiative amplitudes while those where the soft photon is attached to an internal fermion line are called "internal" radiative amplitudes. These two types of amplitudes are illustrated in Fig. 1. In Chapters 3 and 4, we will adapt these definitions to a factorized form of the radiative amplitude.

The explicit forms of the external radiative amplitudes from Fig. 1 are

$$M_a^{ext,\mu}(p_1, p_2, k_1, k_2, q) = \bar{u}(p_2)(-ie\gamma^\mu)\frac{i}{\not{p}_2 + \not{q} - m}\tilde{M}_{el}(p_1, p_2 + q, k_1, k_2)u(p_1)\,,$$

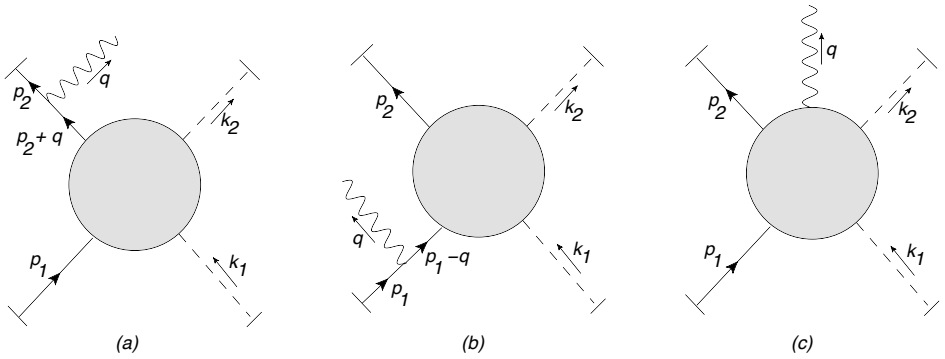

Figure 1: Diagrams (a) and (b) represent the external amplitudes. Diagram (c) is the internal amplitude where the soft photon is attached to an internal fermion propagator.

$$M_b^{ext,\mu}(p_1,p_2,k_1,k_2,q) = \bar{u}(p_2)\tilde{M}_{el}(p_1-q,p_2,k_1,k_2)\frac{i}{\not{p}_1-\not{q}-m}(-ie\gamma^\mu)u(p_1)\,. \tag{4}$$

In the above, we denote the elastic amplitude stripped of the external spinors by $\tilde{M}_{el}(\dots)$. The internal radiative amplitude is denoted with the symbol $M^{int,\mu}(p_1,p_2,k_1,k_2,q)$. This notation allows us to express the QED Ward identity in a form that corresponds to the separation of the photon emission amplitude into emission from external or internal legs,

$$q_\mu M_a^{ext,\mu} + q_\mu M_b^{ext,\mu} + q_\mu M^{int,\mu} = 0\,. \tag{5}$$

Substituting the explicit forms for the external amplitudes of Eq. (4) into Eq. (5), we find that the Ward identity becomes

$$e\,\bar{u}(p_2)\tilde{M}_{el}(p_1,p_2+q,k_1,k_2)u(p_1) + (-e)\,\bar{u}(p_2)\tilde{M}_{el}(p_1-q,p_2,k_1,k_2)u(p_1) + q_\mu M^{int,\mu} = 0\,. \tag{6}$$

This Ward identity is illustrated in Fig. 2.

Equation (6) allows us to solve for the internal amplitude $M^{int,\mu}$ in terms of derivatives of the elastic amplitude. We assume, following Low, that it is consistent to expand the stripped elastic amplitude $\tilde{M}_{el}(\dots)$ in powers of q about the point (p_1,k_1,p_2,k_2). Using charge conservation, one then finds

$$\begin{aligned} q_\mu M^{int,\mu} \;=& -e\,q_\mu\,\bar{u}(p_2)\frac{\partial}{\partial p_{1,\mu}}\tilde{M}_{el}(p_1,p_2,k_1,k_2)\,u(p_1) \\ & -e\,q_\mu\,\bar{u}(p_2)\frac{\partial}{\partial p_{2,\mu}}\tilde{M}_{el}(p_1,p_2,k_1,k_2)\,u(p_1) + O(\lambda^4)\,. \end{aligned} \tag{7}$$

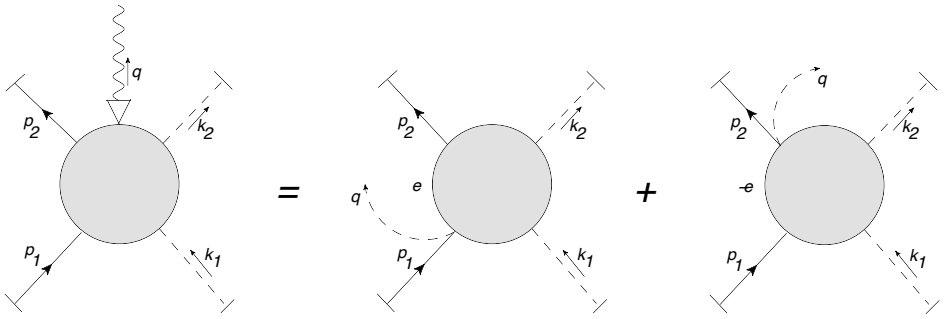

Figure 2: The Ward identity relates the internal radiative amplitude to the elastic amplitude with external momenta shifted by q. The arrow at the end of the photon line on the left hand side indicates that the current operator corresponding to the emitted photon is contracted with the photon momentum q. On the right, the photon momentum q is pictured as exiting the diagram through a composite scalar-fermion-photon vertex.

A possible problem with this procedure, as discussed by Burnett and Kroll in [2], is that we are left with a formula where the elastic amplitude is evaluated at a point outside the locus of momentum conservation. This unphysical formula could be ambiguous in realistic applications and thus an alternative would be preferrable.

Following Burnett and Kroll, we define an elastic momentum configuration $\{p_1', k_1', p_2', k_2'\}$ where p_1' and k_1' are the respective momenta of the incoming fermion and scalar while p_2' and k_2' are the momenta of the outgoing fermion and scalar – see Fig. 3. These elastic momenta are all on-shell and obey momentum conservation in the absence of the soft photon,

$$p_1' + k_1' = p_2' + k_2' \,. \tag{8}$$

We want the elastic momenta to be shifted slightly away from the radiative configuration. Hence, we introduce the small deviations $\xi_1(q)$, $\xi_2(q)$, $\eta_1(q)$, and $\eta_2(q)$ satisfying

$$\begin{aligned} p_i &= p_i'(q) + \xi_i(q) \quad \text{for } i = 1, 2, \\ k_i &= k_i'(q) + \eta_i(q) \quad \text{for } i = 1, 2. \end{aligned} \tag{9}$$

We also want that when $q = 0$, the radiative fermion and scalar momenta coincide with the elastic ones. This motivates the requirement that the ξ_i's and η_i's be polynomials in q whose leading term is linear in q, and in particular, $\xi_i, \eta_i = O(\lambda^2)$, as for q^μ.

Now, insisting on preserving momentum conservation and having on-shell particles in the elastic amplitude induces the following constraints on the ξ_i's and η_i's,

$$\xi_1 + \eta_1 - \xi_2 - \eta_2 = q \,,$$

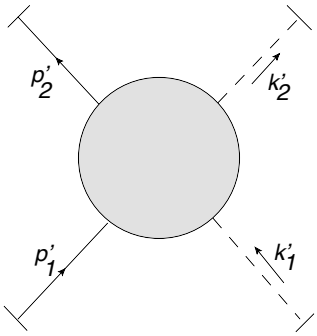

Figure 3: The elastic $fs \to fs$ amplitude involves no photon emission. The external momenta are on-shell and obey momentum conservation.

$$\begin{aligned} 2p_i \cdot \xi_i &= \xi_i^2 \quad \text{for } i = 1, 2, \\ 2k_i \cdot \eta_i &= \eta_i^2 \quad \text{for } i = 1, 2. \end{aligned} \tag{10}$$

To leading order in λ, the latter two equations in (10) above become

$$p_i \cdot \xi_i = k_i \cdot \eta_i = 0 \quad \text{for } i = 1, 2. \tag{11}$$

To construct the ξ_i's and η_i's at leading order in λ, it is convenient to introduce an orthonormal frame about each external fermion and scalar momentum. About the fermion momenta $\vec{p}_1$ and $\vec{p}_2$, we introduce the three dimensional vectors $\vec{n}_{p_i}$, $\vec{\bar{n}}_{p_i}$, and $\vec{e}_{p_i}$. The vector $\vec{e}_{p_i} = \vec{p}_i/|\vec{p}_i|$ points in the direction parallel to $\vec{p}_i$ while the vectors $\vec{n}_{p_i}$ and $\vec{\bar{n}}_{p_i}$ span the plane orthonormal to $\vec{p}_i$. Likewise, to each scalar's momentum $\vec{k}_i$, we associate the orthonormal frame $\vec{n}_{k_i}$, $\vec{\bar{n}}_{k_i}$, and $\vec{e}_{k_i}$. We then decompose the $\vec{\xi}_i$'s and $\vec{\eta}_i$'s in their corresponding orthonormal bases

$$\begin{aligned} \vec{\xi}_i &= \alpha_{p_i}\vec{n}_{p_i} + \beta_{p_i}\vec{\bar{n}}_{p_i} + \delta_{p_i}\vec{e}_{p_i} \quad \text{for } i = 1, 2, \\ \vec{\eta}_i &= \alpha_{k_i}\vec{n}_{k_i} + \beta_{k_i}\vec{\bar{n}}_{k_i} + \delta_{k_i}\vec{e}_{k_i} \quad \text{for } i = 1, 2, \end{aligned} \tag{12}$$

where all coefficients α_*, β_*, and δ_* are $O(\lambda^2)$.

Since the p_i's and k_i's are on-shell, we have

$$\begin{aligned} p_i^0 &= \sqrt{|\vec{p}_i|^2 + m^2} \quad \text{for } i = 1, 2, \\ k_i^0 &= |\vec{k}_i| \qquad\qquad\quad \text{for } i = 1, 2. \end{aligned} \tag{13}$$

Combining this with (11) and (12), we find that

$$\xi_i^0 = \delta_{p_i} v_{p_i} \quad \text{for } i = 1, 2,$$

$$\eta_i^0 = \delta_{k_i} \qquad \text{for } i = 1, 2, \tag{14}$$

where we have defined the velocities $v_{p_i} \equiv |\vec{p}_i|/\sqrt{|\vec{p}_i|^2 + m^2}$ for $i = 1, 2$. This fully characterizes the components ξ_i^0 and η_i^0, and takes care of ensuring that the elastic momenta are on-shell to leading order in λ. We still need to solve for momentum conservation in Eqs. (10). This requirement is most conveniently written in matrix notation,

$$\begin{pmatrix} 0 & 0 & v_{p_1} & 0 & 0 & 1 & 0 & 0 & -v_{p_2} & 0 & 0 & -1 \\ \vec{n}_{p_1} & \vec{\bar{n}}_{p_1} & \vec{e}_{p_1} & \vec{n}_{k_1} & \vec{\bar{n}}_{k_1} & \vec{e}_{k_1} & -\vec{n}_{p_2} & -\vec{\bar{n}}_{p_2} & -\vec{e}_{p_2} & -\vec{n}_{k_2} & -\vec{\bar{n}}_{k_2} & -\vec{e}_{k_2} \end{pmatrix} \begin{pmatrix} \alpha_{p_1} \\ \beta_{p_1} \\ \delta_{p_1} \\ \alpha_{k_1} \\ \beta_{k_1} \\ \delta_{k_1} \\ \alpha_{p_2} \\ \beta_{p_2} \\ \delta_{p_2} \\ \alpha_{k_2} \\ \beta_{k_2} \\ \delta_{k_2} \end{pmatrix} = \begin{pmatrix} q^0 \\ \vec{q} \end{pmatrix} . \tag{15}$$

The columns of the leftmost matrix above are made of the components of the orthonormal frame vectors relative to some fixed common frame. Assuming the rank of the resulting matrix to be maximal, we can determine the four coefficients α_{p_1}, β_{p_1}, δ_{p_1}, and α_{k_1} in terms of the remaining α_*, β_*, δ_*, and q. If we choose the undetermined components to be $O(\lambda^2)$, then the solution for α_{p_1}, β_{p_1}, δ_{p_1}, and α_{k_1} will also be $O(\lambda^2)$. Therefore, the construction we have outlined allows us to derive ξ_i's and η_i's that are of the same order of magnitude as the soft momentum q. It is then clear that one must include these deviations from the elastic configuration in a complete expansion of the radiative amplitude.

Returning to Eq. (6), we proceed with the expansion of $\tilde{M}_{el}(\dots)$ to $O(\lambda^2)$ about (p_1', p_2', k_1', k_2'), taking the ξ_i's and η_i's into account,

$$\begin{aligned} & q_\mu M^{int,\mu}(p_1, p_2, k_1, k_2, q) = \\ & \quad e\,\bar{u}(p_2) \left(\tilde{M}_{el}(p_1', \dots) + \sum_{i=1,2} \left(\xi_i^\mu \frac{\partial}{\partial p_i'^\mu} + \eta_i^\mu \frac{\partial}{\partial k_i'^\mu} \right) \tilde{M}_{el}(p_1', \dots) - q^\mu \frac{\partial}{\partial p_1'^\mu} \tilde{M}_{el}(p_1', \dots) \right) u(p_1) \\ & \quad - e\,\bar{u}(p_2) \left(\tilde{M}_{el}(p_1', \dots) + \sum_{i=1,2} \left(\xi_i^\mu \frac{\partial}{\partial p_i'^\mu} + \eta_i^\mu \frac{\partial}{\partial k_i'^\mu} \right) \tilde{M}_{el}(p_1', \dots) + q^\mu \frac{\partial}{\partial p_2'^\mu} \tilde{M}_{el}(p_1', \dots) \right) u(p_1) \\ & \quad + O(\lambda^4)\,. \end{aligned} \tag{16}$$

When taking derivatives in the above, we first treat the momenta p_1', p_2', k_1', and k_2' as variables upon which the elastic amplitude $\tilde{M}_{el}$ depends. The differentiated amplitude is then evaluated at the elastic configuration (p_1', p_2', k_1', k_2') that we constructed. Charge conservation reduces (16) to

$$\begin{aligned} q_\mu M^{int,\mu}(p_1,p_2,k_1,k_2,q) = &- e\, q^\mu\, \bar{u}(p_2) \frac{\partial}{\partial p_1'^\mu} \tilde{M}_{el}(p_1', p_2', k_1', k_2')\, u(p_1) \\ &- e\, q^\mu\, \bar{u}(p_2) \frac{\partial}{\partial p_2'^\mu} \tilde{M}_{el}(p_1', p_2', k_1', k_2')\, u(p_1) + O(\lambda^4)\,. \end{aligned} \tag{17}$$

We see that the ξ_i and η_i terms have cancelled because of charge conservation. This means that the way we choose to transition from radiative to elastic kinematics does not affect the essence of Low's theorem, which is the determination of the internal radiative amplitude in terms of the external one. To obtain a full expansion of the radiative amplitude however, we also need to expand the external amplitudes in Eq. (4) to $O(\lambda^2)$. As we shall see, the ξ_i and η_i terms no longer cancel in the expansion of these external amplitudes.

Note that the elastic configuration p_1', p_2', k_1', k_2' is not unique. If we were to solve Eq. (15) by making a different choice for the undetermined coefficients, we would obtain a different set of ξ_i's and η_i's. However, as long as we choose coefficients that are $O(\lambda^2)$, the difference in the elastic configuration we obtain will also be $O(\lambda^2)$. This would induce corrections to the internal radiative amplitude that are beyond $O(\lambda^0)$, and hence beyond our order of accuracy in Low's theorem.

The obvious particular solution to Eq. (17) is derived by simply "factoring out" the soft photon momentum q_μ,

$$\begin{aligned} M^{int,\mu}(p_1,p_2,k_1,k_2,q) = &- e\, \bar{u}(p_2) \frac{\partial}{\partial p_{1,\mu}'} \tilde{M}_{el}(p_1', p_2', k_1', k_2')\, u(p_1) \\ &- e\, \bar{u}(p_2) \frac{\partial}{\partial p_{2,\mu}'} \tilde{M}_{el}(p_1', p_2', k_1', k_2')\, u(p_1) + O(\lambda^2)\,. \end{aligned} \tag{18}$$

However, one may inquire about the possibility of separately gauge invariant contributions to $M^{int,\mu}$. These have the generic form

$$\begin{aligned} B^\mu(l,q) = &\sum_{l\in S} f_{1,l}(S,q)\, (l\cdot q\, q^\mu - q^2 l^\mu)\, \bar{u}(p_2) u(p_1) \\ &+ \sum_{l\in S} f_{2,l}(S,q)\, (l\cdot q\, q^\mu - q^2 l^\mu)\, \bar{u}(p_2)\gamma_5 u(p_1) \\ &+ f_3(S,q)\, \bar{u}(p_2)[\gamma^\mu, \not{q}] u(p_1)\,, \end{aligned} \tag{19}$$

where $S = \{p_1, p_2, k_1, k_2\}$ is the set of external momenta excluding the soft photon momentum. The tensor structures corresponding to f_1, f_2, and f_3 are of order λ^4, λ^4, and λ^2 respectively. Accordingly, to have contributions of order λ^0, f_1, f_2, and f_3 must have enhancements of orders λ^{-4}, λ^{-4}, and λ^{-2}. Such enhancements do not appear in the low energy regime $E \sim m$ where the classic form of Low's theorem holds. At high energies $E \gg m$ however, these enhancements are intimately linked to the infrared behavior of loop integrals and the need to generalize the classic form of Low's theorem, as we will see in Secs. 2.1, 3.1, and 3.3.

We conclude this section by showing the full radiative amplitude deduced from the classic form of Low's argument,

$$\begin{aligned}
M^\mu =& \bar{u}(p_2)(-ie\gamma^\mu)\frac{i}{\not{p}_2 + \not{q} - m}\tilde{M}_{el}(p_1', p_2', k_1', k_2')\, u(p_1) \\
&+ \bar{u}(p_2)\tilde{M}_{el}(p_1', p_2', k_1', k_2')\frac{i}{\not{p}_1 - \not{q} - m}(-ie\gamma^\mu)\, u(p_1) \\
&+ \bar{u}(p_2)\left[\sum_{i=1,2}\left(\xi_i^\alpha \frac{\partial}{\partial p_i'^\alpha} + \eta_i^\alpha \frac{\partial}{\partial k_i'^\alpha}\right) - q^\alpha \frac{\partial}{\partial p_1'^\alpha}\right]\tilde{M}_{el}(p_1', p_2', k_1', k_2')\frac{i}{\not{p}_1 - \not{q} - m}(-ie\gamma^\mu)\, u(p_1) \\
&+ \bar{u}(p_2)(-ie\gamma^\mu)\frac{i}{\not{p}_2 + \not{q} - m}\left[\sum_{i=1,2}\left(\xi_i^\alpha \frac{\partial}{\partial p_i'^\alpha} + \eta_i^\alpha \frac{\partial}{\partial k_i'^\alpha}\right) + q^\alpha \frac{\partial}{\partial p_2'^\alpha}\right]\tilde{M}_{el}(p_1', p_2', k_1', k_2')\, u(p_1) \\
&- e\,\bar{u}(p_2)\frac{\partial}{\partial p_{1,\mu}'}\tilde{M}_{el}(p_1', p_2', k_1', k_2')\, u(p_1) \\
&- e\,\bar{u}(p_2)\frac{\partial}{\partial p_{2,\mu}'}\tilde{M}_{el}(p_1', p_2', k_1', k_2')\, u(p_1) \\
&+ O(\lambda^2)\,, \qquad (20)
\end{aligned}$$

where we retain the necessary ξ_i and η_i dependence for the external connections, which enter with different Dirac structure, and hence do not cancel in general. In the next chapter, we show precisely why the classic form of Low's theorem we have just described requires generalization in the regime $q = O(\lambda^2)$.

1.3 Review of Cachazo and Strominger's soft graviton theorem

The full soft graviton theorem [3,6,10] applies to an $n+1$-point amplitude $\mathcal{M}_{n+1}(p_1, ..., p_n, q)$ where the $p_1, ..., p_n$ are hard momenta with $p_i \cdot p_j >> p_i^2, p_j^2$ for all i, j, and q is a soft graviton momentum. In the limit that q^μ vanishes in all components relative to all $p_i \cdot p_j$, we can

expand in q, starting with the leading, $1/q$, behavior

$$\mathcal{M}_{n+1}(p_1,...,p_n,q) = (S_0+S_1+S_2)\mathcal{M}_n(p_1,...,p_n) \;+\; O(q^2)\,, \tag{21}$$

where the S_i specify in closed form the leading and the first two subleading power corrections in the graviton momentum, q^μ,

$$\begin{aligned} S_0 &= \sum_{i=1}^{n} \frac{E_{\mu\nu}p_i^\mu p_i^\nu}{p_i\cdot q} \\ S_1 &= \sum_{i=1}^{n} \frac{E_{\mu\nu}p_i^\mu (q_\rho \mathcal{J}_i^{\rho\nu})}{p_i\cdot q} \\ S_2 &= \frac{1}{2}\sum_{i=1}^{n} \frac{E_{\mu\nu}(q_\rho \mathcal{J}_i^{\rho\mu})(q_\sigma \mathcal{J}_i^{\sigma\nu})}{p_i\cdot q}\,. \end{aligned} \tag{22}$$

Here $E_{\mu\nu}$ is the soft graviton polarization tensor and $\mathcal{J}_i^{\mu\nu}$ is the angular momentum tensor of the i^{th} external particle, of the form

$$\mathcal{J}_i^{\mu\nu} \equiv p_i^\mu \frac{\partial}{\partial p_{i\nu}} - p_i^\nu \frac{\partial}{\partial p_{i\mu}} \;+\; \Sigma_i^{\mu\nu}\,, \tag{23}$$

with $\Sigma^{\mu\nu}$ a spin term. Newton's constant, κ, has been normalized so that $\kappa/2 = 1$, and we will also make this choice whenever convenient.

In [6], Cachazo and Strominger proved that Eqs. (21)-(23) apply for arbitrary n at tree level using the BCFW construction [7,8]. We will refer to their result as "CS" below. Subsequently, the CS result was rederived from the gravitational Ward identity [9] that decouples scalar-polarized gravitational radiation [10], following the analysis of Low [1] for soft photon radiation in Quantum Electrodynamics. References [10, 15] discussed modifications associated with loop corrections and soft singularities, both for pure gravity and for gravitational radiation associated with massive and massless matter fields.

As in the problem of soft photon emission at high energies, the soft graviton theorem can be thought of as an expansion of the graviton radiative amplitude in powers of the small parameter λ,

$$\mathcal{M}^{\mu\nu}(k_1,\ldots,k_n,q) = \sigma_{-2}^{\mu\nu} + \sigma_{-1}^{\mu\nu} + \sigma_0^{\mu\nu} + \sigma_1^{\mu\nu} + \sigma_2^{\mu\nu}\,, \tag{24}$$

where $\sigma_\gamma^{\mu\nu} = O(\lambda^\gamma)$. Note that in the CS result, only even γ terms are present. As we will demonstrate, this is no longer the case when we consider loop corrections at high energies.

2 Analytic Structure of the Radiative and Elastic Amplitude

This chapter studies the analytic properties of the radiative and elastic amplitudes in the $q = O(\lambda^2)$ region, both for the emission of a soft photon, and a soft graviton. In Sec. 2.1, we begin with a demonstration of why an expansion of the elastic amplitude to linear order in q is inaccurate. To circumvent this obstacle to the application of a Low type analysis as presented in Sec. 1.2, we first find all sources of nonanalyticity in the elastic amplitude and classify them by their order of magnitude using power counting techniques. In Sec. 2.3, we then introduce factorized amplitudes that isolate these nonanalyticities and provide an adequate formalism for applying Ward identities to the derivation of soft theorems.

2.1 Failure of the linear expansion

In Sec. 1.2, our ability to deduce $M^{int,\mu}$ from the Ward identity (5) depends on being able to expand the elastic amplitude $\tilde{M}_{el}(\dots)$ in (6) to linear order in q. The accuracy of this expansion is intimately tied to the infrared behavior of the loop integrals contributing to the radiative and elastic amplitude.

Once all loop integrals contributing to the radiative and elastic amplitudes have been carried out, some regions of the loop integration will have yielded functions of q that are either singular at $q = 0$, or are analytic with a "very small" radius of convergence. Examples of the former include pole terms such as $1/p_i \cdot q$. The latter category includes logarithmic terms such as $f(q) \equiv \log(1 + ap_i \cdot q/m^2)$ where $a = O(1)$ is some constant. The Taylor series for this logarithmic function of q has radius of convergence $R \sim m^2/E = O(\lambda^2)$ since there is a branch cut within a distance of order $O(\lambda^2)$ of $q = 0$. When expanding $f(q)$ to linear order, the remainder has a small upper bound only in the vanishingly small region $q << m^2/E$. It is convenient here to apply the term "nonanalytic" to functions whose power series have radius of convergence $R = O(\lambda^2)$. Our claim is then that in general, loop integrals have singular and nonanalytic contributions that either cannot be Taylor expanded about $q = 0$ altogether, or whose linear expansion in q is accurate only for vanishingly small photon momenta $q << O(\lambda^2)$. Either way, in our region of interest, such contributions prevent us from carrying out Low's argument as described in Sec. 1.2.

To extend Low's theorem to high energy scattering, it is necessary first to identify singular and nonanalytic contributions, and then factorize them from terms that can be legitimately expanded to linear order in q. Fortunately, identifying these contributions can be done by studying the loop integrand rather than fully evaluating the loop integral [48, 50–55]. We introduce these methods through an example.

Consider a triangle integral where two massive on-shell particles of mass m and momenta

p_1 and p_2 exchange a massless scalar,

$$I \equiv \int d^4k \frac{1}{(k^2+i\epsilon)((k+p_1)^2-m^2+i\epsilon)((k+p_2)^2-m^2+i\epsilon)}\,, \tag{25}$$

with $p_1^2 = p_2^2 = m^2$ and $(p_1-p_2)^2 < 0$. Although they would have to be included in general, we ignore numerator factors in this illustrative example. Our goal is to locate regions of the d^4k integration that may result in singular or nonanalytic terms. At high energy, the coordinates best suited to this goal are light cone coordinates. An arbitrary vector v is defined by its components (v^+, v^-, v_T) with the standard definitions

$$\begin{aligned} v^\pm &\equiv \frac{1}{\sqrt{2}}(v^0 \pm v^3)\,, \\ v_T &\equiv (v^1, v^2)\,. \end{aligned} \tag{26}$$

Scalar products take the form

$$v \cdot w = v^+ w^- + v^- w^+ - v_T \cdot w_T\,. \tag{27}$$

Collinear and soft momenta are defined by the scaling of their light cone coordinates. Suppose that p_1 is moving in the z direction. The components of a momentum k collinear to p_1 scale as $(1, \lambda^2, \lambda)E$. Those of a soft momentum, on the other hand, scale as $(\lambda^2, \lambda^2, \lambda^2)E$. An arbitrary hard momentum scales as $(1,1,1)E$. Note that in our example, p_2 is hard relative to p_1. Focusing on the region where k is collinear to p_1 in our example, it is straightforward to see that

$$\begin{aligned} k^2 &= O(\lambda^2)\,, \\ k^2 + 2p_1 \cdot k &= O(\lambda^2)\,, \\ k^2 + 2p_2 \cdot k &= 2p_2^- k^+ + O(\lambda) = O(\lambda^0)\,. \end{aligned} \tag{28}$$

We can now explain why it is inaccurate to expand $\tilde{M}_{el}(p_1 - q, p_2, k_1, k_2)$ to linear order in q by studying the integrand. Consider Eq. (25) with the external momentum p_1 replaced with $p_1 - q$ similarly to $\tilde{M}_{el}(p_1 - q, p_2, k_1, k_2)$ in (6),

$$I' \equiv \int d^4k \frac{1}{(k^2+i\epsilon)(k^2+2(p_1-q)\cdot k + q^2 - 2p_1\cdot q + i\epsilon)(k^2+2p_2\cdot k + i\epsilon)}\,. \tag{29}$$

The sum of the invariants with a factor of q in the middle denominator is

$$q^2 - 2p_1 \cdot q - 2k \cdot q = O(\lambda^2)\,,$$

which is of the same order of magnitude as $k^2+2p_1\cdot k$ in region (28). Therefore, when q flows through a momentum collinear to p_1, we may not treat terms in propagator denominators with factors of q as small quantities in which we can expand using a power series. Further, the scaling $k^2+2p_1\cdot k=O(\lambda^2)$ implies that $k+p_1$ is very close to the mass shell. Similar conclusions apply when k is collinear to p_2 rather than p_1.

It turns out that internal momenta going on-shell are a necessary condition for having singular or nonanalytic terms. To see this, consider the generic multiloop integral

$$\tilde{F}(p_1,\ldots,p_n)=\int\prod_{l=1}^{L}d^4k_l\int\prod_{j=1}^{M}d\alpha_j\,\delta\left(1-\sum_{j=1}^{M}\alpha_j\right)\frac{\mathcal{N}(\{p_i,k_l,\alpha_j\})}{\left[\sum_{j=1}^{M}\alpha_j(l_j^2(\{p_i,k_l\})-m_j^2)+i\epsilon\right]^{\sum_{j=1}^{M}\delta_j}}\,, \tag{30}$$

where the Feynman parameters $\alpha_1,\ldots,\alpha_M$ have been introduced. The numerator factor $\mathcal{N}(\{p_i,k_l,\alpha_j\})$ gathers all vertex factors, propagator numerators, and external spinors in the amplitude. The exponents δ_i are the powers of the original propagator denominators. As in our previous example, introducing a q dependence in the integral by shifting one of the p_i's will result in a function depending on q through invariants of order $O(\lambda^2)$ in the denominator,

$$\begin{aligned}\tilde{F}(p_1,\ldots,p_{i_0}+q,\ldots,p_n)=&\int\prod_{l=1}^{L}d^4k_l\int\prod_{j=1}^{M}d\alpha_j\,\delta\left(1-\sum_{j=1}^{M}\alpha_j\right)\times\\ &\times\frac{\mathcal{N}(\{p_i,k_l,\alpha_j\},q)}{\left[\sum_{j=1}^{M}\alpha_j(l_j^2(\{p_i,k_l\})-m_j^2)+G(\{p_i\cdot q,k_l\cdot q,\alpha_j\},q^2)+i\epsilon\right]^{\sum_{j=1}^{M}\delta_j}}\,,\end{aligned} \tag{31}$$

with $G(\{p_i\cdot q,k_l\cdot q,\alpha_j\},q^2)=O(\lambda^2)$. If we have

$$\sum_{j=1}^{M}\alpha_j(l_j^2(p_i,k_l)-m_j^2)=O(\lambda^2)\,, \tag{32}$$

then a power series expansion in q of the denominator becomes inaccurate. Regions in loop variables space where (32) holds are close to submanifolds where the denominator of the loop integrand in (30) vanishes. The latter can be thought of as "singular submanifolds". If the integration contour in (30) can be deformed away from a singular submanifold by a deviation larger than $O(\lambda^2)$, then a power series expansion in q is possible. This can be achieved as long as the singular submanifold does not coincide with the endpoint of one of the integration contours or is not pinched between pairs of coallescing singularities in the

complex plane. Therefore, a necessary condition for having singular or nonanalytic terms in q in our loop integrals is the presence of *pinch surfaces*.

To summarize, to extend Low's theorem to soft photon and graviton emission in the high energy regime, we need to find all pinch surfaces of the loop integrand for the elastic amplitude. These pinch surfaces may yield singular or nonanalytic terms in the elastic amplitude which prevent us from performing the expansion in q that is crucial to the classic form of Low's argument. To derive a soft radiation expansion at high energies using an argument similar to Low's, it is therefore necessary to factorize the elastic amplitude into components that may legitimately be expanded to linear order in q, and nonanalytic components. This will be achieved by defining matrix elements that capture the dependence of the radiative and elastic amplitudes on the infrared regions. These will be the jet functions and soft functions that will appear in Sec. 2.3. The full elastic or radiative amplitude is then matched onto the factorized amplitude by the hard functions. These hard functions can be accurately expanded to linear order in q and are reminiscent of the matching coefficients of soft collinear effective theory [18]. We will, however, think of them as being constructed by a series of nested subtractions similar to [56, 57].

For reasons that will become clear in Sec. 2.4, the extension of the soft photon theorem will require us to consider all factorized contributions to the elastic amplitude of order up to $O(\lambda^2)$. The soft graviton theorem, on the other hand, will require us to identify all factorized terms of order up to $O(\lambda^4)$. These factorized contributions will be identified by first locating all pinch surfaces of the elastic amplitude, and then defining jet and soft functions that capture the analytic structure of the loop integral in the neighborhood of those pinch surfaces. Pinch surfaces are found by solving the Landau equations [50]. Solutions to these equations can be visualized as physical processes with classical propagation of particles, following an observation first made by Coleman and Norton [51]. Physical propagation of on-shell particles is represented using "reduced diagrams" where all off-shell lines are shrunk to a point. In general, loop integration over a neighborhood of a pinch surface will yield nonanalytic logarithmic dependence on the soft momentum q which must be factorized as described below. Not all pinch surfaces result in singular terms however, and in the majority of cases, integration about a given pinch surface will yield a contribution of order higher than is relevant for the soft photon or the soft graviton theorem. In the next section, we will use power counting techniques [52] to determine the order of magnitude of integrals over regions neighboring pinch surfaces, and also to determine if the resulting term is singular or not.

2.2 Application of power counting to the elastic amplitude

Following Akhoury and Sen [58, 59], finding pinch surfaces using the reduced diagrams of Coleman and Norton is straightforward. Once we have found a pinch surface, we will use power counting techniques to put an upper bound on the loop integral over a region close to that pinch surface. This will allow us to determine whether this pinch surface corresponds to a factorized contribution of order up to $O(\lambda^4)$.

Power counting techniques also allow us to determine if the integral about a pinch surface is singular and in fact, these were first introduced to search for infrared singularities in higher loop integrals. We will begin with a brief review of this technology. More detailed treatments are given in [48, 53–55].

2.2.1 Review of power counting

Arbitrary multiloop Feynman diagrams have infrared singularities associated with various limits in their loop integration momenta [60, 61]. These singularities come from singular submanifolds where propagator denominators vanish. A necessary condition for a singular submanifold to result in a singularity is that it must be a pinch surface. However, a pinch surface need not yield a divergent integral. To determine whether that is the case or not requires the use of power counting techniques [52]. Power counting allows us to determine the order of growth of a loop integral over a region close to a pinch surface. This procedure is best explained by studying a concrete example.

Consider again the triangle integral in (25). We consider the pinch surface arising from the limit where k becomes collinear with p_1. To capture how singular this pinch surface is, we need to change the loop integration variables to "intrinsic" and "normal" coordinates. Normal coordinates are the variables that vanish as we approach the singular submanifold. Intrinsic coordinates, on the other hand, are variables whose variation moves a point along the submanifold without leaving it.

The scalings in (28) tell us that as we approach the collinear region by taking the limit $\lambda \to 0$, two denominators vanish as $O(\lambda^2)$, as is required for a singularity. Further, the collinear region is approached by making k^- and k_T small, which leads us to identify these as the normal variables. The remaining large component k^+ of k is the intrinsic component. Changing integration variables to the normal and intrinsic coordinates, (25) becomes

$$I = \pi \int_{c^+}^{b^+} dk^+ \int_{c^-\lambda^2}^{b^-\lambda^2} dk^- \int_{c_T\lambda^2}^{b_T\lambda^2} dk_T^2 \, \frac{1}{2k^+k^- - k_T^2 + i\epsilon} \times \frac{1}{2k^+k^- - k_T^2 + 2p_1^+k^- + 2p_1^-k^+ + i\epsilon}$$

$$\times \frac{1}{2k^+k^- - k_T^2 + 2p_2^+k^- + 2p_2^-k^+ - 2k_T\cdot p_{2T} + i\epsilon}\,. \tag{33}$$

In the bounds of integration, we have introduced the numbers b^* and c^* which are all $O(1)$. The bounds include an appropriate power of λ since we are interested in the order of magnitude of the loop integral over a region of integration that borders the collinear pinch surface where k^- and k_T vanish. To obtain an estimate of the order of the loop integral about the collinear region, we then perform the changes of variables

$$\begin{aligned} k^+ &= \kappa^+ \\ k^- &= \lambda^2\kappa^- \\ k_T &= \lambda\kappa_T\,. \end{aligned} \tag{34}$$

Eq. (33) becomes

$$\begin{aligned} I = \pi\int_{c^+}^{b^+} d\kappa^+ \int_{c^-}^{b^-} \lambda^2 d\kappa^- \int_{c_T}^{b_T} \lambda^2 d\kappa_T^2\, &\frac{1}{\lambda^2(2\kappa^+\kappa^- - \kappa_T^2 + i\epsilon)} \\ &\times \frac{1}{\lambda^2(2\kappa^+\kappa^- - \kappa_T^2 + 2p_1^+\kappa^- + 2p_1^-\kappa^+/\lambda^2 + i\epsilon)} \\ &\times \frac{1}{2\lambda^2\kappa^+\kappa^- - \lambda^2\kappa_T^2 + 2\lambda^2 p_2^+\kappa^- + 2p_2^-\kappa^+ - 2\lambda\kappa_T\cdot p_{2T} + i\epsilon}\,. \end{aligned} \tag{35}$$

Factoring out the leading powers of λ in the numerator and denominators, we are left with an overall scaling of λ^0 times an integral where all three denominators are $O(1)$ and whose domain of integration is well separated from the pinch surface, since its bounds are all $O(1)$. This is the case even though the integration volume vanishes as a power of λ. Note that the term $2p_1^-\kappa^+/\lambda^2$ in the second line is $O(1)$ since the component p_1^- scales as $\lambda^2 = \frac{m^2}{2p_1^+}$. An overall scaling for the integral of λ^0 indicates the potential for a logarithmic term. In fact, any scaling as a power of λ is valid up to multiplication by a logarithmic function of λ.

The procedure we have just employed to find the potential for a logarithmic divergence without going through a full calculation of a loop integral can be systematized and applied as above to any higher order multiloop diagram for $M_{el}(\{p_i\})$ whenever none of the p_i are parallel. The key points are the identification of candidate pinch surfaces, the proper definition of normal variables and their scaling, and finally power counting to put bounds on the order of growth of the integral. The final step will tell us that the loop integral scales as some power λ^γ of the small parameter λ. This power γ is called the infrared degree of divergence of the pinch surface, in analogy with the ultraviolet degree of divergence of renormalization theory. A strictly positive degree of divergence $\gamma > 0$ means that we have

a nonsingular integral. Conversely, a degree of divergence $\gamma \leq 0$ indicates that we have an infrared divergence in the loop integration when $\lambda \to 0$ i.e. in the massless limit. More specifically, $\gamma < 0$ tells us that the pinch surface leads to a power divergence while $\gamma = 0$ indicates the presence of a logarithmic divergence. In our analysis of soft photon emission, we are interested in retaining a finite mass for the fermion, but we can still apply power counting techniques, as we have described, to determine the order of magnitude of contributions from pinch surfaces to loop integrals. To derive an expansion of the elastic amplitude in powers of λ, one can, therefore, separate the whole range of a loop integral into regions surrounding the pinch surfaces of the integrand, with each pinch surface yielding a factorized contribution of order $O(\lambda^\gamma)$.

2.2.2 Power counting analysis of n particle scattering

Armed with the tools we have described, we begin our study of the infrared structure of the elastic amplitude through the search for pinch surfaces that correspond to factorized contributions of order up to $O(\lambda^4)$. Although we will only consider outgoing external fermions and antifermions in the interest of conciseness, extending our analysis to include external scalars is straightforward. To classify pinch surfaces based on the order of magnitude of their contribution as a power of λ, we introduce a separate set of light cone coordinates for each external particle $p_1, \ldots, p_n$. As in the example we studied, the normal variables are the transverse and "minus" components for a collinear loop momentum, or all momentum components for a soft loop momentum. These definitions of the scaling of momenta in singular regions result in the power counting rules listed in Table 1. When analyzing a reduced diagram that represents a given pinch surface, we use the rules in the table to determine the contribution to the infrared degree of divergence from all components of the reduced diagram – *i.e.* collinear fermion lines, soft fermion lines, etc. Using the Euler identity, it is possible to obtain a general formula for the degree of divergence of the most general reduced diagram [54]. Although we will not review the details of such a treatment, we will outline the main intermediate results for convenience.

As shown in Refs. [58, 59], the application of the Coleman-Norton analysis [51] gives the most general reduced diagram for the elastic scattering of n particles, which is shown in Fig. 4. The hard part labelled H has several jets of collinear particles emerging from it. In our notation, the jet of lines collinear to the i^{th} external particle is linked to the hard part by N_f^i collinear fermion lines and N_s^i collinear scalar lines. Each jet can also have soft particles emerging from it; for the i^{th} jet, we denote the number of such soft fermions by n_f^i and the number of soft scalars by n_s^i. The number $n_f^i + N_f^i$ is odd in the case we study, when the i^{th} external particle is a fermion, and would be even if the external particle were a scalar. The soft fermions and scalars emerge from the n jets and combine at a soft cloud denoted

S. Finally, there are m_f soft fermions and m_s soft scalars connecting the soft cloud to the hard part.

The i^{th} jet's contribution to the degree of divergence of Fig. 4 is denoted by γ_{J_i} and the contribution from the soft cloud S will be denoted by γ_S. Then using the rules from Table 1 and the Euler identity, one can derive the following,

$$\begin{aligned}\gamma_{J_i} &= N_f^i + N_s^i - n_f^i - n_s^i - 1 \\ \gamma_S &= 4\sum_i n_f^i + 2\sum_i n_s^i + I_f + 4m_f + 2m_s\,,\end{aligned} \tag{36}$$

where we have introduced the symbol I_f to stand for the number of soft fermion lines internal to the soft cloud S. The suppression associated with a Yukawa vertex in Table 1 enters in the derivation of γ_{J_i}, and follows from the relation $(\gamma^-)^2 = 0$ and the Dirac equation. The above formulas remain valid whether the i^{th} external particle is a fermion or a scalar. Combining the formulas in (36), we obtain that the degree of divergence of the most general reduced diagram is

$$\gamma = \sum_i (N_f^i + N_s^i + 3n_f^i + n_s^i - 1) + I_f + 4m_f + 2m_S\,. \tag{37}$$

From this result, one sees immediately that there are no diagrams with $\gamma < 0$, meaning that the elastic amplitude is at most logarithmically singular in the limit $\lambda \to 0$. This conclusion was derived long ago by Akhoury in the fully massless case [58].

It is convenient to define the quantities

$$\begin{aligned}\tilde{\gamma} &\equiv \gamma - I_f - 4m_f - 2m_S \\ &= \sum_i (N_f^i + N_s^i + 3n_f^i + n_s^i - 1) \equiv \sum_i \gamma_i\,.\end{aligned} \tag{38}$$

One can think of γ_i as an effective contribution to the degree of divergence from the i^{th} jet after the effect of the soft cloud has been taken into account. Finding all diagrams with $0 \le \gamma \le 4$ can be accomplished by first searching for all reduced diagrams with $0 \le \tilde{\gamma} \le 4$ and then enforcing the necessary constraints on I_f, m_f, and m_S.

The first step in identifying all reduced diagrams with $0 \le \tilde{\gamma} \le 4$ is to determine all jets with $\gamma_i = 0, 1, 2, 3$, or 4. The results follow from an inspection of the γ_i, defined in (38) and are shown in Figs. 5, 6, and 7.

From the definition $\tilde{\gamma} = \sum_i \gamma_i$, it is then clear that to find all reduced diagrams with a given value of $\tilde{\gamma}$, we need to find first all distinct partitions of that value into a sum of positive integers. Then, for each of the summands, we need to choose one jet with matching γ_i. For

Table 1: The power counting rules below define how much each component of a reduced diagram contributes to the degree of divergence of the corresponding pinch surface. These rules are for Yukawa and scalar theories where the fermions are massive and the scalars are massless. In the case of massless fermions, soft fermions yield an enhancement of -2 rather than -1.

	Enhancement	Suppression
Collinear fermion line	-2	
Collinear scalar line	-2	
Soft fermion line	-1	
Soft scalar line	-4	
Collinear loop integral		+4
Soft loop integral		+8
Yukawa vertex on collinear fermion line		+1

example, suppose we want to find a reduced diagram with $\tilde{\gamma} = 4$. One of the partitions of 4 is $4 = 2 + 1 + 1$. We then need one jet with $\gamma_i = 2$ and two jets with $\gamma_i = 1$ from Fig. 5.

To find all reduced diagrams with $\tilde{\gamma} = 4$, we first write down all partitions of 4,

$$\begin{aligned} \tilde{\gamma} &= 4 \\ &= 3 + 1 \\ &= 2 + 2 \\ &= 2 + 1 + 1 \\ &= 1 + 1 + 1 + 1 \,. \end{aligned} \tag{39}$$

The classes of diagrams with $\tilde{\gamma} = 4$ corresponding to each partition are shown in Figs. 9 to 13. Note that we have not shown diagrams where the soft cloud attaches to a single jet, such as in Fig. 8. We opt to combine the jet in Fig. 8 with the class of jets having three collinear fermions attached to the hard part from Fig. 17. This will be justified in Sec. 2.4 when we show that soft photon and graviton emission from the soft cloud does not contribute any enhancement.

The same approach yields all diagrams with $\tilde{\gamma} = 3$. These are labelled by their corresponding partition of 3 and shown in Figs. 14, 15, and 16. Likewise, by considering the trivial partitions of $\tilde{\gamma} = 2$ and $\tilde{\gamma} = 1$, we find that the diagrams with $\tilde{\gamma} \leq 2$ belong to the classes shown in Figs. 17 and 18.

We may now return to the original definition of the degree of divergence $\gamma \equiv \tilde{\gamma} + I_f + 4m_f + 2m_s$. When restricting ourselves to $\gamma \leq 2$, as is required for the soft photon theorem,

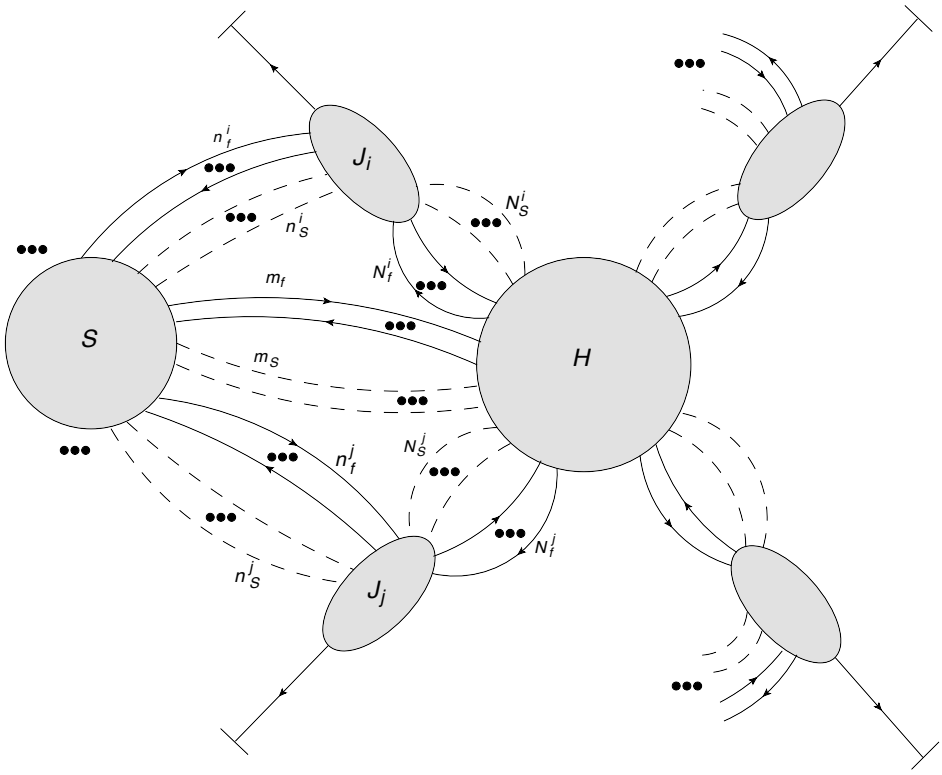

Figure 4: The most general reduced diagram incorporating the hard vertex, the soft function, and well separated jets.

we may set $m_f = 0$. In that case, setting I_f to 1 or 2 forces us to have $\tilde{\gamma} = 1$ or 0 respectively. Either way, we are left with a soft vacuum bubble disconnected form the rest of the diagram. This disconnected piece may be set to vanish by renormalization and need not be considered further. Similarly, setting $m_S = 1$ requires $\tilde{\gamma} = 0$ and results in our having a tadpole soft diagram attached to the hard part by one scalar. Such a diagram vanishes in ϕ^4 theory. Therefore, we find that the elastic diagrams required for an analysis of loop corrections to the soft photon theorem are precisely those from Figs. 17 and 18.

In gravity, the need to consider diagrams with degree of divergence up to $\gamma = 4$ brings about the possibility of having soft lines connecting the soft cloud to the hard part. Suppose we consider a diagram with $\tilde{\gamma} = 4$, then the constraint $\gamma \leq 4$ forces us to have $I_f = m_f = m_S = 0$ and $\gamma = \tilde{\gamma} = 4$ in this case. If $\tilde{\gamma} = 3$, then $m_f = m_S = 0$, but we may have $I_f = 0$ or 1. The former case gives us diagrams with $\gamma = 3$, which are identical to those shown in Figs. 14, 15, and 16. The latter case allows us to have exactly one fermion ring with no scalars attaching to it. This disconnected piece can be renormalized to 0 and therefore we ignore it.

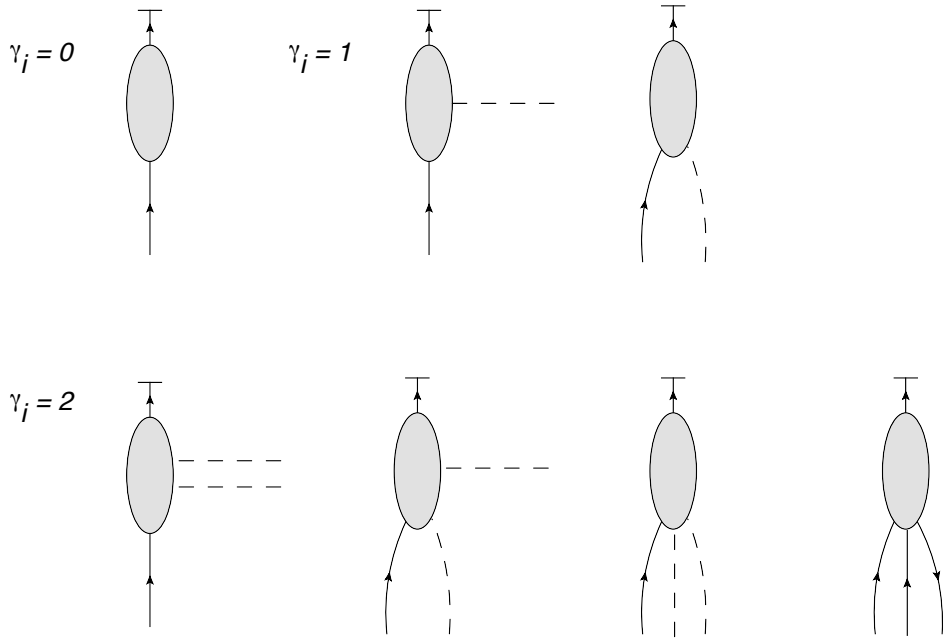

Figure 5: These jets have effective degree of divergence $\gamma_i \leq 2$.

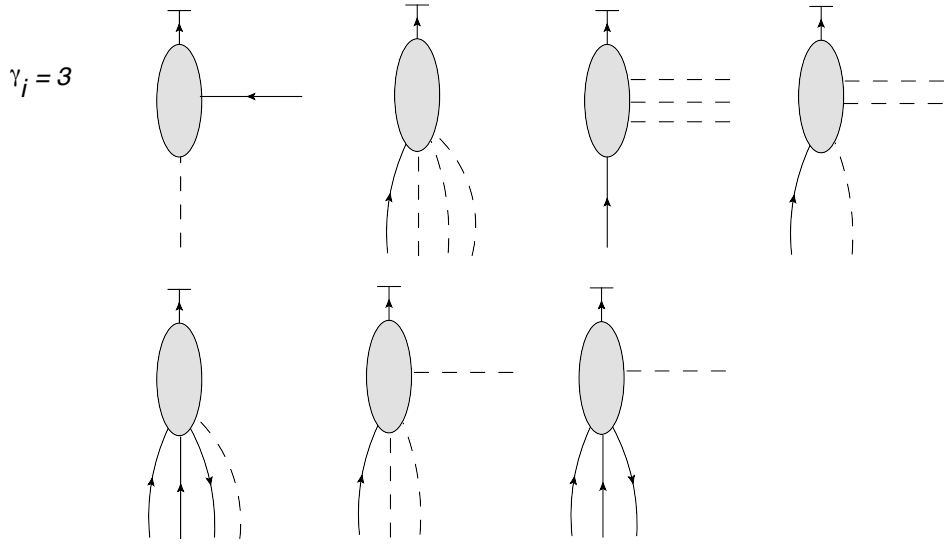

Figure 6: These jets have effective degree of divergence $\gamma_i = 3$.

The situations where $\tilde{\gamma} = 0$, 1, or 2 give us the freedom to have soft fermions internal to the soft cloud, or soft fermions and scalars connecting the soft cloud to the hard part.

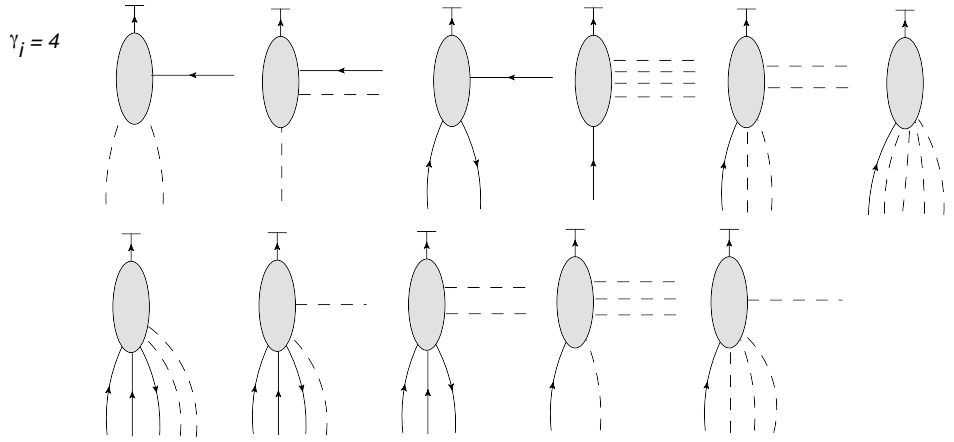

Figure 7: These jets have effective degree of divergence $\gamma_i = 4$.

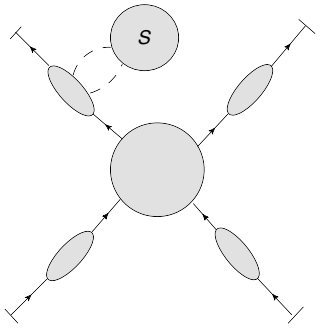

Figure 8: This class of diagrams has $\gamma = 2$ but will be combined with the leading jet class.

For example, if $\tilde{\gamma} = 1$, we may have $\gamma = 3$ and $m_S = 1$. The resulting diagram is shown in Fig. 19 (a). The other possibilities are also shown in Fig. 19 and we will refer to these diagrams as "exceptional" diagrams. Of course, when $I_f = m_f = m_S = 0$, we have that $\gamma = \tilde{\gamma}$. Consequently, the diagrams shown in Figs. 9 to 18 all have a degree of divergence that matches their $\tilde{\gamma}$ value. Finally, we remark that diagrams containing a soft cloud with an odd number of external soft scalars vanish in ϕ^4 theory and, therefore, may be ignored in our analysis.

The class of diagrams in Fig. 17(a) corresponds to the logarithmic leading term of Akhoury [58]. This class consists only of the hard part attached by single fermions to several jets of virtual on-shell lines collinear to the external particles. Since jets attached to the hard part by a single fermion line give the leading term in the elastic amplitude, we will henceforth refer to such jets as "leading jets".

In order to have a comprehensive naming convention for nonleading jets, we introduce the

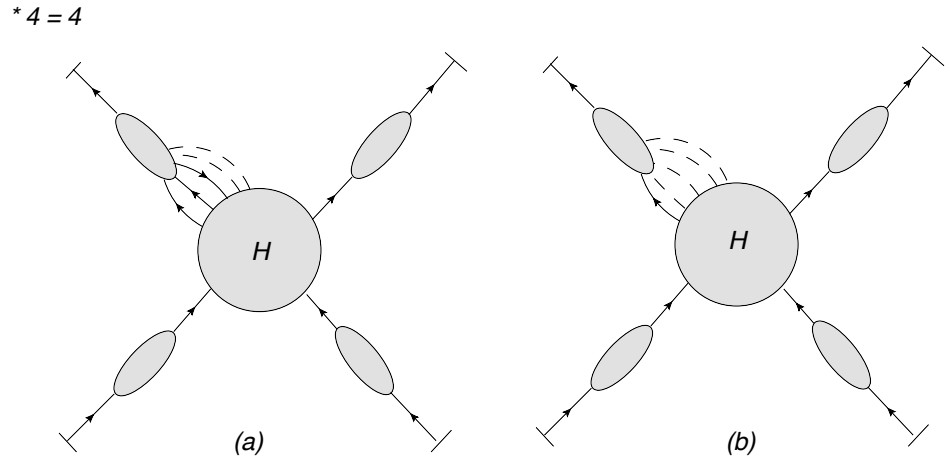

Figure 9: These diagrams have $\tilde{\gamma} = 4$ and correspond to the trivial partition $4 = 4$.

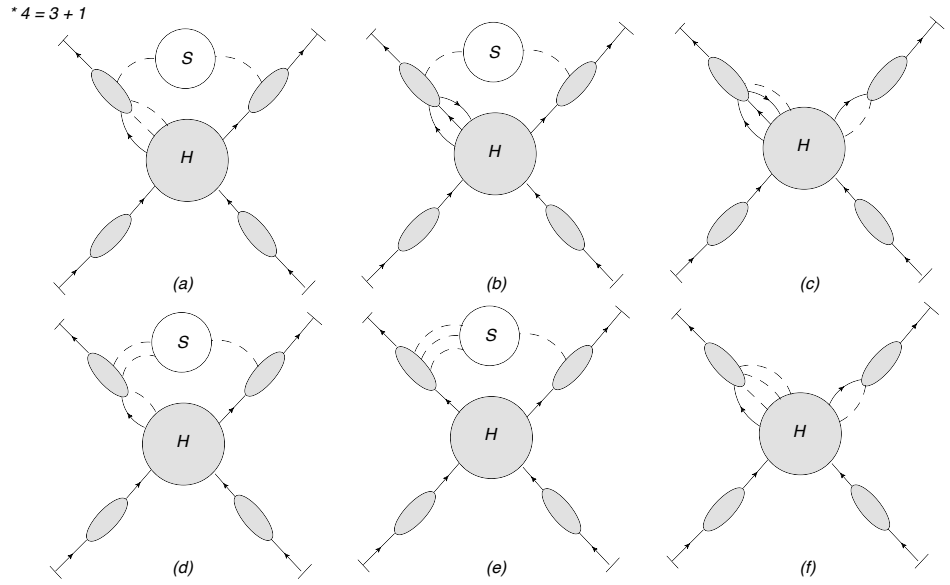

Figure 10: These diagrams have $\tilde{\gamma} = 4$ and correspond to the partition $4 = 3 + 1$. Diagram (d) vanishes in ϕ^4 theory since the soft cloud has three scalars emerging from it.

labels f and s to refer to the particle contents of the jets. These labels indicate whether the collinear particles connecting the jets to the hard part are scalars (s) or fermions/antifermions (f). We underline the labels f and s whenever we need to indicate that a particle coming out of a jet is soft, rather than collinear. Thus, the jets with $\gamma_i = 2$ from Fig. 5 are $f\underline{ss}$, $fs\underline{s}$,

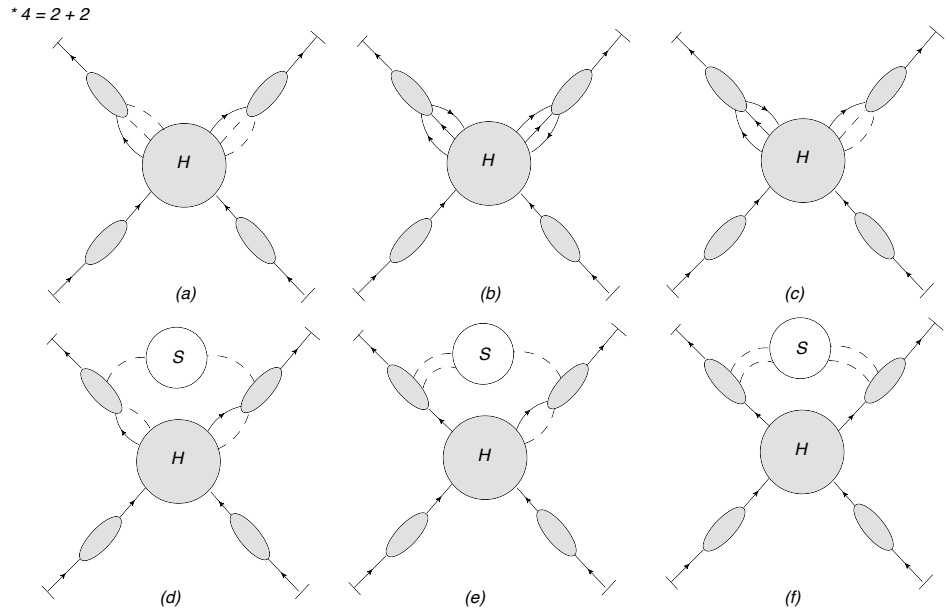

Figure 11: These diagrams have $\tilde{\gamma} = 4$ and correspond to the partition $4 = 2 + 2$. Diagram (e) vanishes in ϕ^4 theory since the soft cloud has three scalars emerging from it.

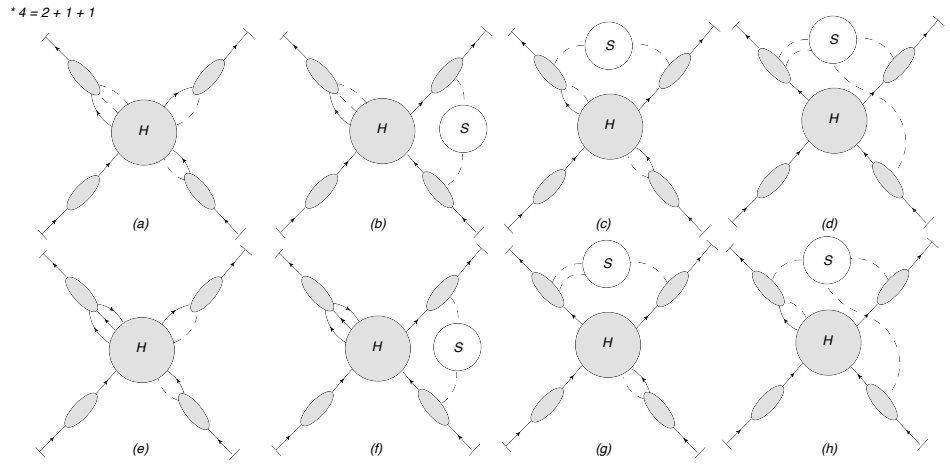

Figure 12: These diagrams have $\tilde{\gamma} = 4$ and correspond to the partition $4 = 2 + 1 + 1$. Diagrams (g) and (h) vanish in ϕ^4 theory since their soft clouds have three scalars emerging from them.

fss, and fff-jets, from left to right.

Having found all pinch surfaces corresponding to loop corrections to Low's theorem and

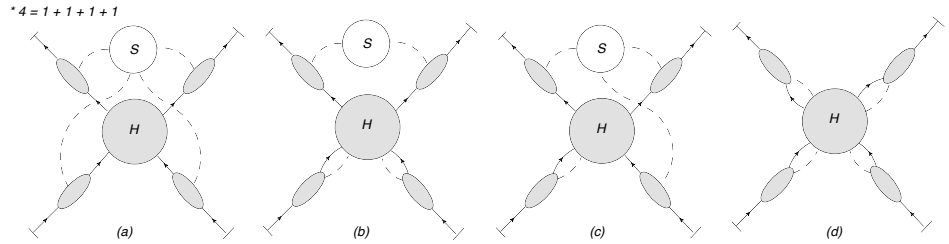

Figure 13: These diagrams have $\tilde{\gamma} = 4$ and correspond to the partition $4 = 1 + 1 + 1 + 1$. Diagram (c) vanishes in ϕ^4 theory since the soft cloud has three scalars emerging from it.

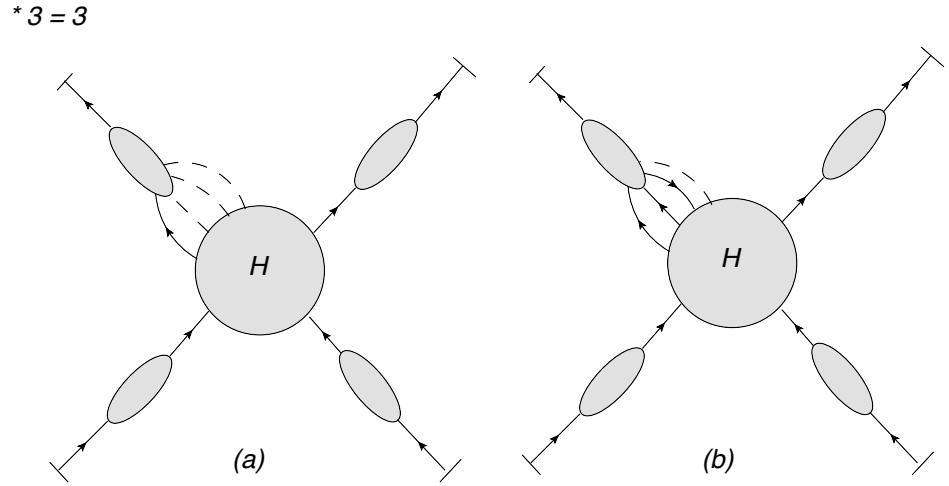

Figure 14: These diagrams have $\tilde{\gamma} = 3$ and correspond to the trivial partition $3 = 3$.

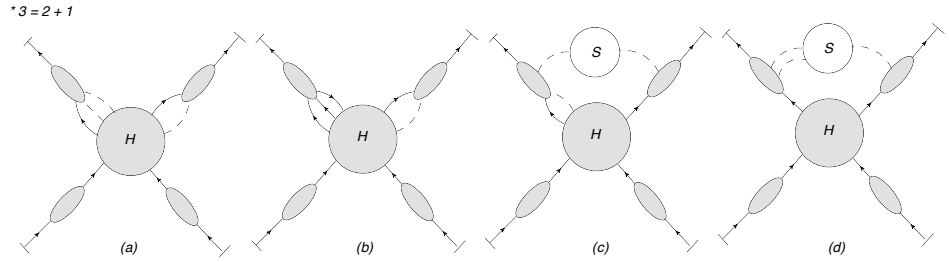

Figure 15: These diagrams have $\tilde{\gamma} = 3$ and correspond to the partition $3 = 2 + 1$. Diagram (d) vanishes in ϕ^4 theory since the soft cloud has three scalars emerging from it.

the CS formula at high energies, we need to factorize their contributions into jet functions. This will allow us to factor the radiative and elastic amplitude into parts that can or cannot

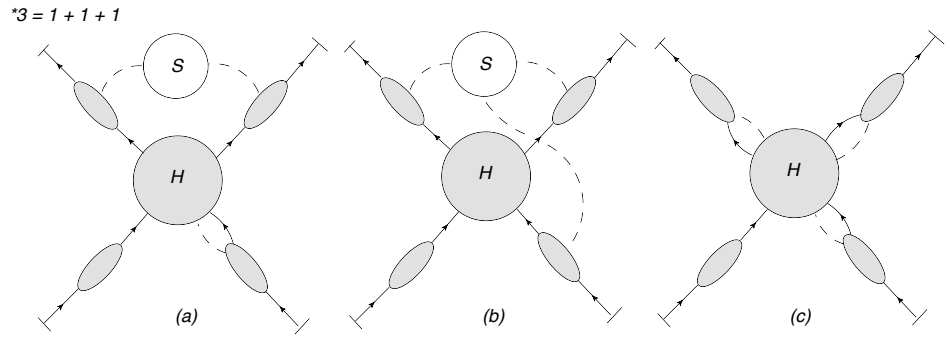

Figure 16: These diagrams have $\tilde{\gamma} = 3$ and correspond to the partition $3 = 1 + 1 + 1$. Diagram (b) vanishes in ϕ^4 theory since the soft cloud has three scalars emerging from it.

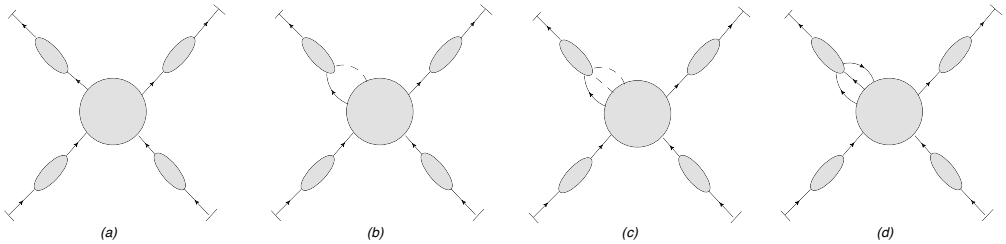

Figure 17: Four of the classes of elastic amplitude diagrams that we need to include when attaching a photon for performing Low's analysis. These are the only ones contributing to the soft photon theorem in the massless limit – see the opening remarks of Chapter 3 for a discussion of this limit. The diagrams in (a) are the leading terms with $\gamma = 0$. Diagrams in (b) have $\gamma = 1$ in the massive case and $\gamma = 2$ in the massless case. The classes of diagrams in (c) and (d) always have $\gamma = 2$.

be expanded in a power series in q. We turn to this task in Sec. 2.3.

2.3 Factorization of nonanalytic contributions

Our approach to extending Low's analysis will rely on factorization. The effect of the pinches producing jet-like momentum configurations can be captured by universal "jet functions" having the same pinch surfaces and singularities as the original Feynman diagrams. The product of jet functions is then matched onto the full amplitude by a "hard function" or "hard part". The hard part gets its leading contribution from exchanges of hard virtual particles. We assume it can be constructed from an algorithm consisting of nested subtractions similar to the procedure described in [55–57]. The jet functions have matrix element definitions,

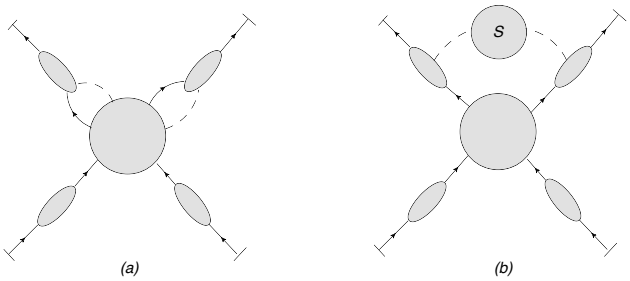

Figure 18: In the massive case, these diagrams have $\gamma = 2$ and contribute to the soft photon theorem. The soft two-point function in (b) includes only soft scalars.

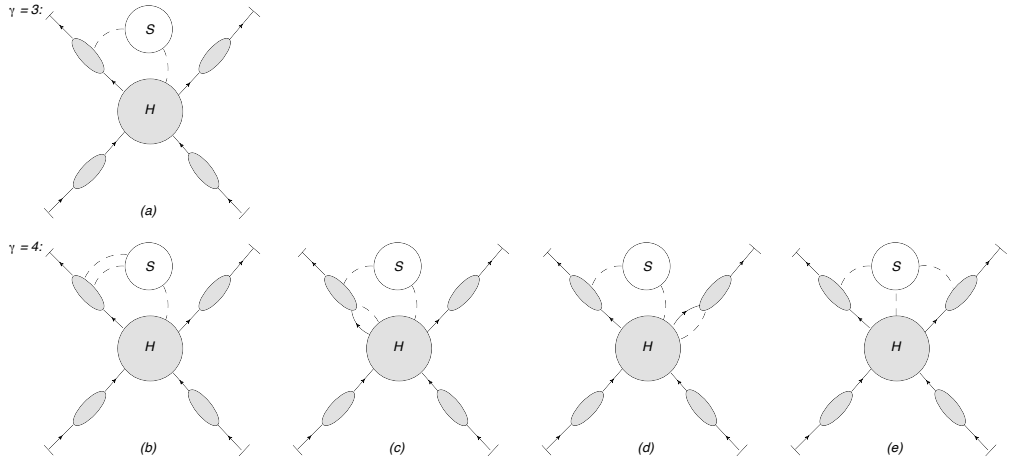

Figure 19: The "exceptional" diagrams with a soft scalar connecting the soft cloud to the hard part. Diagrams (b) and (e) vanish in ϕ^4 theory since their soft clouds have three scalars emerging from them.

which are closely related to the soft collinear effective theory approach to soft radiation theorems [18] and the treatment of bound states in [62–64]. In the soft collinear effective theory approach, the role of our hard part is played by the matching coefficients.

To set the stage for our adaptation of Low's analysis, we need to introduce a unifying notation for jet functions. For Akhoury's leading jets, we use the notation $J^f(p_i)$. The superscript f represents the single fermion or antifermion emerging from the hard part and attaching to the collinear lines comprising the jet. The corresponding hard part is simply denoted $H(p_1, \ldots, p_n)$. Since leading jets are attached to the hard part by a single fermion line, $J^f(p_i)$ is essentially a reduced on-shell self energy. For example, for an outgoing fermion,

$J^f(p_i)$ has the matrix element definition

$$J^f(p_i) = \langle p_i|\overline{\psi}(0)|0\rangle\,. \tag{40}$$

We now introduce a standard notation appropriate for the factorized amplitude. As is customary when using light cone coordinates, we define the vectors n_i^μ and $\bar{n}_i^\mu$ by

$$\begin{aligned} \vec{n}_i &= \frac{\vec{p}_i}{\sqrt{2}\,|\vec{p}_i|} = -\vec{\bar{n}}_i\,, \\ n_i^2 &= \bar{n}_i^2 = 0\,, \\ n_i\cdot\bar{n}_i &= 1\,. \end{aligned} \tag{41}$$

The vector n_i points in the direction collinear to p_i, while the vector $\bar{n}_i$ points in the anti-collinear direction.

The hard part H with which the jets are combined is only sensitive to the collinear components of the external momenta p_i. These collinear components are defined by

$$\hat{p}_i = p_i^+ n_i\,. \tag{42}$$

This collinear vector is the natural argument for the hard part. In the case of a jet loop momentum k collinear to p_i, we proceed analogously and define $\hat{k} \equiv k^+ n_i$. In hard parts, the other components of jet loop momenta are set to zero, or expanded about zero (see below).

In the notation just introduced, the leading term in the expansion of the elastic amplitude is

$$M_{el}^{leading} = \left(\prod_{i=1}^{n} J^f(p_i)\right) \otimes H(\hat{p}_1,\ldots,\hat{p}_n)\,. \tag{43}$$

Each jet function and hard part carries implicit Dirac spinor indices. The tensor product symbol "$\otimes$" will stand for a product of Dirac spinors contracted with matching indices in the jet functions and the hard part.

The nonleading jet function in Fig. 17(b) is denoted by $J^{fs}(p_i - \hat{k}, \hat{k})$. The fs superscript indicates that the first momentum in the argument belongs to the collinear fermion connecting the hard part to the jet and the second momentum to the collinear scalar. The corresponding hard part is then denoted $H_i^{fs}(\hat{p}_1,\ldots;\hat{p}_i - \hat{k}, \hat{k};\ldots,\hat{p}_n)$. The subscript i and superscript fs indicate that the i^{th} outgoing momentum p_i is split between the collinear fermion momentum $p_i - k$ and the collinear scalar momentum k that are shown between the semicolons for clarity. This fs-jet function has the matrix element definition

$$J^{fs}(p_i - \hat{k}, \hat{k}) = \int_{-\infty}^{\infty} d\xi\, e^{-i\hat{k}\cdot(\xi\bar{n}_i)} \langle p_i|\phi(\xi\bar{n}_i)\overline{\psi}(0)|0\rangle\,, \tag{44}$$

for an outgoing fermion, and the subleading amplitude formed from this jet and hard part has the expression

$$M^{fs} = \sum_{i=1}^{n} \left(\prod_{j \neq i} J^f(p_i) \right) \int_0^{p_i^+} dk^+ \, J^{fs}(p_i - \hat{k}, \hat{k}) \otimes H_i^{fs}(\hat{p}_1, \ldots; \hat{p}_i - \hat{k}, \hat{k}; \ldots, \hat{p}_n) \,. \tag{45}$$

In (44), the argument of the field ϕ is $\xi \bar{n}_i$ because we integrate over all noncollinear components of the loop momentum k. Therefore, ξ is the "$-$" component of the original position space argument of the field ϕ, conjugate to the collinear component k^+.

Since fs-jets scale as $O(\lambda)$, it is possible to obtain a contribution of order $O(\lambda^2)$ by expanding the hard part H^{fs} to first order in the transverse loop momentum k_T before it is integrated over. This results in contributions captured by a derivative operator and a separate corresponding hard part. The derivative fs-jet is denoted $J^{f\partial s}$ and given by the operator definition

$$J^{f\partial s} = \int_{-\infty}^{\infty} d\xi \, e^{-i\hat{k}\cdot(\xi\bar{n}_i)} \langle p_i | (\partial_T \phi)(\xi \bar{n}_i) \overline{\psi}(0) | 0 \rangle \,. \tag{46}$$

The transverse index in the derivative is suppressed. It is contracted with a corresponding index in the matching hard part, which will be denoted by $H^{f\partial s}$. Analogously to (45), we have

$$M^{f\partial s} = \sum_{i=1}^{n} \left(\prod_{j \neq i} J^f(p_j) \right) \int_0^{p_i^+} dk^+ \, J^{f\partial s}(p_i - \hat{k}, \hat{k}) \otimes H_i^{f\partial s}(\hat{p}_1, \ldots; \hat{p}_i - \hat{k}, \hat{k}; \ldots, \hat{p}_n) \,, \tag{47}$$

for the amplitude with an $f\partial s$-jet, where the symbol $\otimes$ now includes a sum over the transverse index of the derivative, just as for the implicit Dirac indices.

For Fig. 17(c), the symbol $J^{fss}(p_i - \hat{k}_1 - \hat{k}_2, \hat{k}_1, \hat{k}_2)$ represents the fss-jet where two scalars and a fermion merge at the hard part from a bundle of collinear lines. The momenta k_1 and k_2 are the momenta of the collinear scalars and $p_i - k_1 - k_2$ is the momentum of the collinear fermion. This jet has the matrix element definition

$$J^{fss}(p_i - \hat{k}_1 - \hat{k}_2, \hat{k}_1, \hat{k}_2) = \int_{-\infty}^{\infty} d\xi_1 \, e^{-i\hat{k}_1\cdot(\xi_1\bar{n}_i)} \int_{-\infty}^{\infty} d\xi_2 \, e^{-i\hat{k}_2\cdot(\xi_2\bar{n}_i)} \langle p_i | \phi(\xi_1 \bar{n}_i) \phi(\xi_2 \bar{n}_i) \overline{\psi}(0) | 0 \rangle \,. \tag{48}$$

Following the same logic as in the previous case, the corresponding hard part is $H_i^{fss}(\hat{p}_1, \ldots; \hat{p}_i - \hat{k}_1 - \hat{k}_2, \hat{k}_1, \hat{k}_2; \ldots, \hat{p}_n)$ and the expression for the amplitude with a single fss-jet is

$$M^{fss} = \sum_{i=1}^{n} \left(\prod_{j \neq i} J^f(p_j) \right) \int_0^{p_i^+} dk_1^+ \int_0^{p_i^+} dk_2^+ \, \theta(p_i^+ - k_1^+ - k_2^+)$$

$$\times J^{fss}(p_i - \hat{k}_1 - \hat{k}_2, \hat{k}_1, \hat{k}_2) \otimes H_i^{fss}(\hat{p}_1, \ldots; \hat{p}_i - \hat{k}_1 - \hat{k}_2, \hat{k}_1, \hat{k}_2; \ldots, \hat{p}_n)\,. \qquad (49)$$

Finally, the fff-jet function in Fig. 17(d) is denoted $J^{fff}(p_i - \hat{k}_1 - \hat{k}_2, \hat{k}_1, \hat{k}_2)$ and its corresponding hard part is $H_i^{fff}(\hat{p}_1, \ldots; \hat{p}_i - \hat{k}_1 - \hat{k}_2, \hat{k}_1, \hat{k}_2; \ldots, \hat{p}_n)$. Similarly to the above, this jet has matrix element definition

$$J^{fff}(p_i - \hat{k}_1 - \hat{k}_2, \hat{k}_1, \hat{k}_2) = \int_{-\infty}^{\infty} d\xi_1\, e^{-i\hat{k}_1\cdot(\xi_1\bar{n}_i)} \int_{-\infty}^{\infty} d\xi_2\, e^{-i\hat{k}_2\cdot(\xi_2\bar{n}_i)} \langle p_i|\overline{\psi}(\xi_1\bar{n}_i)\psi(\xi_2\bar{n}_i)\overline{\psi}(0)|0\rangle\,, \qquad (50)$$

and the amplitude involving a single fff-jet is

$$M^{fff} = \sum_{i=1}^{n} \left(\prod_{j\neq i} J^f(p_j)\right) \int_0^{p_i^+} dk_1^+ \int_0^{p_i^+} dk_2^+\, \theta(p_i^+ - k_1^+ - k_2^+)$$
$$\times J^{fff}(p_i - \hat{k}_1 - \hat{k}_2, \hat{k}_1, \hat{k}_2) \otimes H_i^{fff}(\hat{p}_1, \ldots; \hat{p}_i - \hat{k}_1 - \hat{k}_2, \hat{k}_1, \hat{k}_2; \ldots, \hat{p}_n)\,. \qquad (51)$$

Here, the symbol $\otimes$ includes the contraction of three implicit Dirac indices.

It should be clear at this point that we could generalize our notation to jets with an arbitrary number of particles merging into a jet of collinear lines. It will be convenient to use the same notation for jets of collinear lines in reduced diagrams and the jet functions themselves. Just like the jets themselves, J^{fs}, J^{fss}, and J^{fff} will also be referred to as fs-jets, fss-jets, and fff-jets respectively. We will also sometimes include convolution over the collinear component of loop momenta in the tensor product symbol "$\otimes$" and omit the full momentum arguments of jet functions and hard parts when they are clear from the context.

It is interesting to remark that the power-suppressed contributions we have identified are closely related to exclusive amplitudes for bound states [62–64] and next-to-leading power inclusive cross sections for pair production [65, 66].

With our notation set up, we can also write down the contribution to the elastic amplitude involving two fs-jets,

$$M^{fsfs} = \sum_{1\leq i<j\leq n} \left(\prod_{l\neq i,j} J^f(p_l)\right) \int_0^{p_i^+} dk_1^+ \int_0^{p_j^+} dk_2^+\, J^{fs}(p_i - \hat{k}_1, \hat{k}_1)$$
$$\times J^{fs}(p_j - \hat{k}_2, \hat{k}_2) \otimes H_{ij}^{fsfs}(\hat{p}_1, \ldots; \hat{p}_i - \hat{k}_1, \hat{k}_1; \ldots; \hat{p}_j - \hat{k}_2, \hat{k}_2; \ldots, \hat{p}_n)\,. \qquad (52)$$

As to the fs-jets from diagrams in Fig. 18(b), we use the label $J^{f\underline{s}}(p_i + k, k)$ with the understanding that the momentum argument corresponding to the label $\underline{s}$ is soft rather than collinear. Accordingly, the contribution to the elastic amplitude from diagrams where two fs-jets are connected by a single soft scalar two-point function $S_{ij}(k)$ is

$M^{f\underline{s}f\underline{s}} =$

$$\sum_{1\le i<j\le n}\left(\prod_{l\neq i,j} J^{f}(p_l)\right)\int d^4k\, S_{ij}(k) J^{f\underline{s}}(p_i+k,k)\, J^{f\underline{s}}(p_j-k,-k)\otimes H_{ij}^{f\underline{s}f\underline{s}}(\hat{p}_1,\ldots,\hat{p}_n)\,. \tag{53}$$

The hard part has no scalars emerging from it in this case. As we mentioned previously, Eq. (37) implies that $S(k)$ only contains soft internal scalars and cannot radiate any photon at $O(\lambda^0)$. It can, however, emit a soft graviton and yield a contribution of $O(\lambda^2)$, as we will see in Sec. 2.4. The matrix element definition of the $f\underline{s}$-jet in Eq. (53) is

$$J^{f\underline{s}}(p_i+k,k)=\int d^4y\, e^{ik\cdot y}\langle p_i|\,\frac{\delta S_I}{\delta\phi(y)}\,\overline{\psi}(0)|0\rangle\,, \tag{54}$$

where $S_I=\int d^4x\,\mathcal{L}_I$. In Yukawa theory, $\mathcal{L}_I(x)=g\,\phi(x)\overline{\psi}(x)\psi(x)+\frac{g'}{4!}\,\phi^4(x)$, where g is the Yukawa coupling and g' is the four-scalar coupling. No component of the soft momentum k is integrated out. Also, the loop momentum k bears no hat in the above because it is a soft rather than a collinear momentum.

Combining the above definitions allows us to write the fully factorized elastic amplitude expanded to $O(\lambda^2)$,

$$\begin{aligned}
M_{el}=&\left(\prod_{i=1}^{n} {J_i}^{f}\right)\otimes H\\
&+\sum_{i=1}^{n}\left(\prod_{j\neq i}{J_j}^{f}\right){J_i}^{fs}\otimes {H_i}^{fs}+\sum_{i=1}^{n}\left(\prod_{j\neq i}{J_j}^{f}\right){J_i}^{f\partial s}\otimes {H_i}^{f\partial s}\\
&+\sum_{i=1}^{n}\left(\prod_{j\neq i}{J_j}^{f}\right){J_i}^{fss}\otimes {H_i}^{fss}+\sum_{i=1}^{n}\left(\prod_{j\neq i}{J_j}^{f}\right){J_i}^{fff}\otimes {H_i}^{fff}\\
&+\sum_{1\le i<j\le n}\left(\prod_{l\neq i,j}{J_l}^{f}\right){J_i}^{fs}{J_j}^{fs}\otimes H_{ij}^{fs;fs}+\sum_{1\le i<j\le n}\left(\prod_{l\neq i,j}{J_l}^{f}\right){J_i}^{f\underline{s}}{J_j}^{f\underline{s}}\,S_{ij}\otimes H_{ij}^{f\underline{s};f\underline{s}}\\
&+O(\lambda^3)\,.
\end{aligned} \tag{55}$$

When we derive the small q expansion of the soft photon radiative amplitude, we will have to consider emission from each factor in each term: the leading jets, the nonleading jets, and the hard part.

In (55), the soft function S_{ij} is a two-point function with soft external scalar momenta connecting to jets i and j. It is useful to extend this notation in a straightforward way, so that for example, S_{iikl} stands for a four-point function with soft external scalar momenta, two of which connect to jet i, and with the two others connecting to jets k and l. In the

notation for the hard parts, the superscripts indicate which nonleading jets are present, separated by semicolons. The subscripts indicate which external particle is coming from the corresponding nonleading jet in the superscript. For example, the hard part $H_{ij}^{fff;fs}$ has an fff-jet at the i^{th} external particle and an fs-jet at the j^{th} external particle.

To include all loop corrections to the soft graviton theorem, it is necessary to expand the elastic amplitude as in (55), but all the way up to $O(\lambda^4)$ rather than $O(\lambda^2)$. In the interest of space, we will not write the $O(\lambda^3)$ and $O(\lambda^4)$ terms in equation format. The $O(\lambda^3)$ terms derive from the diagrams shown in Figs. 14, 15, and 16. The associated factorized terms are listed in Table 2. The $O(\lambda^4)$ terms correspond to the reduced diagrams shown in Figs. 9, 10, 11, 12, and 13. The associated factors are displayed in Table 3. Finally, we also need to consider the "exceptional contributions" whose diagrams appear in Fig. 19, with the associated factorized contributions listed in Table 4. To generate the explicit $O(\lambda^3)$ and $O(\lambda^4)$ terms, one would need to contract the factors found in these tables analogously to (55).

It should be mentioned that additional derivative jet functions need to be defined at $O(\lambda^3)$ and $O(\lambda^4)$. These arise when one expands the hard parts of lower order terms in the transverse components of the loop momenta of the collinear particles connecting hard parts to jets. Although we will not list these explicitly, their construction is entirely analogous to (46).

Table 2: The factors corresponding to the diagrams with $\gamma = 3$. A horizontal line separates factorized forms corresponding to distinct partitions of $\gamma = 3$. These factorized contributions are associated with the diagrams shown in Figs. 14, 15, and 16.

Nonleading jets	Soft function	Hard part
J_i^{fsss}	1	H_i^{fsss}
J_i^{ffffs}	1	H_i^{ffffs}
$J_i^{fss} J_j^{fs}$	1	$H_{ij}^{fss;fs}$
$J_i^{fff} J_j^{fs}$	1	$H_{ij}^{fff;fs}$
$J_i^{fs\underline{s}} J_j^{f\underline{s}}$	S_{ij}	H_i^{fs}
$J_i^{f\underline{s}} J_j^{f\underline{s}} J_k^{fs}$	S_{ij}	H_k^{fs}
$J_i^{fs} J_j^{fs} J_k^{fs}$	1	$H_{ijk}^{fs;fs;fs}$

Table 3: The factors corresponding to the diagrams with $\gamma = 4$. A horizontal line separates factorized forms corresponding to distinct partitions of $\gamma = 4$. These factorized contributions are associated with the diagrams shown in Figs. 9, 10, 11, 12, and 13.

Non leading jets	Soft function	Hard part
J_i^{fffss}	1	H_i^{fffss}
J_i^{fssss}	1	H_i^{fssss}
$J_i^{fss\underline{s}} J_j^{f\underline{s}}$	S_{ij}	$H_{ij}^{fss;f}$
$J_i^{fff\underline{s}} J_j^{f\underline{s}}$	S_{ij}	$H_{ij}^{fff;f}$
$J_i^{fffs} J_j^{fs}$	1	$H_{ij}^{fffs;fs}$
$J_i^{f\underline{sss}} J_j^{f\underline{s}}$	S_{iiij}	H
$J_i^{fsss} J_j^{fs}$	S_{ij}	$H_{ij}^{fsss;fs}$
$J_i^{fss} J_j^{fss}$	1	$H_{ij}^{fss;fss}$
$J_i^{fff} J_j^{fff}$	1	$H_{ij}^{fff;fff}$
$J_i^{fff} J_j^{fss}$	1	$H_{ij}^{fff;fss}$
$J_i^{fs\underline{s}} J_j^{fs\underline{s}}$	S_{ij}	$H_{ij}^{fs;fs}$
$J_i^{f\underline{ss}} J_j^{f\underline{ss}}$	S_{iijj}	H
$J_i^{fss} J_j^{fs} J_k^{fs}$	1	$H_{ijk}^{fss;fs;fs}$
$J_i^{fss} J_j^{f\underline{s}} J_k^{f\underline{s}}$	S_{jk}	H_i^{fss}
$J_i^{fs\underline{s}} J_j^{f\underline{s}} J_k^{fs}$	S_{ij}	$H_{ik}^{fs;fs}$
$J_i^{f\underline{ss}} J_j^{f\underline{s}} J_k^{f\underline{s}}$	S_{iijk}	H
$J_i^{fff} J_j^{fs} J_k^{fs}$	1	$H_{ijk}^{fff;fs;fs}$
$J_i^{fff} J_j^{f\underline{s}} J_k^{f\underline{s}}$	S_{jk}	H_i^{fff}
$J_i^{f\underline{s}} J_j^{f\underline{s}} J_k^{f\underline{s}} J_l^{f\underline{s}}$	S_{ijkl}	H
$J_i^{f\underline{s}} J_j^{f\underline{s}} J_k^{fs} J_l^{fs}$	S_{ij}	$H_{kl}^{fs;fs}$
$J_i^{fs} J_j^{fs} J_k^{fs} J_l^{fs}$	1	$H_{ijkl}^{fs;fs;fs;fs}$

2.4 Modification of power counting from photon and graviton emission

Having obtained an expansion of the elastic amplitude in powers of λ, with each term factored into jet functions, a soft cloud, and a hard part, we now move on to understanding how the radiative amplitudes are derived from these factorized forms. Recall the expansions of the

Table 4: The exceptional factorized terms contributing to the elastic amplitude. In the soft function subscript, the label H indicates that a soft scalar is attaching the soft cloud to the hard part. Likewise, in the hard part superscript, the label S indicates that a soft scalar connects the hard part to the soft cloud. These factorized contributions are associated with the diagrams shown in Fig. 19.

Order	Non leading jets	Soft function	Hard part
λ^3	J_i^{fs}	S_{iH}	H^S
λ^4	$J_i^{fs} J_j^{fs}$	S_{iH}	$H_j^{fs;S}$
λ^4	J_i^{fss}	S_{iH}	$H_i^{fs;S}$

radiative amplitude for the emission of a soft photon, and a soft graviton,

$$\begin{aligned} M^\mu(q) &= \sigma_{-2}^\mu + \sigma_{-1}^\mu + \sigma_0^\mu \quad \text{for a soft photon,} \\ \mathcal{M}^{\mu\nu}(q) &= \sigma_{-2}^{\mu\nu} + \sigma_{-1}^{\mu\nu} + \sigma_0^{\mu\nu} + \sigma_1^{\mu\nu} + \sigma_2^{\mu\nu} \quad \text{for a soft graviton,} \end{aligned} \tag{56}$$

where $\sigma_\gamma = O(\lambda^\gamma)$. One approach to deriving the coefficients σ is to identify all pinch surfaces of the radiative amplitude, analogously to the elastic amplitude, and construct the radiative hard parts by brute force. The radiative jet functions are universal, but the nested subtractions required to derive the hard parts differ for every process, and, therefore, such an approach would not be practical. A better alternative, following Low, is to take advantage of the fact that every diagram contributing to the radiative amplitude can be generated from the elastic amplitude by considering all points of attachment of the soft photon or soft graviton. One can then apply an argument similar to Low's by considering separately photon, or graviton, emission from the external jets, the soft cloud, and the hard part. To carry out this approach, we need, however, to determine how the infrared degree of divergence γ of a radiative diagram is related to the degree of divergence of an elastic diagram when a soft photon, or graviton, is attached to obtain the former from the latter.

We will focus on gravitons, since the case of photons is simpler. The amplitude for soft graviton emission from a jet is generated by inserting a matter-graviton vertex into the matrix element definition of the corresponding jet function. For instance, in the case of a leading jet, we obtain the following radiative jet function,

$$J_{\mu\nu}(p_i, q) = \int d^4x\, e^{-iq\cdot x} \left\langle p_i \left| \mathcal{T}^* \left(i T_{\mu\nu}(x) \phi_i(0) \right) \right| 0 \right\rangle , \tag{57}$$

where $T_{\mu\nu}$ is the stress tensor through which we assume gravity couples to matter. This stress tensor is defined by taking the variational derivative of the matter action, as shown in

the following equation [67, 68],

$$\delta S_{matter} \equiv \frac{1}{2}\int d^4x\, T^{\mu\nu}(x)\, \delta g_{\mu\nu}(x). \tag{58}$$

The dynamics of the graviton field is dictated by the full Einstein-Hilbert action. We will, however, not be concerned with graviton loops, and thus, our prescription for coupling matter to gravity is to make insertions of the operator $iT_{\mu\nu}$ to generate a matter graviton vertex.

We now analyze the effect of emitting a graviton from one of the lines, or vertices, in the reduced diagrams that give the terms of order $O(\lambda^0)$ up to $O(\lambda^4)$ identified in Sec. 2.2.2. In doing this, we need to take into account the possibility of emitting the graviton from a collinear line, a soft line, or directly from the vertices of Yukawa and scalar theory.

We begin by considering graviton emission from a fermion line. The graviton-fermion vertex is given by

$$V^{\mu\nu}_{ffG} = -\frac{i\kappa}{2}\left[\frac{1}{4}(\gamma^\mu(p+p')^\nu + \gamma^\nu(p+p')^\mu) - \eta^{\mu\nu}\left(\frac{1}{2}(\not{p}+\not{p}') - m\right)\right], \tag{59}$$

where κ is Newton's constant, and p and p' are the incoming and outgoing fermion momenta – see Fig. 20(a).

Figure 20: The fermion-graviton (ffG) and scalar-graviton (ssG) vertices.

Starting from a fermion line carrying momentum p, emitting a graviton from this line changes the propagator according to

$$\frac{i}{\not{p}-m} \mapsto \frac{i\kappa}{8}\left[\frac{\not{p}+m}{p^2-m^2}(\gamma^\mu(2p+q)^\nu + \gamma^\nu(2p+q)^\mu)\frac{\not{p}+\not{q}+m}{(p+q)^2-m^2} - \frac{2\eta^{\mu\nu}}{\not{p}+\not{q}-m} - \frac{2\eta^{\mu\nu}}{\not{p}-m}\right]. \tag{60}$$

Suppose we had started with a collinear fermion line. On the right hand side of the arrow, the leading term is the first on the left. It has two collinear denominators, each of which scales as λ^2, and a numerator whose leading term scales as λ^0 when $\mu\nu = ++$. Since we started with only one collinear denominator scaling as λ^2, we conclude that the net effect of adding a graviton is to reduce the degree of divergence γ of the whole diagram by 2.

On the other hand, suppose we had started with a soft fermion. Then we begin with a propagator where the numerator and denominator are dominated by the mass term. Therefore, this soft fermion propagator scales as λ^{-1} and, as seen from (60), emitting the graviton from this line either introduces an additional soft fermion propagator and a numerator that scales as λ^2, or does not introduce any new factor as in the rightmost two terms. The net effect is therefore to leave the scaling power γ unchanged.

Consider now emitting the soft graviton from a scalar line as in Fig. 20 (b). The scalar-graviton vertex is given by

$$V_{ssG}^{\mu\nu} = \frac{-i\kappa}{2}(p^\mu p'^\nu + p^\nu p'^\mu - \eta^{\mu\nu}(p\cdot p' - m^2))\,. \tag{61}$$

The starting massless scalar propagator is therefore replaced according to

$$\frac{i}{p^2} \mapsto \frac{i\kappa}{2}\frac{1}{p^2}\frac{1}{(p+q)^2}(2p^\mu p^\nu + p^\mu q^\nu + p^\nu q^\mu - \eta^{\mu\nu}(p^2 + p\cdot q))\,. \tag{62}$$

If the original scalar is collinear, then as before we have added a denominator scaling as λ^2 and a numerator scaling as 1 when $\mu\nu = ++$, for a net change of $\gamma \mapsto \gamma - 2$. If, however, the scalar is soft, then the addition of a denominator scaling as λ^4 is entirely compensated by the numerator scaling as λ^4 as well. Hence, emitting a soft graviton from a soft scalar does not alter the degree of divergence of the whole diagram.

It remains to analyze the effect of emitting a graviton directly from the interaction vertices of Yukawa and scalar theory – see Fig. 21. Let g be the Yukawa coupling and g' be the four-scalar coupling. Then, emitting the graviton from the Yukawa vertex introduces a factor of $-\frac{ig\kappa}{2}\eta^{\mu\nu}$ into the diagram and nothing else. This does not alter the degree of divergence. Similarly, emitting the soft graviton from the four-scalar vertex introduces a factor of $-\frac{ig'\kappa}{2}\eta^{\mu\nu}$ and does not alter the degree of divergence.

Consider now emitting a soft graviton from a hard line internal to the hard part. Our notation for radiative hard parts is derived from the elastic hard parts by simply adding $\mu\nu$ indices, where μ and ν couple to the spacetime indices of the graviton polarization tensor $E^{\mu\nu}$. We thereby obtain the radiative hard parts $H_{\mu\nu}(\hat{p}_1,\ldots,\hat{p}_n,q)$, $H^{fs}_{i,\mu\nu}(\hat{p}_1,\ldots;\hat{p}_i - \hat{k},\hat{k};\ldots,\hat{p}_n,q)$, $H^{fss}_{i,\mu\nu}(\hat{p}_1,\ldots;\hat{p}_i - \hat{k}_1 - \hat{k}_2,\hat{k}_1,\hat{k}_2;\ldots,\hat{p}_n,q)$, and so on. Soft graviton insertions into hard lines will only result in the addition of another hard line to the diagram, since a soft momentum cannot possibly alter the scaling of a hard momentum. Hence, the degree of divergence of a radiative diagram obtained by inserting a soft graviton into the hard part of an elastic diagram is the same as the degree of divergence of the original elastic diagram.

The effects of emitting a soft graviton from a reduced diagram of the elastic amplitude are gathered in Table 5. We see that the greatest enhancement occurs when the graviton is emitted from a collinear fermion or scalar line. Further, in this case, the infrared degree of

Figure 21: The scalar-two-fermion-graviton (sffG) and the four-scalar-graviton (ssssG) vertices.

divergence of the newly obtained radiative diagram is equal to the degree of divergence of the original elastic amplitude diagram minus 2.

Table 5: This table describes how to obtain the degree of divergence of a radiative diagram from the degree of divergence of the corresponding elastic diagram. The effect of graviton emission depends on which component of the elastic diagram the graviton is emitted from.

Component emitting the soft graviton	Net effect on degree of divergence of elastic diagram
Collinear fermion line	-2
Collinear scalar line	-2
Soft fermion line	+0
Soft scalar line	+0
Yukawa vertex	+0
Four-scalar vertex	+0
Hard part	+0

In Eq. (24), we noted that the soft graviton theorem can be thought of as an expansion of the radiative amplitude in power of the small scale λ. Any diagram contributing to this expansion can be derived by attaching a soft graviton to a diagram contributing to the elastic amplitude. Further, we have just shown that the resulting radiative diagram will be of order $O(\lambda^{\gamma-2})$, where we assume that the original elastic amplitude diagram was of order $O(\lambda^{\gamma})$. Therefore, to get all contributions to the radiative amplitude between $O(\lambda^{-2})$ and $O(\lambda^{2})$, we need to begin our construction with all elastic diagrams of orders between $O(\lambda^{0})$ and $O(\lambda^{4})$, as we claimed in Sec. 2.1.

Graviton emission from the hard part or the soft cloud needs to be considered only for elastic diagrams with scaling power γ between 0 and 2. Indeed, emitting a graviton from the hard part or the soft cloud has no effect on the degree of divergence, and hence we need

to start from an elastic diagram with $\gamma \leq 2$ to remain within the order of accuracy of the soft graviton theorem.

The photon emission amplitudes are described by the radiative jet functions $J^f_{i,\mu}(p_l+q,q)$, $J^{fs}_{i,\mu}(p_i+q-\hat{k},\hat{k},q)$, etc., and the radiative hard parts $H_\mu(\hat{p}_1,\ldots,\hat{p}_n,q)$, $H^{fs}_{i,\mu}(\hat{p}_1,...,\hat{p}_i-\hat{k},\hat{k},...,\hat{p}_n,q)$, etc. The notation is the same as for nonradiative jet functions and hard parts, with the photon index μ coupling to the polarization of the emitted photon. The radiative jet functions are derived from the matrix element definitions of Sec. 2.3 by inserting an electromagnetic current operator [14]. For example, the elastic jet function in (40) becomes the radiative leading jet

$$J^{f,\mu}(p_i,q) = \int d^4x\, e^{iq\cdot x}\langle p_i|j^\mu(x)\overline{\psi}(0)|0\rangle\,, \tag{63}$$

where $j^\mu(x)$ is the electromagnetic current operator and q is the photon momentum.

Following a similar line of reasoning as for gravitons, we find that the regions of integration about the pinch surfaces with $0 \leq \gamma \leq 2$ are precisely the ones we need to consider for extending the soft photon theorem. The soft photon momentum q scales as $(\lambda^2,\lambda^2,\lambda^2)E$, and, hence, attaching a soft photon to a collinear or soft fermion line will not alter the scaling of the pre-existing fermion line. The net effect as far as our power counting procedure is concerned will be the addition of a supplementary collinear or soft fermion line. Therefore, following the rules in Table 1, attaching an external soft photon to an elastic amplitude diagram will reduce its degree of divergence by 2 if the photon is attached to a collinear fermion line, or 1 if it is attached to a soft fermion line. If we start from diagrams with $0 \leq \gamma \leq 2$, this will leave us with radiative diagrams of order between $O(\lambda^{-2})$ and $O(\lambda^0)$, which is precisely the range of magnitudes relevant to Low's theorem. We mention that in both the photon and graviton cases, the leading order $O(\lambda^{-2})$ term in the radiative amplitude is generated by attaching the soft external particle to a leading jet.

3 Loop Corrections to the Soft Photon Theorem

The objective of this chapter is to show how to derive a soft photon theorem that fully takes loop corrections and infrared behavior into account. Our approach will start from the factorized amplitude (55), and apply Ward identities similarly to Low's argument. Before tackling this task, however, we make a few more comments on the power counting results of Chapter 2, and also illustrate our general conclusions with two examples in Sec. 3.1.

As we mentioned in Sec. 2.4, attaching a soft photon to a leading jet yields the leading $O(\lambda^{-2})$ term in the radiative amplitude. The diagrams (c) and (d) of Fig. 17 have $\gamma = 2$ and inserting a photon into them produces diagrams that are $O(\lambda^0)$ up to multiplication by a logarithmic term in q. When the fermions have nonzero mass m, the diagrams in 17(b) have $\gamma = 1$ and inserting a soft photon into them produces a term scaling as λ^{-1}, thereby yielding a contribution of the same order as m/q.

One can take the limit where $m \to 0$ and retain the definitions of collinear and soft scaling provided another suitable small scale λ is identified. We will assume this has been done when discussing the fully "massless limit" here and below. In this case, the fs-jets scale as λ^2, unlike the λ scaling predicted by power counting in the massive case. This makes the whole class of diagrams in Fig. 17(b) scale as λ^2. Hence, the term of intermediate order of magnitude λ^{-1} disappears in the massless limit. The $O(\lambda)$ contribution is absent from fs-jets in the massless limit because the denominator of the loop integrand is symmetric under simultaneous reflection of all transverse loop momenta while the leading term in the numerator is odd under such a transformation. Consequently, the term that would scale as λ, and thereby conform to the power counting rules of Table 1, actually vanishes. This vanishing of the would-be leading term pushes the scaling of fs-jets back to the next available order, namely λ^2. We illustrate how this happens explicitly in Sec. 3.1.1.

In Fig. 18, we show two additional classes of diagrams that only contribute in the massive case. Both of these have $\gamma = 2$. Diagram 18(a) contains two distinct nonleading jets but can be treated similarly to diagrams appearing in Fig. 17. Diagram 18(b) includes a two-point function of soft particles connected to two distinct jets. From the requirement $\gamma \leq 2$ with γ given by Eq. (37), we find that this two-point function consists only of soft scalars and therefore no photon is emitted from it.

The disappearance of contributions from diagrams 18(a) in the massless limit takes place because with massless fermions, fs-jets scale as λ^2 rather than λ, as we mentioned when discussing Fig. 17(b). This makes the diagrams of Fig. 18(a) scale as λ^4 rather than λ^2. As for contributions from diagrams 18(b), the $f\underline{s}$-jets will scale as λ^0 rather than λ^{-1} in the massless case, making the whole diagram scale as λ^4. As in the case of fs-jets, the scaling of $f\underline{s}$-jets in the massless limit is due to the leading term in the integrand being odd under simultaneous reflection of all transverse loop momenta.

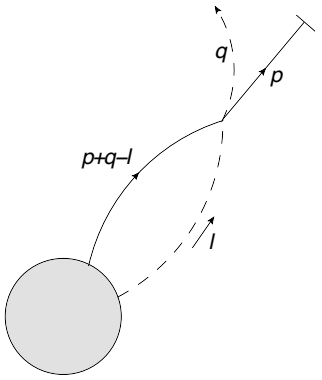

Figure 22: Lowest order fs-jet after the application of the Ward identity. The photon momentum exits the jet at a composite scalar-photon-fermion vertex as in the Ward identity shown in Fig. 2.

3.1 Examples

Our discussion of the soft photon theorem above relies on a treatment of the analytic structure of soft photon radiation. In particular, we have used a power counting analysis to determine that nonleading jets do contribute to Low's theorem. It is instructive to verify our claims by studying explicit examples. To this end, we study the lowest order fs-jet, and a diagram with two one-loop $f\underline{s}$-jets. We will consider a massless pseudoscalar coupled to massive fermions in this section. A pseudoscalar coupling lets us use the Dirac equation to obtain more compact formulas for the jet functions but still obeys our power counting rules shown in Sec. 2.2.2.

3.1.1 Lowest order fs-jet

Consider first the lowest order fs-jet in a pseudoscalar theory, shown in Fig. 22. In the classic form of Low's argument, we would encounter this jet when deducing the internal emission amplitude from the external amplitude as in Eq. (6) – see Fig. 2. In Eq. (6), the elastic amplitude is given a q dependence by shifting one of the external momentum arguments p to $p+q$. We have introduced such a q dependence in our fs-jet as well, and in doing so aim at exhibiting the logarithmic dependence on q that we described in Sec. 2.1.

The loop integral for the elastic amplitude with a single fs-jet takes the form

$$M^{fs}(p+q) = \int_0^1 dx \int \frac{d^d l}{(2\pi)^d}\, \bar{u}(p) \frac{(-ig\mu^\epsilon \gamma_5) i(\not{p} + \not{q} - \not{l} + m)}{((p+q-l)^2 - m^2 + i\epsilon)} H^{fs}(x)\, \frac{i}{l^2 + i\epsilon}\, p^+ \delta(l^+ - x p^+)\,. \tag{64}$$

We work in dimension $d = 4 - 2\epsilon$. Our coupling constant for Yukawa theory is $g\mu^\epsilon$, where we introduce the mass scale μ to retain a dimensionless coupling.

The hard part as we have presented it in Sec. 2.3 depends on the collinear components of the fermion and pseudoscalar momenta: $H^{fs} = H^{fs}(\hat{p} - \hat{l}, \hat{l})$. We can choose our coordinates such that the collinear parts of p and l coincide with their + components. Then, through the delta function $\delta(x - l^+/p^+) = p^+\delta(l^+ - xp^+)$, we introduce the new integration variable x. This is the fraction of the collinear component of the fermion momentum p taken by the collinear scalar. Since the hard part is only sensitive to the collinear components of its arguments, H^{fs} is a function of x only. Introducing x allows us to integrate over the whole range of loop momenta l while leaving the x integration undone.

The loop integral for M^{fs} can be evaluated analytically without making any simplifying assumption. However, for our purposes, it is convenient to use the frame chosen above with $p_T = 0$. The result of the integration over loop momenta l after retaining the leading term only is then

$$M^{fs}(p+q) = \frac{-gm\mu^{-\epsilon}}{(4\pi)^{2-\epsilon}}\Gamma(\epsilon)\int_0^1 dx\, x\, \bar{u}(p)\gamma_5 H^{fs}(x)\left(x^2\frac{m^2}{\mu^2} - 2x(1-x)\frac{p^+q^-}{\mu^2}\right)^{-\epsilon}, \qquad (65)$$

which is of order λ for $\epsilon = 0$, as predicted by the power counting rules of Sec. 2.2.2. The presence of the factor $\Gamma(\epsilon)$ indicates that there is an ultraviolet divergence coming from the loop integral in the definition of the jet function. Therefore, the jet function must be renormalized and thereby becomes a scale dependent quantity. However, the hard part must also be renormalized so that the factorized amplitude matches the original amplitude. This induces evolution equations for the jet functions and the hard parts, as for the treatment of bound states [62–64] and in soft collinear effective theory [18].

If we apply an on-shell renormalization scheme and subtract the $q = 0$ part of the nonradiative fs-jet in (65), we obtain at order ϵ^0

$$M^{fs}(p+q) = \frac{gm}{(4\pi)^2}\int_0^1 dx\, x\, \bar{u}(p)\gamma_5 H^{fs}(x)\log\left(1 - 2\left(\frac{1-x}{x}\right)\frac{p^+q^-}{m^2}\right), \qquad (66)$$

which exhibits the logarithmic dependence on q that we predicted in Sec. 2.1. A standard analysis following Low would treat radiative fs-jets as part of the internal emission amplitude and deduce their values by expanding (66) to linear order in q. This is inaccurate for a photon momentum in the region $q \sim \lambda^2 E$ since we then have $\frac{p^+q^-}{m^2} \sim 1$, thereby precluding an expansion of $\log\left(1 - 2\left(\frac{1-x}{x}\right)\frac{p^+q^-}{m^2}\right)$ in powers of q. We therefore confirm that we are required to include radiative fs-jets in the *external* amplitude.

Another prediction of our power counting rules is that adding a photon to the internal collinear fermion line of the nonradiative fs-jet reduces its degree of divergence by 2. We may

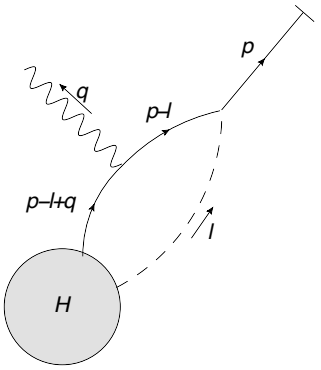

Figure 23: Lowest order radiative fs-jet.

verify this expectation by considering the radiative fs-jet shown in Fig. 23. The expression we need to calculate the radiative fs-jet function is

$$M_{ext}^{fs,\mu} = \int_0^1 dx \int \frac{d^dl}{(2\pi)^d}\, \bar{u}(p)(-ig\mu^\epsilon\gamma_5)\frac{i(\not{p}-\not{l}+m)}{(p-l)^2-m^2+i\epsilon}(-ie\mu^\epsilon\gamma^\mu)\times$$
$$\times\, \frac{i(\not{p}-\not{l}+\not{q}+m)}{(p-l+q)^2-m^2+i\epsilon}H^{fs}(x)\frac{i}{l^2+i\epsilon}p^+\delta(l^+-xp^+)\,. \tag{67}$$

This can also be evaluated analytically without making any simplifying assumption. However, we do not need to go into that amount of detail to confirm the results of power counting and will, as before, keep the fermion moving in the + direction. Retaining only the leading term yields the expression

$$M_{ext}^{fs,\mu} = -\frac{egm}{32\pi^2q^-}\int_0^1 dx\, x\, \bar{u}(p)\gamma_5\gamma^\mu\gamma^- H^{fs}(x)\, \log\left(1-2\left(\frac{1-x}{x}\right)\frac{p^+q^-}{m^2}\right)\,. \tag{68}$$

The order of the radiative fs-jet is λ^{-1} as predicted by power counting. This is qualitatively new since there are no terms of order $O(\lambda^{-1})$ in the classic form of Low's theorem. The factor of magnitude $O(\lambda^{-1})$ appears as m/q^- in our example.

We conclude our study of the lowest order fs-jet by confirming that in the fully massless case, $m = 0$, the nonradiative fs-jet is pushed back to $O(\lambda^2)$. To see this, we consider the lowest order fs-jet loop integral after the massless condition has been implemented,

$$M^{fs}(p) = \int_0^1 dx \int \frac{dl^+dl^-d^{d-2}l_T}{(2\pi)^d}\,\frac{\bar{u}(p)(-ig\mu^\epsilon\gamma_5)i(-l^+\gamma^- - l^-\gamma^+ + \gamma_T\cdot l_T)H^{fs}(x)}{l^2-2p\cdot l+i\epsilon}$$
$$\times\,\frac{i}{l^2+i\epsilon}\,p^+\delta(l^+-xp^+)\,. \tag{69}$$

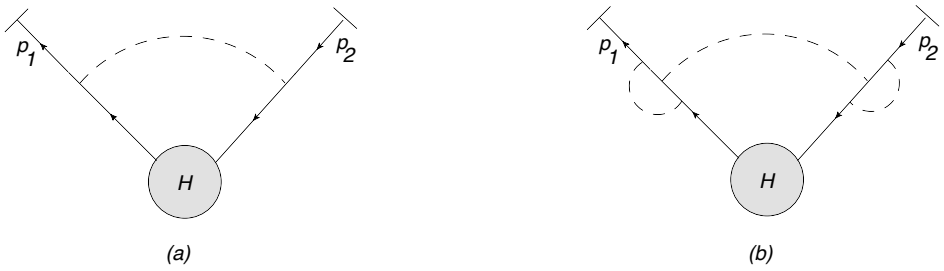

Figure 24: Diagram (a) shows the leading order (in g) case where a soft pseudoscalar connects two leading jets. This diagram is too suppressed to affect our extension of Low's theorem but diagram (b) is not.

Since $p_T = 0$, the denominator of the integrand is even in l_T and therefore the transverse term in the numerator can be ignored. Further, from the massless Dirac equation, $\bar{u}(p)\gamma^- = 0$ when $p_T = 0$, which implies that the leading term in the numerator is $O(\lambda^2)$ since $\gamma^+ l^- = O(\lambda^2)$. It is then a simple matter to finish estimating the magnitude of the integral and conclude that it is $O(\lambda^2)$. This result can be extended to arbitrary order $f\underline{s}$-jets by proving that any term in the integrand scaling as an odd power of λ must be odd under simultaneously reversing the sign of every transverse momentum integration variable.

3.1.2 One-loop jets with soft line

The next example we study belongs to the class of diagrams where two $f\underline{s}$- jets are connected by a two-point function of soft scalars such as in Fig. 18(b). In pseudoscalar theories, the leading order diagram in the Yukawa coupling g with two $f\underline{s}$-jets shown in Fig. 24(a) has degree of divergence $\gamma > 2$ and hence does not contribute to Low's theorem when a soft photon is attached to it. However, this does not extend to higher loop diagrams, as we demonstrate through this section's example.

Consider then the diagram shown in Fig. 24(b). This diagram has a single soft scalar connecting two one-loop $f\underline{s}$-jets. We consider each $f\underline{s}$-jet individually – see Fig. 25. The expression for a single $f\underline{s}$-jet is

$$J^{f\underline{s}}(p,s) = \int \frac{d^dk}{(2\pi)^d} \frac{\bar{u}(p)(-ig\mu^\epsilon\gamma_5)i(\not{p}+\not{k}+m)(-ig\mu^\epsilon\gamma_5)i(\not{p}+\not{k}+\not{s}+m)(-ig\mu^\epsilon\gamma_5)i(\not{p}+\not{s}+m)}{((p+k)^2-m^2)((p+k+s)^2-m^2)((p+s)^2-m^2)} \frac{i}{k^2}\,. \tag{70}$$

The momentum s is the connecting soft pseudoscalar momentum. The loop momentum k is the collinear pseudoscalar momentum. The leading term of this jet function in four

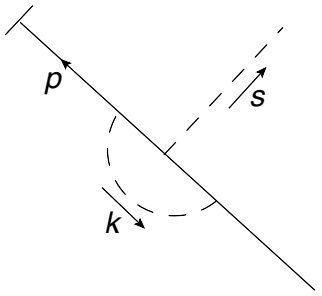

Figure 25: The momenta assignments for the one-loop jet with soft scalar emission that we are considering.

dimensions is

$$J^{f\underline{s}}(p,s) = \frac{g^3}{32\pi^2}\,\frac{m}{p\cdot s}\,\bar{u}(p)\gamma_5\left[\mathrm{Li}_2(1+2a) + \frac{2a}{1+2a}\log(-2a) - \frac{\pi^2}{6}\right]\Bigg|_{a=\frac{p\cdot s}{m^2}}, \qquad (71)$$

which is $O(\lambda^{-1})$. Returning to Fig. 24(b), the expression for the full diagram is

$$M^{f\underline{s}f\underline{s}}(p_1,p_2) = \int d^4s\,\frac{i}{s^2+i\epsilon}\,J^{f\underline{s}}(\hat{p}_1,s)\,J^{f\underline{s}}(-\hat{p}_2,-s)\otimes H(\hat{p}_1+s,-\hat{p}_2-s)\,. \qquad (72)$$

Bearing in mind that when calculating the degree of divergence, a soft loop integration measure contributes a suppression of $+8$ while a soft pseudoscalar propagator supplies an enhancement of -4, we find that the entire amplitude in (72) has degree of divergence $\gamma = 8\times1-1\times2-4\times1 = 2$. This result is the same as if we had proceeded by applying power counting rules to the diagram directly without going through an explicit calculation of the $f\underline{s}$-jet function. Consequently, attaching a soft photon to diagram 24(b) will yield a correction to the soft theorem of order $O(\lambda^0)$ possibly multiplied by nonanalytic polylogarithms. Finally, as in the case of fs-jets, the leading term of $f\underline{s}$-jets vanishes in the massless fermion limit because its integrand is odd under reflection of all transverse loop momenta.

3.2 Adapting Low's argument to the factorized amplitude

In this section, we will show a preliminary version of our extension of Low's theorem and see that to order $O(\lambda^0)$, we need only consider photon emission from the hard part corresponding to diagrams with leading jets. Photon emission from hard parts connecting to nonleading jets will also be derived for completeness. This treatment adapts Low's argument to our factorized elastic amplitude (55).

3.2.1 Preliminary form of Low's theorem

To set the stage for the appearance of our preliminary version of Low's theorem, we first represent the full radiative amplitude in the generic form

$$\begin{aligned} M_\mu = & \sum_{i=1}^{n} \left(\prod_{j\neq i} J_j^f \right) J_{i,\mu}^f \otimes H + \left(\prod_{i=1}^{n} J_i^f \right) \otimes H_\mu \\ & + \sum_{\theta\in\Theta_1} \sum_{i=1}^{n} \left[\left(\prod_{j\neq i} J_j^f \right) J_{i,\mu}^\theta \otimes H_i^\theta + \sum_{l\neq i} \left(\prod_{j\neq i,l} J_j^f \right) J_{l,\mu}^f J_i^\theta \otimes H_i^\theta \right] \\ & + \sum_{\theta\in\Theta_2} \sum_{i\neq j} \left[\left(\prod_{l\neq i,j} J_l^f \right) J_{i,\mu}^\theta J_j^\theta \, S^\theta \otimes H_{ij}^{\theta\theta} + \frac{1}{2} \sum_{h\neq i,j} \left(\prod_{l\neq i,j,h} J_l^f \right) J_i^\theta J_j^\theta J_{h,\mu}^f \, S^\theta \otimes H_{ij}^{\theta\theta} \right] \\ & + O(\lambda) \,, \end{aligned} \tag{73}$$

where $S^\theta = 1$ if $\theta = fs$ and $S^\theta = S_{ij}$ if $\theta = f\underline{s}$. The symbols Θ_1 and Θ_2 stand for the sets of labels $\{fs, f\partial s, fss, fff\}$ and $\{fs, f\underline{s}\}$ respectively. Comparing with Eq. (55), one sees that each term corresponds to a factorized form describing photon emission from a leading jet, a nonleading jet, or a hard part – as illustrated in Fig. 26. Notice, however, that we have omitted the following radiative contributions,

$$E_\mu \equiv \sum_{\theta\in\Theta_1} \sum_{i=1}^{n} \left(\prod_{j\neq i} J_j^f \right) J_i^\theta \otimes H_{i,\mu}^\theta + \frac{1}{2} \sum_{\theta\in\Theta_2} \sum_{i\neq j} \left(\prod_{l\neq i,j} J_l^f \right) J_i^\theta J_j^\theta \, S^\theta \otimes H_{ij,\mu}^{\theta\theta} \,. \tag{74}$$

These correspond to attaching a photon to the hard parts of the diagrams from Figs. 17 (b), (c), (d), and 18, all of which have $\gamma > 0$. Attaching a photon to a hard line does not modify the degree of divergence of the diagram. Therefore, the radiative contributions in (74) are of order higher than $O(\lambda^0)$ and do not need to be included in our extension of Low's theorem.

The only radiative hard part contributing at our order in λ is the one corresponding to the diagram with leading jets only. We adapt Low's analysis to this diagram by introducing new notation for the external and internal amplitudes,

$$\begin{aligned} M_{ldg}^{ext,\mu} &= \left(\prod_{j\neq i} J_j^f \right) J_i^{f,\mu} \otimes H \,, \\ M_{ldg}^{int,\mu} &= \left(\prod_{i=1}^{n} J_i^f \right) \otimes H^\mu \,. \end{aligned} \tag{75}$$

As in Sec. 1.2, these are related by the Ward identity,

$$q_\mu M_{ldg}^{ext,\mu} + q_\mu M_{ldg}^{int,\mu} = 0 \,, \tag{76}$$

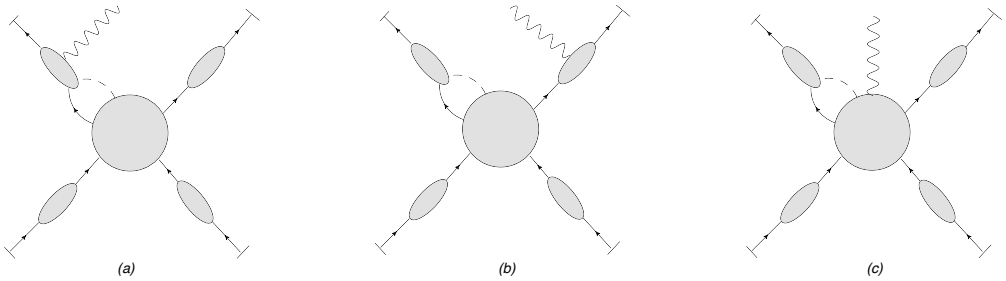

Figure 26: In applying Low's argument, the radiative amplitude diagrams are split between those with external photon emission as in (a) and (b), and those with internal photon emission as in (c).

which we can use to deduce the radiative hard part H^μ. Indeed, once the jets have been factorized as in Eqs. (73) and (74), the nonradiative and radiative hard parts can be reliably expanded in powers of q even in the regime $q \sim \lambda^2 E$. We emphasize that it is possible to expand the hard parts because the jet functions are engineered to contain all the leading and nonleading pinch surfaces of the original Feynman diagrams. All the infrared singularity structure of the radiative amplitude is contained within the jet functions. As noted above, the hard parts correspond to the matching coefficients of soft collinear effective theory [18] and are assumed to be constructible by nested subtractions similar to [55–57]. Hence, hard parts get their leading contributions from off-shell lines and are dominated by hard momenta in the factorized form. Adding a q dependence to hard lines will produce only subleading behavior. This subleading behavior can be represented by higher order terms in an expansion of the hard line propagators in q.

It is important to bear in mind that the Ward identity holds not only diagram by diagram, but also at fixed loop momenta, and therefore pinch surface by pinch surface. By this we mean that given a single reduced diagram contributing to an elastic scattering amplitude, the Ward identity will apply to this diagram by itself if we sum over all points of photon insertion [54]. The only exception arises in fermion loops where a shift of the loop momentum by the photon momentum q is required. Therefore, in (76), it is not necessary to include the contributions from all reduced diagrams at once. Rather, we can focus on each class of diagrams individually.

In the case of nonleading jets, say an fs-jet for definiteness, the internal radiative amplitude $M_{fs}^{int,\mu}$ is of order $O(\lambda)$. The external amplitude $M_{fs}^{ext,\mu}$, on the other hand, is of order $O(\lambda^{-1})$, and the Ward identity has the form

$$q^\mu M_{fs}^{ext,\mu} = -q^\mu M_{fs}^{int,\mu} \,. \tag{77}$$

A naive estimate tells us that the left hand side is $O(\lambda)$ while the right hand side is $O(\lambda^3)$.

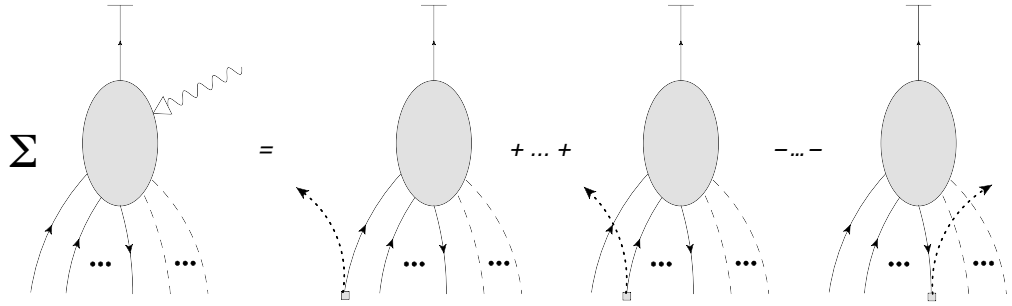

Figure 27: The general diagrammatic form of the Ward identity for jet functions. Each fermion line that does not form a closed loop has a term corresponding to the photon exiting the jet at the end of the line and a term for the photon exiting at the beginning of the line. The exception to this rule is the through going fermion line that becomes the outgoing fermion – this line only has a term with the soft photon exiting the diagram from the beginning and not at the on-shell external line. The terms with the photon exiting at the beginning of a fermion line appear in the identity with a relative + sign whereas those where the photon exits at the end of fermion line carry a − sign.

Therefore, leading terms in the external amplitudes must cancel each other in the Ward identity. In Sec. 3.2.2, we will see that this necessary cancellation also follows from charge conservation – see the discussion below (89).

If we were to try and calculate the internal radiative amplitude M^{μ}_{int} directly, we would need to delve into the construction of the hard part at each order and find all ways of inserting a soft photon, thereby making the calculation different for each process. The alternative, following Low, is to calculate the contraction of the soft momentum q with the universal external radiative amplitudes and then use the Ward identity to extract M^{μ}_{int}. However, to detemine $q_\mu M^{\mu}_{ext}$, we still need to express the quantity $q_\mu J_i^{f,\mu}$ in a form that also does not depend on the details of the radiative jet function. To this end, we introduce the jet Ward identities. In their most general form, these are expressed diagrammatically as in Fig. 27.

The jet QED Ward identity for photon emission is derived straightforwardly using diagrammatic or path integral techniques [54,69]. The special case we need involves the leading jet,

$$q_\mu J^{f,\mu}(p_i+q,q) = e_i J^f(p_i)\,. \tag{78}$$

It is then straightforward to extend Low's argument and obtain

$$H^{\mu}(\hat{p}_1,\ldots,\hat{p}_n,q) = -\sum_{l=1}^{n} e_l \frac{\partial}{\partial \hat{p}'_{l\mu}} H(\hat{p}'_1,\ldots,\hat{p}'_n) + O(\lambda^2)\,, \tag{79}$$

for the radiative hard part. The momentum arguments $\hat{p}'_i$ indicate that we have performed the construction described in Sec. 1.2 to transition to an elastic set of momenta.

With (79), we can write the preliminary form of our extension of Low's theorem to high energies. Incorporating the radiative hard part (79) into the generic radiative amplitude (73), we find

$$\begin{aligned} M_\mu = &- \left(\prod_{i=1}^{n} J_i^f\right) \otimes \sum_{l=1}^{n} e_l \frac{\partial}{\partial \hat{p}_l'^\mu} H \bigg|_{P_0} \\ &+ \sum_{i=1}^{n} \left(\prod_{j\neq i} J_j^f\right) J_{i,\mu}^f \otimes H \\ &+ \sum_{\theta\in\Theta_1} \sum_{i=1}^{n} \left[\left(\prod_{j\neq i} J_j^f\right) J_{i,\mu}^\theta \otimes H_i^\theta + \sum_{l\neq i} \left(\prod_{j\neq i,l} J_j^f\right) J_{l,\mu}^f J_i^\theta \otimes H_i^\theta\right] \\ &+ \sum_{\theta\in\Theta_2} \sum_{i\neq j} \left[\left(\prod_{l\neq i,j} J_l^f\right) J_{i,\mu}^\theta J_j^\theta \, S^\theta \otimes H_{ij}^{\theta\theta} + \frac{1}{2} \sum_{h\neq i,j} \left(\prod_{l\neq i,j,h} J_l^f\right) J_i^\theta J_j^\theta J_{h,\mu}^f \, S^\theta \otimes H_{ij}^{\theta\theta}\right] \\ &+ O(\lambda)\,. \end{aligned} \tag{80}$$

We use the P_0 symbol to denote that after the momentum derivatives have acted on the nonradiative hard part, we evaluate the resulting expression at an elastic set of momenta close to the starting radiative configuration, as described in Sec. 1.2. The first term gathers all internal emission at $O(\lambda^0)$. It is remarkable that even at this level, summing over all insertions of a soft photon into the hard part results in the action of a differential operator acting on its external momenta. On the other hand, as has been mentioned in Sec. 1.2, this formula does not yet fully clarify the structure of the radiative jet functions. In contrast to the internal emission, these are universal, and for soft q, their structure can be probed using Grammer and Yennie's KG decomposition. We will turn to this task in Sec. 3.3.

For completeness, we show next how we can adapt Low's insight to analyze the nonleading radiative amplitude E_μ in (74). This amplitude could in fact be included in a higher power treatment of Low's theorem, which would include higher order jets such as the radiative $fsss$-jet shown in Fig. 28, and also depend on the higher order subleading terms in the hard part.

3.2.2 Photon emission beyond $O(\lambda^0)$

Consider first the class of diagrams with a single fs-jet. For the diagrams in Fig. 17(b), the factorized amplitude consists in the fs-jet, the leading jets, and the hard part. As shown

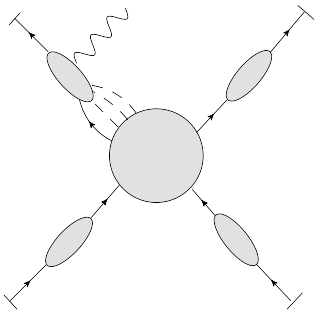

Figure 28: An example of a higher order jet required for a consistent treatment of the radiative amplitude E_μ in (74).

in Eqs. (73) and (74), a soft photon can be emitted from any of those components. The corresponding radiative amplitudes from Eqs. (73) and (74) have the expressions

$$M_{fs}^{ext:fs,\mu} = \sum_{i=1}^{n} \left(\prod_{j\neq i} J^f(p_j) \right) J^{fs,\mu}(p_i + q - \hat{k}, \hat{k}, q) \otimes H_i^{fs}(\hat{p}_1, ...; \hat{p}_i + q - \hat{k}, \hat{k}; ..., \hat{p}_n)\,, \quad (81)$$

when radiating a photon from the fs-jet, and

$$M_{fs}^{ext:f,\mu} = \sum_{i=1}^{n} \sum_{l\neq i} \left(\prod_{j\neq i,l} J^f(p_j) \right) J^{f,\mu}(p_l + q, q) J^{fs}(p_i - \hat{k}, \hat{k}) \otimes H_i^{fs}(\hat{p}_1, ..., \hat{p}_l + q, ...; \hat{p}_i - \hat{k}, \hat{k}; ..., \hat{p}_n)\,, \quad (82)$$

when radiating from a leading jet, and finally

$$M_{fs}^{int,\mu} = \sum_{i=1}^{n} \left(\prod_{j\neq i} J^f(p_j) \right) J^{fs}(p_i - \hat{k}, \hat{k}) \otimes H_i^{fs,\mu}(\hat{p}_1, ...; \hat{p}_i - \hat{k}, \hat{k}; ..., \hat{p}_n, q) \quad (83)$$

when radiating from the hard part. This factorization of photon emission is illustrated in Fig. 26.

The three radiative amplitudes we have identified are related by the Ward identity, which takes the form

$$q_\mu M_{fs}^{ext:fs,\mu} + q_\mu M_{fs}^{ext:f,\mu} + q_\mu M_{fs}^{int,\mu} = 0\,. \quad (84)$$

We recall that this Ward identity applies to each diagram represented in Fig. 26 individually and there is no need to consider all diagrams contributing to an amplitude at once.

The three special cases of the jet Ward identity from Fig. 27 that will be of use to us can be stated as follows using our notation

$$\begin{aligned}
q_\mu J^{fs,\mu}(p_i+q-\hat{k},\hat{k},q) &= e_i J^{fs}(p_i-\hat{k},\hat{k})\,,\\
q_\mu J^{fss,\mu}(p_i+q-\hat{k}_1-\hat{k}_2,\hat{k}_1,\hat{k}_2,q) &= e_i J^{fss}(p_i-\hat{k}_1-\hat{k}_2,\hat{k}_1,\hat{k}_2)\,,\\
q_\mu J^{fff,\mu}(p_i+q-\hat{k}_1-\hat{k}_2,\hat{k}_1,\hat{k}_2,q) &= e_i J^{fff}(p_i-\hat{k}_1-\hat{k}_2,\hat{k}_1,\hat{k}_2)\\
&\quad + e_i J^{fff}(p_i+q-\hat{k}_1-\hat{k}_2,\hat{k}_1-q,\hat{k}_2)\\
&\quad - e_i J^{fff}(p_i+q-\hat{k}_1-\hat{k}_2,\hat{k}_1,\hat{k}_2-q)\,, \qquad (85)
\end{aligned}$$

with e_i the charge of the i^{th} scattering fermion or antifermion. On the left hand side in each case, we choose to route the photon momentum q into the hard function via the through-going fermion line that becomes the external particle. The momenta k, k_1, and k_2 are collinear momenta that become part of a loop once the jet is attached to its corresponding hard part. These Ward identities apply whether the scalars, which are neutral, are soft or collinear.

Considering an fs-jet, the jet Ward identities allow us to expand (84) and cast it into the explicit form

$$\begin{aligned}
&\sum_{i=1}^{n}\left(\prod_{j\neq i}J^f(p_j)\right)J^{fs}(p_i-\hat{k},\hat{k})\otimes q_\mu H_i^{fs,\mu}(\hat{p}_1,...;\hat{p}_i-\hat{k},\hat{k};...,\hat{p}_n,q)\\
&\quad=-\sum_{i=1}^{n}\left(\prod_{j\neq i}J^f(p_j)\right)e_i J^{fs}(p_i-\hat{k},\hat{k})\otimes H_i^{fs}(\hat{p}_1,...;\hat{p}_i+q-\hat{k},\hat{k};...,\hat{p}_n)\\
&\quad\quad-\sum_{i=1}^{n}\sum_{l\neq i}\left(\prod_{j\neq i,l}J^f(p_j)\right)e_l J^f(p_l)J^{fs}(p_i-\hat{k},\hat{k})\otimes H_i^{fs}(\hat{p}_1,...,\hat{p}_l+q,...;\hat{p}_i-\hat{k},\hat{k};...,\hat{p}_n)\,.
\end{aligned} \qquad (86)$$

The next step is to Taylor expand the nonradiative hard parts to $O(\lambda^2)$ in order to deduce the radiative hard part $H_i^{fs,\mu}(\hat{p}_1,...;\hat{p}_i-\hat{k},\hat{k};...,\hat{p}_n,q)$ to $O(\lambda^0)$. We will suppress any consideration of the transition from the radiative kinematics to an elastic configuration such as the one we considered in detail in Sec. 1.2. Our analysis has shown that the ξ_i's of Burnett and Kroll can be constructed in general and will not affect the formula we obtain for the internal amplitude. The expansion of the hard part then, is

$$\begin{aligned}
&H_i^{fs}(\hat{p}_1,...;\hat{p}_i+q-\hat{k},\hat{k};...,\hat{p}_n)=\\
&\quad H_i^{fs}(\hat{p}_1,...;\hat{p}_i-\hat{k},\hat{k};...,\hat{p}_n)+\,q^\mu\frac{\partial}{\partial\hat{p}_i^\mu}H_i^{fs}(\hat{p}_1,...;\hat{p}_i-\hat{k},\hat{k};...,\hat{p}_n)+O(\lambda^4)\,, \qquad (87)
\end{aligned}$$

for the photon attached to the fs-jet i, and,

$$H_i^{fs}(\hat{p}_1,...,\hat{p}_l+q,...;\hat{p}_i-\hat{k},\hat{k};...,\hat{p}_n) = \\ H_i^{fs}(\hat{p}_1,...;\hat{p}_i-\hat{k},\hat{k};...,\hat{p}_n) + q^\mu \frac{\partial}{\partial \hat{p}_l^\mu} H_i^{fs}(\hat{p}_1,...,\hat{p}_l,...;\hat{p}_i-\hat{k},\hat{k};...,\hat{p}_n) + O(\lambda^4)\,, \quad (88)$$

when $l \neq i$ is a leading power jet. The derivative above acts on all the components of each $\hat{p}_i$ for $i = 1,\ldots,n$. These are treated as variables p_i^μ that the hard part depends upon for the sake of the differentiation. Once the differentiation has been performed, the vectors p_i^μ are evaluated at the collinear configurations $\hat{p}_i^\mu$ of the corresponding p_i's.

Substituting the expansions (87) and (88) into (86), we obtain

$$\sum_{i=1}^n \left(\prod_{j\neq i} J^f(p_j)\right) J^{fs}(p_i-\hat{k},\hat{k}) \otimes q_\mu H_i^{fs,\mu}(\hat{p}_1,...;\hat{p}_i-\hat{k},\hat{k};...,\hat{p}_n,q) \\ = -\sum_{i=1}^n \left(\prod_{j\neq i} J^f(p_j)\right) J^{fs}(p_i-\hat{k},\hat{k}) \\ \otimes \sum_{l=1}^n \left[e_l\, H_i^{fs}(\hat{p}_1,...;\hat{p}_i-\hat{k},\hat{k};...,\hat{p}_n) + e_l\, q^\mu \frac{\partial}{\partial \hat{p}_l^\mu} H_i^{fs}(\hat{p}_1,...;\hat{p}_i-\hat{k},\hat{k};...,\hat{p}_n)\right] \\ + O(\lambda^4)\,. \quad (89)$$

After summing over the index l, the first term in the square brackets above vanishes by charge conservation, as in the standard Low analysis. This cancellation confirms that contributions from the hard part associated with fs-jets are higher order in λ, and decouple from the use of the Ward identity for the leading jets. The natural solution to Eq. (89) for the radiative hard part is

$$H_i^{fs,\mu}(\hat{p}_1,...;\hat{p}_i-\hat{k},\hat{k};...,\hat{p}_n,q) = -\sum_{l=1}^n e_l \frac{\partial}{\partial \hat{p}_{l\mu}} H_i^{fs}(\hat{p}_1,...;\hat{p}_i-\hat{k},\hat{k};...,\hat{p}_n) + O(\lambda^2)\,. \quad (90)$$

In fact, (90) is the full solution to Eq. (89). Additional gauge invariant terms would require the radiative hard part to have enhancements in λ – see the discussion of Eq. (19). These are not allowed since any dependence of the hard part on q or m comes as a subleading correction to the hard exchanges.

Since $f\partial s$-jets correspond to higher order contributions to fs-jet amplitudes, they are treated using the same steps. Similarly, the analysis for photon emission from diagrams with a single fss-jet is virtually unchanged. We need only include two collinear scalar momenta k_1 and k_2 rather than a single one. The final result is

$$H_i^{fss,\mu}(\hat{p}_1,...;\hat{p}_i-\hat{k}_1-\hat{k}_2,\hat{k}_1,\hat{k}_2;...,\hat{p}_n,q)$$

$$= -\sum_{l=1}^{n} e_l \frac{\partial}{\partial \hat{p}_{l\mu}} H_i^{fss}(\hat{p}_1, ...; \hat{p}_i - \hat{k}_1 - \hat{k}_2, \hat{k}_1, \hat{k}_2; ..., \hat{p}_n) + O(\lambda^2)\,. \tag{91}$$

For diagrams with fff-jets, the analysis involves one additional step because the corresponding jet Ward identity has three terms as shown in Eq. (85) and Fig. 27. The momentum flow through the jets enables us to shift the collinear loop integration momenta, after which we obtain

$$\begin{aligned} H_i^{fff,\mu}(\hat{p}_1, ...; \hat{p}_1 - \hat{k}_1 - \hat{k}_2, \hat{k}_1, \hat{k}_2; ..., \hat{p}_n, q) = \\ - \sum_{l=1}^{n} e_l \frac{\partial}{\partial \hat{p}_{l\mu}} H_i^{fff}(\hat{p}_1, ...; \hat{p}_i - \hat{k}_1 - \hat{k}_2, \hat{k}_1, \hat{k}_2; ..., \hat{p}_n) \\ - e_i \frac{\partial}{\partial \hat{k}_{1\mu}} H_i^{fff}(\hat{p}_1, ...; \hat{p}_i - \hat{k}_1 - \hat{k}_2, \hat{k}_1, \hat{k}_2; ..., \hat{p}_n) \\ + e_i \frac{\partial}{\partial \hat{k}_{2\mu}} H_i^{fff}(\hat{p}_1, ...; \hat{p}_i - \hat{k}_1 - \hat{k}_2, \hat{k}_1, \hat{k}_2; ..., \hat{p}_n) + O(\lambda^2)\,. \end{aligned} \tag{92}$$

In the above, the partial derivatives $\frac{\partial}{\partial \hat{k}_{l\mu}}$ only act on the explicit dependence of H_i^{fff} on $\hat{k}_1$ and $\hat{k}_2$. That is, there is no contribution to the derivative from the implicit dependence of H_i^{fff} on $\hat{k}_1$ and $\hat{k}_2$ through $\hat{p}_i - \hat{k}_1 - \hat{k}_2$.

This concludes our description of photon emission at orders beyond $O(\lambda^0)$. In the next section, we return to Eq. (80) and analyze the external amplitude using the KG decomposition.

3.3 The KG decomposition

By making use of the jet Ward identities once again, it is possible to unravel some structure in the small q expansion of the radiative jet functions. Following del Duca [14], who drew inspiration from Grammer and Yennie [49], we consider the two tensors

$$\begin{aligned} K_{i\,\mu}{}^{\nu} &\equiv \frac{(2p_i + q)_\mu\, q^\nu}{2p_i \cdot q + q^2}\,, \\ G_{i\,\mu}{}^{\nu} &\equiv g_\mu{}^{\nu} - K_{i\,\mu}{}^{\nu}\,. \end{aligned} \tag{93}$$

We will use the K and G tensors to decompose the soft photon polarization $\epsilon^\mu(q)$ into two complementary polarizations. It will turn out that the K polarized photon emission amplitude contains all the leading $O(\lambda^{-2})$ terms while the G polarized photon amplitude supplies transverse corrections that begin at $O(\lambda^{-1})$. Note that transversality of G polarized photons, $q^\mu\, G_{i\,\mu}{}^{\nu} = 0$, follows immediately from (93).

So far, we have only been considering the stripped amplitude M_μ, that is, we have derived the photon emission amplitude with the photon polarization tensor $\epsilon^\mu(q)$ stripped away. For the purposes of applying the KG decomposition, it is useful to reintroduce this polarization tensor.

Consider first the emission of a K polarized photon. For definiteness, we will illustrate our argument using fss-jets, although the same conclusion applies to any type of jet. The relevant identity is

$$\begin{aligned}\epsilon^\mu(q) K_{i\,\mu}{}^\nu J^{fss}_{i,\nu}(p_i + q - \hat{k}_1 - \hat{k}_2, \hat{k}_1, \hat{k}_2) \otimes H^{fss}_i(\hat{p}_i + q - \hat{k}_1 - \hat{k}_2, \hat{k}_1, \hat{k}_2) \\ = e_i \, \frac{\epsilon \cdot (2p_i + q)}{2p_i \cdot q + q^2} \, J^{fss}_i(p_i - \hat{k}_1 - \hat{k}_2, \hat{k}_1, \hat{k}_2) \otimes H^{fss}_i(\hat{p}_i + q - \hat{k}_1 - \hat{k}_2, \hat{k}_1, \hat{k}_2) \,. \end{aligned} \tag{94}$$

This result follows immediately from the application of the jet Ward identity for fss-jets, as shown in (85). Since the infrared degree of divergence of a nonradiative fss-jet is $\gamma = 2$, the above formula confirms that the emission of a K polarized photon starts at $O(\lambda^0)$. The same conclusion holds when attaching the soft photon to an $f\partial s$-jet, an fff-jet, or to any jet in diagrams containing either two fs -jets or two $f\underline{s}$-jets as these all have degree of divergence $\gamma = 2$ prior to the soft photon insertion. For a diagram with a single fs-jet, the emission of a K polarized photon is $O(\lambda^{-1})$ since fs-jets have degree of divergence $\gamma = 1$ in the massive case. Finally, following the same reasoning, the emission of a K photon from a leading jet is $O(\lambda^{-2})$. Therefore, the K polarization tensor does contain a leading order term, which is derived purely from the application of the jet Ward identity. The question is then whether a leading term also appears in the complimentary polarization.

A G polarized photon is connected to the radiative jet function through the insertion of a field strength tensor operator,

$$\epsilon^\mu(q) \, G_{i\,\mu}{}^\nu = \frac{(2p_i + q)_\mu}{2p_i \cdot q + q^2} F^{\mu\nu}(q, \epsilon) \,, \tag{95}$$

where $F^{\mu\nu}(q, \epsilon) = q^\mu \epsilon^\nu(q) - q^\nu \epsilon^\mu(q)$. An important property of the G polarization tensor following from this form is that it annihilates the scalar photon vertex,

$$\epsilon^\mu(q) \, G_{i\,\mu}{}^\nu (2p_i + q)_\nu = 0 \,. \tag{96}$$

In particular, this implies that $\epsilon^\mu(q) \, G_{i\,\mu}{}^\nu p_{i\nu} = O(q)$. An analysis of the general loop integrand for jet functions shows that their leading term is always proportional to $p_{i\nu}$, where p_i is the external momentum of the jet. The first subleading term is suppressed by at least one power of λ in the massive fermion case. Since contracting $p_{i\nu}$ with the G polarization tensor yields a suppression of λ^2, we find that the emission of a G polarized photon is suppressed by at least one power of λ relative to the corresponding K polarized emission [14].

Using the techniques of Sec. 2.2.2, we found that attaching a soft photon to a nonradiative diagram with an $f\partial s$, fss, or fff-jet, as well as to a diagram with two nonradiative fs or $f\underline{s}$-jets makes the diagram at most logarithmic in q. Hence, emission of a G photon starts at $O(\lambda)$ when attaching a soft photon to any of those diagrams, which is beyond the order of accurary of our extension of Low's theorem to high energies. When a diagram only has a single fs-jet, the emission of a G photon will start at $O(\lambda^0)$. Finally, for leading jets, G photon emission begins at $O(\lambda^{-1})$ when considering massive fermions.

We mention that using an on-shell renormalization scheme further simplifies external emission amplitudes. It is straightforward to verify that in the tree level radiative leading jet, G photon emission starts at $O(\lambda^0)$, and the leading $O(\lambda^{-2})$ term is entirely contained within the K photon emission amplitude. By definition, an on-shell scheme eliminates the $q \to 0$ limit of the radiative loop diagrams. Consequently, all leading $O(\lambda^{-2})$ behavior is contained in the tree level diagram and fully accounted for by K photon emission. Further, G photon emission begins at $O(\lambda^0)$ in this scheme.

We now have all the required pieces to apply the KG decomposition to all external radiative terms in (80) and thereby complete the derivation of the final form of our extension of Low's theorem. It is useful to separate the soft photon amplitude into three contributions: the internal emission amplitude, the external emission amplitude for K polarized photons, and the external emission amplitude for G polarized photons,

$$\epsilon \cdot M = \epsilon \cdot M_{int} + \epsilon \cdot M^K_{ext} + \epsilon \cdot M^G_{ext} \,. \tag{97}$$

The internal emission amplitude simply follows from contracting the photon polarization tensor with the first term in (80),

$$\epsilon \cdot M_{int} = -\left(\prod_{i=1}^{n} J_i^f\right) \otimes \sum_{l=1}^{n} e_l \, \epsilon^\mu \frac{\partial}{\partial \hat{p}_l'^\mu} H \bigg|_{P_0} + O(\lambda) \,, \tag{98}$$

where as above, P_0 indicates that we are evaluating the derivative at a set of momenta constructed from the procedure described in Sec. 1.2.

The KG decomposition allows us to extract the leading $O(\lambda^{-2})$ term from the radiative jet functions. This leading term is contained within the complete K polarized emission amplitude, which is

$$\begin{aligned} \epsilon \cdot M^K_{ext} = &\sum_{i=1}^{n} \left(\prod_{j=1}^{n} J_j^f\right) \otimes e_i \frac{\epsilon \cdot (2p_i + q)}{2p_i \cdot q + q^2} \, H(\hat{p}_i + q) \\ &+ \sum_{i=1}^{n} \sum_{\theta \in \Theta_1} \left(\prod_{j \neq i} J_j^f\right) J_i^\theta \otimes \sum_{h=1}^{n} e_h \frac{\epsilon \cdot (2p_h + q)}{2p_h \cdot q + q^2} \, H_i^\theta(\hat{p}_h + q) \end{aligned}$$

$$+\frac{1}{2}\sum_{i\neq j}\sum_{\theta\in\Theta_2}\left(\prod_{l\neq i,j}J_l^f\right)J_i^\theta J_j^\theta S^\theta\otimes\sum_{h=1}^n e_h\frac{\epsilon\cdot(2p_h+q)}{2p_h\cdot q+q^2}\,H_{ij}^{\theta\theta}(\hat{p}_h+q)$$
$$+O(\lambda)\,, \tag{99}$$

where again $\Theta_1=\{fs,\,f\partial s,\,fss,\,fff\}$ and $\Theta_2=\{fs,\,f\underline{s}\}$, and $S^\theta=1$ if $\theta=fs$ and $S^\theta=S$ if $\theta=f\underline{s}$. In each term, the soft photon polarization is coupled to a tree level leading factor reminiscent of early treatments of the soft theorem [1–3]. We have indicated which argument of the hard parts is shifted by q. One could extend the construction of the ξ_i's and η_i's of Sec. 1.2 and expand the hard parts. However, corrections of order $O(\lambda^2)$ would only be required for the hard part corresponding to the leading jets, $H(\dots,\hat{p}_i+q,\dots)$.

Corrections to the soft theorem also appear as separately transverse emission amplitudes which couple to a tree level leading order factor through the field strength tensor in momentum space. These are always suppressed by at least one power of λ relative to the corresponding K polarized photon emission amplitude. Therefore, at our order in λ, only leading and fs-jets are relevant for these corrections, which are given by

$$\begin{aligned}\epsilon\cdot M_{ext}^G=&\sum_{i=1}^n\sum_{l\neq i}\left(\prod_{j\neq i,l}J_j^f\right)\frac{(2p_l+q)_\mu}{2p_l\cdot q+q^2}F^{\mu\nu}(q,\epsilon)\,J_{l,\nu}^f J_i^{fs}\otimes H_i^{fs}(\hat{p}_l+q)\\&+\sum_{i=1}^n\left(\prod_{j\neq i}J_j^f\right)\frac{(2p_i+q)_\mu}{2p_i\cdot q+q^2}F^{\mu\nu}(q,\epsilon)\left(J_{i,\nu}^f+J_{i,\nu}^{fs}\right)\otimes H_i^{fs}(\hat{p}_i+q)\\&+O(\lambda)\,.\end{aligned} \tag{100}$$

Equations (97)-(100) taken together make up our final version of Low's theorem.

4 Loop Corrections to the Soft Graviton Theorem

In this Chapter, we use the gravitational Ward identity [9] to derive an extension of the soft graviton theorem at high energies that incorporates loop corrections to arbitrary order in Yukawa and scalar theory. Just like for photons, we build the radiative amplitude by considering all points of insertion of the soft graviton into an elastic amplitude diagram. Our starting point is the expansion of the elastic amplitude into factorized contributions of order going up to $O(\lambda^4)$. Because the graviton polarization tensor has two spacetime indices, we will find that the deduction of the radiative hard part from the external amplitude is more involved. We will also, as in Sec. 1.2, provide a careful treatment of the transition between radiative and elastic external kinematics.

Before delving into the proof of our soft graviton theorem, however, we take the time to derive the gravitational off-shell Ward identity, which is analogous to the off-shell Ward identity shown in Fig. 27 for photons, and will be an important tool in our proof.

4.1 Diagrammatic derivation of the off-shell gravitational Ward identity in scalar and Yukawa theory

Diagrammatically, the off-shell Ward identity can be expressed as in Fig. 29 [70–73]. The box vertices represent the emission of a "ghost" graviton – see Fig. 30. Their corresponding expressions are given by

$$\begin{aligned} W_{fG}^{\nu} &= \frac{\kappa}{2}\left(p^{\nu} - \frac{1}{2}q_{\mu}\sigma^{\mu\nu}\right), \\ W_{sG}^{\nu} &= \frac{\kappa}{2}p^{\nu}, \end{aligned} \tag{101}$$

where $\sigma_{\mu\nu} = \frac{1}{4}[\gamma_{\mu}, \gamma_{\nu}]$. The vertex W_{fG} acts on the left of a string of fermion propagators if the fermion arrows point towards the box in the corresponding diagram. Conversely, W_{fG} will act to the right of a string of fermionic propagators if the fermion arrow points away from the box in the diagram.

We give a sketch of how the off-shell Ward identity is derived diagrammatically. This proof clearly shows why the Ward identity holds at fixed loop momenta. The key identity we use is the simplest example of the Feynman identity,

$$\begin{aligned} q_{\mu}V_{ffG}^{\mu\nu} = \left(\frac{i\kappa}{4}\right)\Bigg(&\frac{1}{2}\gamma^{\nu}(p^2 - (p+q)^2) \\ &+ \frac{1}{2}p^{\nu}((1-A)(\not{p} - m) - (1+A)(\not{p} + \not{q} - m)) \end{aligned}$$

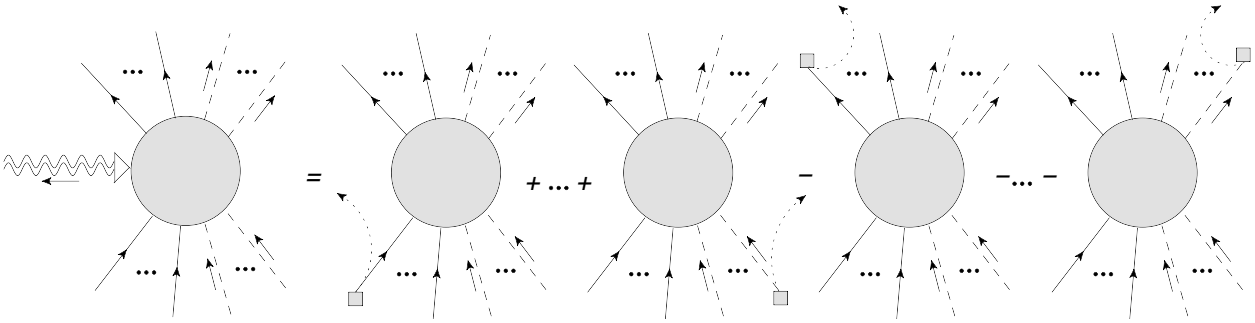

Figure 29: The general off-shell gravitational Ward identity. This identity holds regardless of whether the external particles are collinear, hard, or soft.

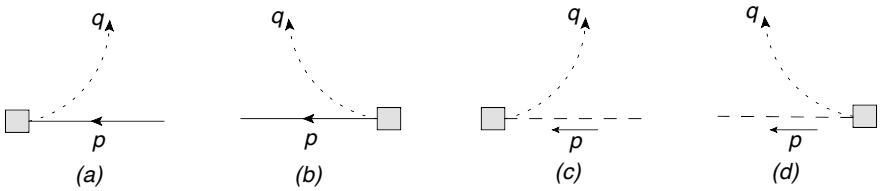

Figure 30: The box vertices represent the emission of a ghost graviton after the graviton momentum q is contracted with the radiative amplitude. Vertices (a) and (b) are denoted W^{μ}_{fG} and have the same expression. In (a), W_{fG} acts to the left of the fermion propagators, whereas in (b), W_{fG} acts on the right. Likewise, vertices (c) and (d) also have the same value, and are both denoted W^{μ}_{sG}.

$$+\frac{1}{2}(p+q)^{\nu}((1+A)(\not{p}-m)-(1-A)(\not{p}+\not{q}-m))\Big)\,, \tag{102}$$

for a fermion emitting a graviton, and

$$q_{\mu}V^{\mu\nu}_{ssG}=\left(\frac{i\kappa}{2}\right)\left((p+q)^{\nu}p^2-p^{\nu}(p+q)^2\right)\,, \tag{103}$$

for a scalar emitting a graviton. The incoming fermion/scalar momentum is taken to be $p+q$ while the outgoing momentum is p – in Fig. 20, this corresponds to making the replacements $p\mapsto p+q$ and $p'\mapsto p$. The parameter A can take the value 1 if we normalize our Lagrangian with the square root of the determinant of the vierbein field $\sqrt{e}$, or 2 if we opt for $\sqrt{g}$, where g is the determinant of the metric. The change in the normalization of the Lagrangian is compensated by a change in the normalization of the fermion field [67, 68].

To illustrate how these identities are used to prove the off-shell Ward identity, we evaluate

the four amplitudes shown in Fig. 31. Note that the ends of the external particle lines are not reduced.

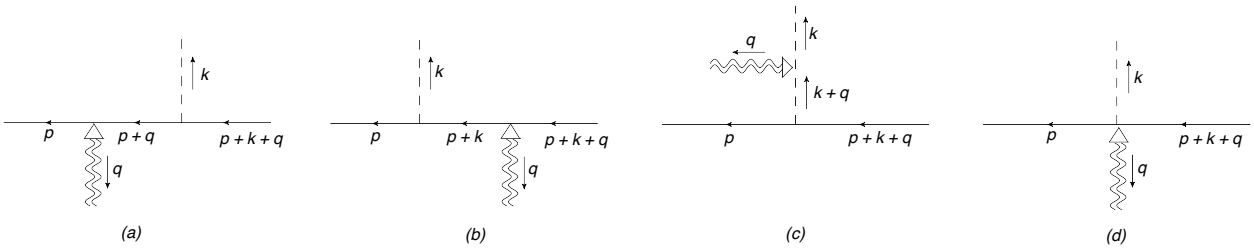

Figure 31: The amplitudes in (a), (b), (c), and (d) will be denoted by $q_\mu M_a^{\mu\nu}$, $q_\mu M_b^{\mu\nu}$, $q_\mu M_c^{\mu\nu}$ and $q_\mu M_d^{\mu\nu}$, respectively.

The amplitudes appearing in Fig. 31 have the expressions,

$$\begin{aligned} q_\mu M_a^{\mu\nu} =& \frac{i}{\not p - m} \\ & \times \left(\frac{i\kappa}{4}\right) \left(\frac{1}{2}\gamma^\nu (p^2 - (p+q)^2) \right. \\ & + \frac{1}{2} p^\nu ((1-A)(\not p - m) - (1+A)(\not p + \not q - m)) \\ & \left. + \frac{1}{2}(p+q)^\nu ((1+A)(\not p - m) - (1-A)(\not p + \not q - m)) \right) \\ & \times \frac{i}{\not p + \not q - m} (-ig) \frac{i}{k^2} \frac{i}{\not p + \not k + \not q - m}\,, \end{aligned} \tag{104}$$

$$\begin{aligned} q_\mu M_b^{\mu\nu} =& \frac{i}{\not p - m} (-ig) \frac{i}{k^2} \frac{i}{\not p + \not k - m} \\ & \times \left(\frac{i\kappa}{4}\right) \left(\frac{1}{2}\gamma^\nu ((p+k)^2 - (p+k+q)^2) \right. \\ & + \frac{1}{2}(p+k)^\nu ((1-A)(\not p + \not k - m) - (1+A)(\not p + \not k + \not q - m)) \\ & \left. + \frac{1}{2}(p+k+q)^\nu ((1+A)(\not p + \not k - m) - (1-A)(\not p + \not k + \not q - m)) \right) \\ & \times \frac{i}{\not p + \not k + \not q - m}\,, \end{aligned} \tag{105}$$

$$q_\mu M_c^{\mu\nu} = \frac{i}{\not p - m}(-ig)\frac{i}{k^2}\left(\frac{i\kappa}{2}\right)\left((k+q)^\nu k^2 - k^\nu (k+q)^2\right)\frac{i}{(k+q)^2}\frac{i}{\not p + \not k + \not q - m}\,, \tag{106}$$

and

$$q_\mu M_d^{\mu\nu} = \frac{i}{\not p - m}\left(\frac{-ig\kappa}{4}\right) A q^\nu \frac{i}{\not p + \not k + \not q - m}\frac{i}{k^2}\,. \tag{107}$$

Summing $q_\mu M_a^{\mu\nu}$, $q_\mu M_b^{\mu\nu}$, $q_\mu M_c^{\mu\nu}$, and $q_\mu M_d^{\mu\nu}$, and performing some routine algebra, we obtain

$$\begin{aligned}
\sum_{\theta=a,b,c,d} q_\mu M_\theta^{\mu\nu} = \\
&\left(\frac{g\kappa}{4}\right)\left(\frac{1}{2}((\not p + m)\gamma^\nu + \gamma^\nu(\not p + \not q - m))\frac{1}{k^2}\frac{1}{\not p + \not q - m}\frac{1}{\not p + \not k + \not q - m}\right. \\
&\qquad \left. + (p + \frac{1}{2}(1+A)q)^\nu \frac{1}{k^2}\frac{1}{\not p + \not q - m}\frac{1}{\not p + \not k + \not q - m}\right) \\
&-\left(\frac{g\kappa}{4}\right)\left(\frac{1}{2}\frac{1}{\not p - m}\frac{1}{\not p + \not k - m}\frac{1}{k^2}(\gamma^\nu(\not p + \not k + \not q + m) + (\not p + \not k - m)\gamma^\nu)\right. \\
&\qquad \left. + (p + k + \frac{1}{2}(1-A)q)^\nu)\frac{1}{\not p - m}\frac{1}{\not p + \not k - m}\frac{1}{k^2}\right) \\
&+\left(\frac{g\kappa}{2}\right)\frac{1}{\not p - m}\frac{1}{\not p + \not k + \not q - m}\frac{(k+q)^\nu}{(k+q)^2}\,.
\end{aligned} \tag{108}$$

Using the relation

$$(\not p + m)\gamma^\nu + \gamma^\nu(\not p + \not q - m) = (2p+q)^\nu + \frac{1}{2}[\gamma^\nu, \not q]\,, \tag{109}$$

and defining $\sigma^{\mu\nu} \equiv \frac{1}{4}[\gamma^\mu, \gamma^\nu]$, we find

$$\begin{aligned}
\sum_{\theta=a,b,c,d} q_\mu M_\theta^{\mu\nu} = &\left(\frac{\kappa}{2}\right)\frac{i}{\not p - m}(-ig)\frac{i}{\not p + \not k - m}\frac{i}{k^2}\left((p+k)^\nu - \frac{1}{2}q_\mu\sigma^{\mu\nu}\right) \\
&-\left(\frac{\kappa}{2}\right)\left((p+q)^\nu - \frac{1}{2}q_\mu\sigma^{\mu\nu}\right)\frac{i}{\not p + \not q - m}(-ig)\frac{i}{\not p + \not k + \not q - m}\frac{i}{k^2} \\
&-\left(\frac{\kappa}{2}\right)\frac{i}{\not p - m}(-ig)\frac{i}{\not p + \not k + \not q - m}\frac{i}{(k+q)^2}(k+q)^\nu\,,
\end{aligned} \tag{110}$$

where we have set $A = 2$. This is exactly the result we expect from the off-shell Ward identity.

To extend our approach to all diagrams, including those with arbitrarily many loops, we need to apply (102) successively to adjacent graviton insertions along a fermion line. The resulting cancellations along each fermion line will give us two terms, one with a + sign and an operator W_{fG} acting to the right of the corresponding series of fermion propagators, and one with a − sign and a W_{fG} operator acting to the left of the corresponding series of fermion propagators. If we need to capture nested cancellations along a fermion loop, a shift in loop momentum by q is required. The treatment of scalars is entirely analogous. This diagrammatic argument shows that the Ward identity holds separately for each pinch surface, since we are working at fixed loop momenta, except in the occurrence of a fermion or scalar loop. Note that a shift of the loop momentum by $O(q)$ does not mix collinear and soft loop momenta.

4.2 Adapting Low's analysis to factorized amplitudes

Our goal is to extend Low's analysis to gravity for a factorized amplitude. Since the pinch surfaces of the radiative amplitude are in correspondence with the reduced diagrams of the elastic amplitude, it will be enough to show how this is done by considering the reduced diagram with n external leading jets. The extension of Low's analysis to diagrams containing nonleading jets involves repeated use of the off-shell Ward identity discussed in Sec. 4.1, and follows the lines of the argument we are about to present.

As in our treatment of Low's theorem in Sec. 1.2, we emphasize the necessity of using the construction of Burnett and Kroll [2] to transition between the radiative and elastic kinematics. This point has mostly been overlooked in the litterature on the soft graviton theorem [12]. Recall that the issue resides in the expansion of the elastic amplitude in powers of q,

$$\mathcal{M}_{el}(p_1,\dots,p_i+q,\dots,p_n) = \\ \mathcal{M}_{el}(p_1,\dots,p_n) + q^\alpha \frac{\partial \mathcal{M}_{el}}{\partial p_i^\alpha}(p_1,\dots,p_n) + \frac{1}{2} q^\alpha q^\beta \frac{\partial^2 \mathcal{M}_{el}}{\partial p_i^\alpha \partial p_i^\beta}(p_1,\dots,p_n) + O(q^3)\,. \tag{111}$$

The momenta $p_1,\dots,p_n$ satisfy momentum conservation in the form

$$p_1 + \cdots + p_n = -q\,, \tag{112}$$

assuming all external momenta are outgoing. The elastic amplitude $\mathcal{M}_{el}$ in (111), however, is defined on the locus of momenta $p_1',\dots,p_n'$ satisfying the constraint

$$p_1' + \cdots + p_n' = 0\,. \tag{113}$$

It thus appears that (111) is ill defined. The solution, following [2, 12], is to define a set of elastic momenta $p'_1, \ldots, p'_n$ that are shifted from the radiative configuration $p_1, \ldots, p_n$ by deviation vectors $\xi_i(q)$ according to

$$p_i = p'_i + \xi_i \text{ for } i = 1, \ldots, n\,. \tag{114}$$

Momentum conservation imposes the requirement that

$$\sum_{i=1}^{n} \xi_i = -q\,. \tag{115}$$

Additionally, we demand that $\xi_i(q) = O(q)$ for all $i = 1, \ldots, n$ and that the p'_i be on-shell. In Sec. 1.2, we show explicitly how to construct the ξ_i's to $O(q)$. The extension of this construction to $O(q^2)$ is straightforward.

The crux of Low's argument is the use of the on-shell gravitational Ward identity [9],

$$q^\mu \mathcal{M}_{\mu\nu} = q^\mu(\mathcal{M}^{ext}_{\mu\nu} + \mathcal{M}^{int}_{\mu\nu}) = 0\,, \tag{116}$$

to relate the external emission amplitude to the internal amplitude. In the context of factorized diagrams, the external amplitude is defined as the amplitude to emit a graviton from a jet, whether leading or nonleading. The internal emission, on the other hand, consists in the amplitude to emit the graviton from the hard part, or the soft cloud, if it is present in the diagram at hand. It is important to bear in mind that the Ward identity holds separately for each reduced diagram – see Sec. 4.1. This property of the Ward identity ensures that it is legitimate to consider individually each of the factorized amplitudes identified in Sec. 2.3.

We will also use the off-shell Ward identity for jet functions that we derived in Sec. 4.1. The result is spin-dependent in the external line, and is given for leading jets by [70–73]

$$\begin{aligned} q^\mu J^s_{\mu\nu}(p_i, q) &= J^s(p_i)\, p_{i,\nu} && \text{for scalars, and} \\ q^\mu J^f_{\mu\nu}(p_i, q) &= J^f(p_i)\, \left(p_{i,\nu} - \frac{1}{2} q^\mu \sigma^{(i)}_{\mu\nu}\right) && \text{for fermions,} \end{aligned} \tag{117}$$

where the spinor indices of the matrix $\sigma^{(i)}_{\mu\nu} = \frac{1}{4}[\gamma_\mu, \gamma_\nu]$ are summed with those of the i^{th} jet function $J^f(p_i)$ and the corresponding indices in the hard part. This form is valid for the case of an outgoing graviton and requires an overall minus sign for an incoming graviton.

We begin with the case of external scalars. In the case of diagrams with leading jets only, the basic factorization we use as a starting point is

$$\mathcal{M}_{el} = \left(\prod_{i=1}^{n} J^s(p_i)\right) \otimes H(p_1, \ldots, p_n)\,,$$

$$\mathcal{M}^{\mu\nu}_{ext} = \sum_{i=1}^{n} \left(\prod_{j\neq i} J^s(p_j) \right) J^{s,\mu\nu}(p_i, q) \otimes H(p_1, \ldots, p_i + q, \ldots, p_n) \,,$$
$$\mathcal{M}^{\mu\nu}_{int} = \left(\prod_{i=1}^{n} J^s(p_i) \right) \otimes H^{\mu\nu}(p_1, \ldots, p_n, q) \,. \tag{118}$$

This factorization is illustrated in Fig. 32. Since both $H(p_1 \ldots p_i + q \ldots p_n)$ and $H_{\mu\nu}(p_1 \ldots p_n, q)$ are fully infrared finite, we can safely expand them in powers of q at fixed values of the p_i, so long as the internal lines are off-shell by a scale set by the invariants formed by the $p_i \cdot p_j$, $i \neq j$, and all loop integrals converge independently of q. We recall that this condition fails in the external jet subdiagrams in general, where, when loop momenta become collinear to p_i, we cannot expand around $q^\mu = 0$. Once the jets are factored, however, the remaining hard subdiagrams can be expanded in powers of q since the soft graviton insertion will not alter the power behavior of their loop integrals – see the discussion in Sec. 2.4.

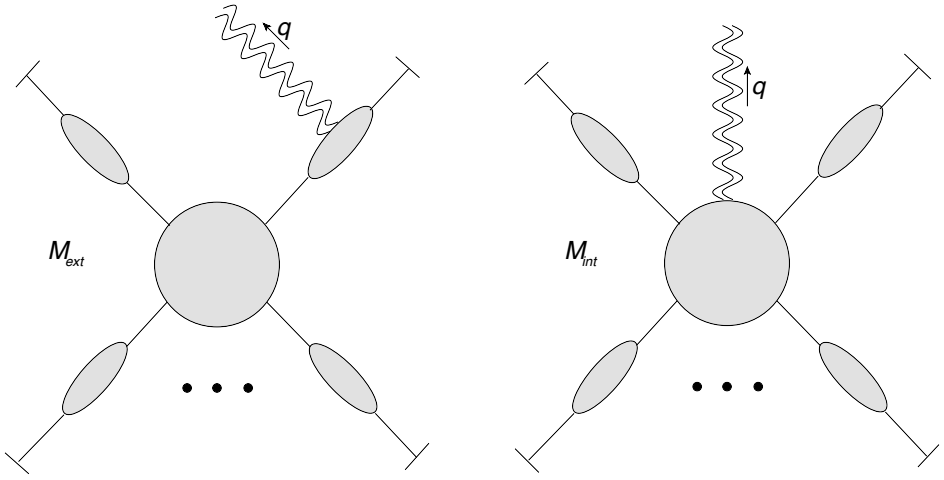

Figure 32: The radiated graviton can be emitted either from an outgoing jet or the internal hard function.

The objective is to solve the two constraints $q_\mu \mathcal{M}^{\mu\nu}_{int} = -q_\mu \mathcal{M}^{\mu\nu}_{ext}$ and $q_\nu \mathcal{M}^{\mu\nu}_{int} = -q_\nu \mathcal{M}^{\mu\nu}_{ext}$ for the radiative hard part $H^{\mu\nu}$. Our approach is motivated by the elementary methods for solving linear equations. Namely, we first find a particular solution $H^{\mu\nu}$ that solves both constraints simultaneously. This will be done by solving one constraint and demanding that $H^{\mu\nu}$ be symmetric. Any other simultaneous solution to the two constraints must differ from $H^{\mu\nu}$ by a gauge invariant quantity $B^{\mu\nu}$ obeying $q_\mu B^{\mu\nu} = 0$ and $q_\nu B^{\mu\nu} = 0$. We will then show that, under the condition that the hard part may not contain any singularity in q, such a $B^{\mu\nu}$ must vanish to $O(q)$.

We now write out each term in the Ward identity (116) explicitly using (117),

$$
\begin{aligned}
q_\mu \mathcal{M}^{\mu\nu}_{ext} &= \left(\prod_{j=1}^{n} J^s(p_j)\right) \otimes \sum_{i=1}^{n} p_i^\nu H(p_1, \ldots, p_i + q, \ldots, p_n)\,, \\
q_\mu \mathcal{M}^{\mu\nu}_{int} &= \left(\prod_{j=1}^{n} J^s(p_j)\right) \otimes q_\mu H^{\mu\nu}(p_1, \ldots, p_n, q)\,,
\end{aligned} \tag{119}
$$

and see that

$$
q_\mu H^{\mu\nu}(p_1, \ldots, p_n, q) = -\sum_{i=1}^{n} p_i^\nu H(p_1, \ldots, p_i + q, \ldots, p_n)\,, \tag{120}
$$

with H the hard function of the elastic amplitude as in (118).

Next, we may proceed with the expansion about the elastic configuration following (114) and (115). Consequently, the hard part is no longer expanded only in q, but also in the ξ_i's,

$$
\begin{aligned}
H(p_1, \ldots, p_i + q, \ldots, p_n) &= H(p_1' + \xi_1, \ldots, p_i' + \xi_i + q, \ldots, p_n' + \xi_n) \\
&= H(p_1', \ldots, p_n') + q^\rho \frac{\partial H}{\partial p_i'^\rho} + \sum_{j=1}^{n} \xi_j^\rho \frac{\partial H}{\partial p_j'^\rho} \\
&\quad + \frac{1}{2} q^\rho q^\sigma \frac{\partial^2 H}{\partial p_i'^\rho \partial p_i'^\sigma} + \sum_{j=1}^{n} q^\rho \xi_j^\sigma \frac{\partial^2 H}{\partial p_i'^\rho \partial p_j'^\sigma} + \frac{1}{2} \sum_{j,l=1}^{n} \xi_j^\rho \xi_l^\sigma \frac{\partial^2 H}{\partial p_j'^\rho \partial p_l'^\sigma}\,.
\end{aligned} \tag{121}
$$

Substituting this into (120), we find

$$
\begin{aligned}
q_\mu H^{\mu\nu}(p_1, \ldots, p_n, q) = q^\nu &\left(H + \sum_{j=1}^{n} \xi_j \cdot \frac{\partial H}{\partial p_j'}\right) \\
&- \sum_{i=1}^{n} \left(p_i'^\nu q \cdot \frac{\partial H}{\partial p_i'}\right) \\
&- \sum_{i=1}^{n} \left(\xi_i^\nu q \cdot \frac{\partial H}{\partial p_i'} + \frac{1}{2} p_i'^\nu (qq) \cdot \frac{\partial^2 H}{\partial p_i' \partial p_i'} + \sum_{j=1}^{n} p_i'^\nu (q\xi_j) \cdot \frac{\partial^2 H}{\partial p_i' \partial p_j'}\right)\,,
\end{aligned} \tag{122}
$$

where we have used the kinematics relations (113) to (115). The "$\cdot$" notation stands for a contraction between matching Minkowski indices, with the understanding that q is always

contracted with $\frac{\partial}{\partial p_i}$ and ξ_j is always paired with $\frac{\partial}{\partial p_j}$. For example, $(q\xi_j)\cdot\frac{\partial H}{\partial p_i \partial p_j} = q^\alpha \xi_j^\beta \cdot \frac{\partial H}{\partial p_i^\alpha \partial p_j^\beta}$. Factoring out q_μ from (122), we obtain a solution to the Ward identity (122),

$$\begin{aligned}\tilde{H}^{\mu\nu} = \eta^{\mu\nu} &\left(H + \sum_{j=1}^{n} \xi_j \cdot \frac{\partial H}{\partial p'_j} \right) \\ &- \sum_{i=1}^{n} \left(p_i'^{\nu} \frac{\partial H}{\partial p'_{i\mu}} \right) \\ &- \sum_{i=1}^{n} \left(\xi_i^\nu \frac{\partial H}{\partial p'_{i\mu}} + \frac{1}{2} p_i'^{\nu} q \cdot \frac{\partial^2 H}{\partial p'_{i\mu} \partial p'_i} + \sum_{j=1}^{n} p_i'^{\nu} \xi_j \cdot \frac{\partial^2 H}{\partial p'_{i\mu} \partial p'_j} \right) . \end{aligned} \tag{123}$$

It is not yet clear, however, whether $\tilde{H}^{\mu\nu}$ gives the full radiative hard part. We could, for instance, be missing a separately gauge invariant contribution. Further, we require the radiative hard part to be symmetric under interchange of μ and ν, which is not immediately obvious from (123). We will return to the issue of separately gauge invariant contributions below and focus on the question of symmetry first.

For scalars, angular momentum conservation implies

$$\sum_{i=1}^{n} \mathcal{J}_{i,\alpha\beta} H = \sum_{i=1}^{n} \left(p'_{i\alpha} \frac{\partial}{\partial p_i'^{\beta}} - p'_{i\beta} \frac{\partial}{\partial p_i'^{\alpha}} \right) H = 0 \,, \tag{124}$$

so that the second term in (123) is actually symmetric under interchange of μ and ν. The operator $\mathcal{J}_i$ is the angular momentum operator from (23). The clearest symmetrization of the ξ_i-independent $O(q)$ term is

$$\frac{1}{2} p_i'^{\nu} q \cdot \frac{\partial^2 H}{\partial p'_{i\mu} \partial p'_i} + \frac{1}{2} p_i'^{\mu} q \cdot \frac{\partial^2 H}{\partial p'_{i\nu} \partial p'_i} - \frac{1}{2} p'_i \cdot q \frac{\partial^2 H}{\partial p'_{i\mu} \partial p'_{i\nu}} \,, \tag{125}$$

where, when contracting with q^μ, the second and third terms cancel and, hence, we recover (122). We reiterate that we are enforcing the symmetry of $H^{\mu\nu}$ in order to construct a particular simultaneous solution to both $q_\mu \mathcal{M}^{\mu\nu}_{int} = -q_\mu \mathcal{M}^{\mu\nu}_{ext}$ and $q_\nu \mathcal{M}^{\mu\nu}_{int} = -q_\nu \mathcal{M}^{\mu\nu}_{ext}$. The uniqueness of this solution will be shown at the end of this subsection. This leaves us with the $O(\lambda^2)$ ξ_i-dependent terms,

$$-\sum_{i=1}^{n} \left(\xi_i^\nu \frac{\partial H}{\partial p'_{i\mu}} + \sum_{j=1}^{n} p_i'^{\nu} \xi_j \cdot \frac{\partial^2 H}{\partial p'_{i\mu} \partial p'_j} \right) = -\sum_{j=1}^{n} \xi_j \cdot \frac{\partial}{\partial p'_j} \left(\sum_{i=1}^{n} p_i'^{\nu} \frac{\partial H}{\partial p'_{i\mu}} \right) , \tag{126}$$

which can also be symmetrized using Eq. (124).

In summary, we find that the extension of the soft graviton theorem including the ξ_i's of Burnett and Kroll is

$$H^{\mu\nu} = \eta^{\mu\nu}\left(H + \sum_{j=1}^{n} \xi_j \cdot \frac{\partial H}{\partial p'_j}\right) - \sum_{i=1}^{n}\left(p_i'^{\nu}\frac{\partial H}{\partial p'_{i\mu}}\right) \\ - \sum_{i=1}^{n}\left[\frac{1}{2}k_i'^{\nu} q\cdot\frac{\partial^2 H}{\partial p'_{i\mu}\partial p'_i} + \frac{1}{2}p_i'^{\mu} q\cdot\frac{\partial^2 H}{\partial p'_{i\nu}\partial p'_i} - \frac{1}{2}p'_i\cdot q\frac{\partial^2 H}{\partial p'_{i\mu}\partial p'_{i\nu}} + \sum_{j=1}^{n}\xi_j\cdot\frac{\partial}{\partial p'_j}\left(\sum_{i=1}^{n} p_i'^{\nu}\frac{\partial H}{\partial p'_{i\mu}}\right)\right], \tag{127}$$

where, again, (124) ensures the symmetry in μ and ν.

In the case of fermions, the relevant jet Ward identity is given in (117),

$$q_\mu J^{f,\mu\nu}(p_i, q) = J^f(p_i)\left(p_i^\nu - \frac{1}{2}q_\mu\sigma_i^{\mu\nu}\right). \tag{128}$$

Applying this Ward identity to the factorized form of the radiative amplitude with leading fermionic jets only, we find that compared with the scalar case, the radiative hard part contracted with q_μ has only the following additional terms,

$$q_\mu \Delta H^{\mu\nu}_{fer} = \sum_{i=1}^{n}\frac{1}{2}q_\mu\sigma_i^{\mu\nu}\left(H + \sum_{j=1}^{n}\xi_j\cdot\frac{\partial H}{\partial p'_j} + q\cdot\frac{\partial H}{\partial p'_i}\right), \tag{129}$$

which are $\frac{1}{2}q_\mu\sigma_i^{\mu\nu}$ times the terms in (121) of order up to $O(q)$.

Working first at $O(q)$ in the fermionic version of (122),

$$(q_\mu H^{\mu\nu})\big|_{O(q)} = q^\nu H - \sum_{i=1}^{n}\left(p_i'^{\nu} q\cdot\frac{\partial H}{\partial p'_i} - \frac{1}{2}q_\mu\sigma_i^{\mu\nu}H\right). \tag{130}$$

From angular momentum conservation, we now have the relation

$$\sum_{i=1}^{n}\mathcal{J}_i H = \sum_{i=1}^{n}\left(p_i'^{\alpha}\frac{\partial}{\partial p'_{i\beta}} - p_i'^{\beta}\frac{\partial}{\partial p'_{i\alpha}} + \sigma_i^{\alpha\beta}\right)H = 0\,, \tag{131}$$

where $\mathcal{J}_i$ is the angular momentum operator from (23). This allows us to rewrite (130) as

$$(q_\mu H^{\mu\nu})\big|_{O(q)} = q^\nu H - \frac{1}{2}\sum_{i=1}^{n}\left(p_i'^{\nu} q\cdot\frac{\partial H}{\partial p'_i} + p'_i\cdot q\frac{\partial H}{\partial p'_{i\nu}}\right). \tag{132}$$

Factoring out q_μ yields the symmetric combination

$$H^{\mu\nu}\big|_{O(q^0)} = \eta^{\mu\nu} H - \frac{1}{2}\sum_{i=1}^{n}\left(p_i'^{\nu}\frac{\partial H}{\partial p'_{i\mu}} + p_i'^{\mu}\frac{\partial H}{\partial p'_{i\nu}}\right), \tag{133}$$

which is the same as in the scalar case (127).

Consider next the $O(q^2)$ terms in $q_\mu H^{\mu\nu}$,

$$\begin{aligned}(q_\mu H^{\mu\nu})\big|_{O(q^2)} = -\sum_{i=1}^{n}\Bigg(&\xi_i^\nu q\cdot\frac{\partial H}{\partial p'_i} + \frac{1}{2}p_i'^{\nu}(qq)\cdot\frac{\partial^2 H}{\partial p'_i\partial p'_i} + \sum_{j=1}^{n} p_i'^{\nu}(q\xi_j)\cdot\frac{\partial^2 H}{\partial p'_i\partial p'_j}\\ &- \frac{1}{2}q_\mu\sigma_i^{\mu\nu}q\cdot\frac{\partial H}{\partial p'_i} - \frac{1}{2}q_\mu\sigma_i^{\mu\nu}\sum_{j=1}^{n}\xi_j\cdot\frac{\partial H}{\partial p'_j}\Bigg) + q^\nu\sum_{j=1}^{n}\xi_j\cdot\frac{\partial H}{\partial p'_j}\,.\end{aligned} \tag{134}$$

Using angular momentum conservation, it is possible to reorganize the ξ_i-dependent terms using steps similar to those in the scalar case. The result is that the $O(q^2)$ terms above become

$$\begin{aligned}(q_\mu H^{\mu\nu})\big|_{O(q^2)} = &-\sum_{i=1}^{n}\left(\frac{1}{2}p_i'^{\nu}(qq)\cdot\frac{\partial^2 H}{\partial p'_i\partial p'_i} - \frac{1}{2}q_\mu\sigma_i^{\mu\nu}q\cdot\frac{\partial H}{\partial p'_i}\right)\\ &- \frac{1}{2}q_\mu\sum_{i,j=1}^{n}\xi_j\cdot\frac{\partial}{\partial p'_j}\left(p_i'^{\mu}\frac{\partial H}{\partial p'_{i\nu}} + p_i'^{\nu}\frac{\partial H}{\partial p'_{i\mu}}\right) + q^\nu\sum_{j=1}^{n}\xi_j\cdot\frac{\partial H}{\partial p'_j}\,.\end{aligned} \tag{135}$$

Factoring out q_μ from this expression, we may finally write down the full radiative hard part when all external particles are fermions,

$$\begin{aligned}H^{\mu\nu} =&\,\eta^{\mu\nu}\left(H + \sum_{j=1}^{n}\xi_j\cdot\frac{\partial H}{\partial p'_j}\right)\\ &- \frac{1}{2}\sum_{i=1}^{n}\left(p_i'^{\mu}\frac{\partial H}{\partial p'_{i\nu}} + p_i'^{\nu}\frac{\partial H}{\partial p'_{i\mu}}\right)\\ &+ \frac{1}{2}\sum_{i=1}^{n}\left(p'_i\cdot q\frac{\partial^2 H}{\partial p'_{i\mu}\partial p'_{i\nu}} - p_i'^{\mu}q^\rho\frac{\partial^2 H}{\partial p_i'^{\rho}\partial p'_{i\nu}} - p_i'^{\nu}q^\rho\frac{\partial^2 H}{\partial p_i'^{\rho}\partial p'_{i\mu}} + q_\rho\sigma_i^{\rho\mu}\frac{\partial H}{\partial p'_{i\nu}} + q_\rho\sigma_i^{\rho\nu}\frac{\partial H}{\partial p'_{i\mu}}\right)\\ &- \frac{1}{2}\sum_{i,j=1}^{n}\xi_j\cdot\frac{\partial}{\partial p'_j}\left(p_i'^{\mu}\frac{\partial H}{\partial p'_{i\nu}} + p_i'^{\nu}\frac{\partial H}{\partial p'_{i\mu}}\right)\\ &+ O(q^2)\,,\end{aligned} \tag{136}$$

where the ξ_i-dependent terms have been symmetrized using (131). We will address the relation of this result to the CS formula (21)-(23) in Sec. 4.4.

In order to complete our derivation of the radiative hard parts (127) and (136), we show that any supplementary contributions $B_{\mu\nu}$ to $H_{\mu\nu}$ statisfying $q^\mu B_{\mu\nu} = 0$ and $q^\nu B_{\mu\nu} = 0$ must vanish to this order. This is equivalent to showing the uniqueness of our solution $H^{\mu\nu}$ to the equations $q_\mu \mathcal{M}^{\mu\nu}_{int} = -q_\mu \mathcal{M}^{\mu\nu}_{ext}$ and $q_\nu \mathcal{M}^{\mu\nu}_{int} = -q_\nu \mathcal{M}^{\mu\nu}_{ext}$.

The most general symmetric tensor structure for $B_{\mu\nu}$ takes the form

$$B_{\mu\nu} = \sum_{i,j=1}^{n} C_{ij}(q) p'_{i\mu} p'_{j\nu} + \sum_{i=1}^{n} D_i(q)(p'_{i\mu} q_\nu + p'_{i\nu} q_\mu) + E(q)\eta_{\mu\nu}\,. \tag{137}$$

The $p'_1, \ldots, p'_n$ dependence of $C_{ij}(q)$, $D_i(q)$, and $E(q)$ are left implicit. There are no singularities in q since we are assuming $H_{\mu\nu}$ contains only hard exchanges, which enables us to Taylor expand it in powers of q.

Taylor expanding $B_{\mu\nu}$ in powers of q, we obtain

$$B_{\mu\nu} = B^{(0)}_{\mu\nu} + B^{(1)}_{\mu\nu}\,, \tag{138}$$

where

$$\begin{aligned} B^{(0)}_{\mu\nu} &= \sum_{i,j=1}^{n} C_{ij}(0) p'_{i\mu} p'_{j\nu} + E(0)\eta_{\mu\nu}\,, \\ B^{(1)}_{\mu\nu} &= \sum_{i,j=1}^{n} q^\alpha \frac{\partial C_{ij}}{\partial q^\alpha}\bigg|_{q=0} p'_{i\mu} p'_{j\nu} + \sum_{i=1}^{n} D_i(0)(p'_{i\mu} q_\nu + p'_{i\nu} q_\mu) + q^\alpha \frac{\partial E}{\partial q^\alpha}\bigg|_{q=0} \eta_{\mu\nu}\,. \end{aligned} \tag{139}$$

$B_{\mu\nu}$ must be gauge invariant at each order in q. Therefore,

$$\begin{aligned} q^\mu B^{(0)}_{\mu\nu} &= q^\nu B^{(0)}_{\mu\nu} = 0 \\ q^\mu B^{(1)}_{\mu\nu} &= q^\nu B^{(1)}_{\mu\nu} = 0\,. \end{aligned} \tag{140}$$

Since $B^{(0)}_{\mu\nu}$ has no q dependence, this implies that $B^{(0)}_{\mu\nu} = 0$. On the other hand, $B^{(1)}_{\mu\nu}$ does depend on q, so the implication is not immediate. We can, however, rewrite $B^{(1)}_{\mu\nu}$ as follows

$$B^{(1)}_{\mu\nu} = q^\alpha B^{(1)}_{\alpha\mu\nu}\,, \tag{141}$$

with

$$B^{(1)}_{\alpha\mu\nu} = \sum_{i,j=1}^{n} \frac{\partial C_{ij}}{\partial q^\alpha}\bigg|_{q=0} p'_{i\mu} p'_{j\nu} + \sum_{i=1}^{n} D_i(0)(\eta_{\mu\alpha} p'_{i\nu} + \eta_{\nu\alpha} p'_{i\mu}) + \frac{\partial E}{\partial q^\alpha}\bigg|_{q=0} \eta_{\mu\nu}\,. \tag{142}$$

Notice that unlike $B^{(1)}_{\mu\nu}$, $B^{(1)}_{\alpha\mu\nu}$ is independent of q. Now, by gauge invariance, we know that

$$q^\alpha q^\mu B^{(1)}_{\alpha\mu\nu} = 0\,. \tag{143}$$

Considering each value of ν independently, the above condition implies that $B^{(1)}_{\alpha\mu\nu}$ is antisymmetric in its first two indices, that is

$$B^{(1)}_{\alpha\mu\nu} = -B^{(1)}_{\mu\alpha\nu}\,. \tag{144}$$

Of course, the same argument yields the analogous antisymmetry property in the first and third indices. Further, we recall that $B_{\mu\nu}$ is symmetric in μ and ν, a property which necessarily makes $B^{(1)}_{\alpha\mu\nu}$ symmetric in its second and third indices. Combining all of these properties, we obtain the following chain of interchanges of indices

$$B^{(1)}_{\alpha\mu\nu} = -B^{(1)}_{\mu\alpha\nu} = -B^{(1)}_{\mu\nu\alpha} = B^{(1)}_{\nu\mu\alpha} = -B^{(1)}_{\alpha\mu\nu}\,, \tag{145}$$

from which we deduce that $B^{(1)}_{\alpha\mu\nu} = 0$ and hence $B_{\mu\nu}$ vanishes up to order $O(q^1)$. Our results Eqs. (127) and (136) are therefore the full graviton emission amplitudes from the hard parts with external scalars and fermions respectively, even in the off-shell scenario. Note that the entire graviton emission amplitude is gauge invariant, but the presence of singular terms in q prevents the argument we have just described from showing it has to vanish as well.

4.3 Graviton emission from nonleading Jets

Having discussed the derivation of the radiative hard part for diagrams with leading jets only, we move on to graviton emission from nonleading jets. Up to $O(\lambda^2)$, the nonleading factorized contributions to the elastic amplitude, as well as the leading term, are all gathered in Eq. (55). The factorized contributions to the elastic amplitude at $O(\lambda^3)$ and $O(\lambda^4)$ are listed in Tables 2, 3, and 4.

Consider the contributions appearing in Eq. (55). To generate radiative contributions from these factorized terms, we need to consider attaching a graviton to each factor separately: the jet functions, the soft cloud, and the hard part. This results in the generic radiative amplitude,

$$\begin{aligned}\mathcal{M}_{\mu\nu} = &\sum_{i=1}^{n}\left(\prod_{j\neq i} J_j^f\right) J^f_{i,\mu\nu}\otimes H + \left(\prod_{i=1}^{n} J_i^f\right)\otimes H_{\mu\nu}\\ &+\sum_{\theta\in\Theta_1}\sum_{i=1}^{n}\left[\left(\prod_{j\neq i} J_j^f\right) J^\theta_{i,\mu\nu}\otimes H_i^\theta + \sum_{l\neq i}\left(\prod_{j\neq i,l} J_j^f\right) J^f_{l,\mu\nu} J_i^\theta\otimes H_i^\theta + \left(\prod_{j\neq i} J_j^f\right) J_i^\theta\otimes H^\theta_{i,\mu\nu}\right]\end{aligned}$$

$$
\begin{aligned}
&+ \sum_{\theta\in\Theta_2} \sum_{1\le i<j\le n} \Bigg[\left(\prod_{l\neq i,j} J_l^f \right) J^\theta_{i,\mu\nu} J^\theta_j \, S^\theta \otimes H^{\theta\theta}_{ij} + \left(\prod_{l\neq i,j} J_l^f \right) J^\theta_i J^\theta_{j,\mu\nu} \, S^\theta \otimes H^{\theta\theta}_{ij} \\
&\qquad + \sum_{h\neq i,j} \left(\prod_{l\neq i,j,h} J_h^f \right) J^\theta_i J^\theta_j J^f_{h,\mu\nu} \, S^\theta \otimes H^{\theta\theta}_{ij} + \left(\prod_{l\neq i,j} J_l^f \right) J^\theta_i J^\theta_j \, S^\theta_{\mu\nu} \otimes H^{\theta\theta}_{ij} \\
&\qquad + \left(\prod_{l\neq i,j} J_l^f \right) J^\theta_i J^\theta_j \, S^\theta \otimes H^{\theta\theta}_{ij,\mu\nu} \Bigg] \\
&+ O(\lambda) \,,
\end{aligned}
\tag{146}
$$

where $\Theta_1 = \{fs, fss, fff, f\partial s\}$ and $\Theta_2 = \{fs, f\underline{s}\}$ are two sets of jet labels. We define $S^\theta \equiv 1$ if $\theta = fs$, and $S^\theta \equiv S_{ij}$ if $\theta = f\underline{s}$. Also, we set $S^\theta_{\mu\nu} \equiv 0$ if $\theta = fs$, and $S^\theta_{\mu\nu} = S_{ij,\mu\nu}$ if $\theta = f\underline{s}$. As in Sec. 2.3, in the jet labels, the superscripts f, s, and $\underline{s}$ stand for a collinear fermion/antifermion, a collinear scalar, and a soft scalar respectively. The ∂ symbol in a jet label refers to the higher dimensional jet function obtained when expanding the hard part in the transverse component of a loop momentum.

To derive the radiative hard parts, we need to apply the general off-shell Ward identity expressed diagrammatically in Fig. 29 of Sec. 4.1. This was done in Sec. 3.2.2 in the case of photons. The main difference in this case is that gravitons can also couple to scalars, and in particular, it is possible to emit a graviton from the soft cloud, as shown in Fig. 33. This diagram is, in fact, the only instance of graviton emission from a soft cloud to $O(q)$. All other diagrams with a soft cloud identified in Sec. 2.2.2 are of order $O(\lambda^3)$ or $O(\lambda^4)$. Since attaching a soft graviton to the soft cloud does not lower the scaling power γ of the diagram (see Sec. 2.4), emitting a graviton from the soft cloud of these diagrams would not generate a diagram of order $O(\lambda^2)$ or less, as is required to contribute to the soft graviton theorem. The possibility of emitting a graviton from a soft cloud makes contact with the emission of soft gluons in gauge theory, which is the subject of ongoing work, some of which is presented in [28–30, 46, 47].

Applying the off-shell Ward identity to (146) in order to deduce the radiative hard parts yields formulas of the form

$$
H^\theta_{\mu\nu} = \mathcal{O}_{\partial,\sigma^{\mu\nu}} H^\theta \,,
\tag{147}
$$

where $\mathcal{O}_{\partial,\sigma^{\mu\nu}}$ is an operator built from $\sigma^{\mu\nu}$ and derivatives with respect to external momenta. This is similar to Eqs. (127) and (136), although the number of terms will be greater due to the increased number of collinear and soft legs in nonleading jets.

For factorized contributions of order higher than $O(\lambda^2)$, as those listed in Tables 2 to 4, one need only consider graviton emission from the jets, since emitting a graviton from the

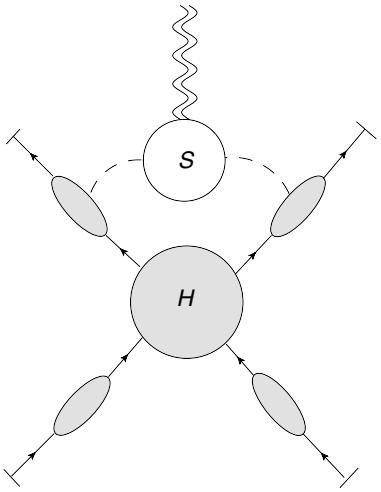

Figure 33: Since the graviton can couple to scalars, it is possible to emit a graviton from the soft cloud at $O(\lambda^2)$.

soft cloud or hard part would leave the scaling power of the diagram unchanged, and hence yield a contribution of order too high to correct the soft graviton theorem.

4.4 Low energy limit

Suppose that we are interested in graviton emission in the regime where Low's theorem applies. Specifically, we consider the case of external fermions of mass $m \neq 0$ and take the limit $q \ll \frac{m^2}{E}$, where E is the center of mass energy. Then the elastic amplitude may be expanded in q when applying Low's original analysis and there is no need to consider graviton emission from the jets $J^i(p_i)$. We can simply split the amplitude $\mathcal{M}_{\mu\nu}(p_1 \dots p_n, q)$ into the emission from the external and the internal lines. In (118), this corresponds to making the replacement $H \mapsto \mathcal{M}_{el}(p_1 \dots p_n)$. Because we have massless scalars, however, the vertex function through which gravity couples to matter has a branch cut starting at $q = 0$. This branch cut is associated with the annihilation of the graviton into two soft scalars and will be shown explicitly in Sec. 4.5.2. The result of these prescriptions, then, is the expansion

$$\begin{aligned}\mathcal{M}_{\mu\nu}(p_1, \dots, p_n, q) = &\sum_{i=1}^{n} \frac{\mathcal{V}_{\mu\nu}^{ffG}(p_i, q)}{2p_i \cdot q + q^2} \left(1 + q^\rho \frac{\partial}{\partial p_i^\rho} + \frac{1}{2} q^\rho q^\sigma \frac{\partial^2}{\partial p_i^\rho \partial p_i^\sigma}\right) \mathcal{M}_{el} \\ &+ \eta_{\mu\nu} \mathcal{M}_{el} - \frac{1}{2} \sum_{i=1}^{n} \left(p_{i\mu} \frac{\partial}{\partial p_i^\nu} + p_{i\nu} \frac{\partial}{\partial p_i^\mu}\right) \mathcal{M}_{el}\end{aligned}$$

$$+\frac{1}{2}\sum_{i=1}^{n}\Bigg((p_i\cdot q)\frac{\partial^2}{\partial p_i^\mu \partial p_i^\nu}-p_{i\mu}q^\rho\frac{\partial^2}{\partial p_i^\rho \partial p_i^\nu}-p_{i\nu}q^\rho\frac{\partial^2}{\partial p_i^\rho \partial p_i^\mu}$$
$$+q^\rho\sigma^i_{\rho\mu}\frac{\partial}{\partial p_i^\nu}+q^\rho\sigma^i_{\rho\nu}\frac{\partial}{\partial p_i^\mu}\Bigg)\mathcal{M}_{el}\,, \tag{148}$$

in which all q-dependence is explicit to $O(q)$ and the ξ_j's have been omitted for brevity. In the external emission, the function $\mathcal{V}^{ffG}_{\mu\nu}$ combines the external spinor, the fully dressed fermion-graviton vertex, and the numerator of the external fermion propagator. At low energies, we have that $\lambda = m/E \sim 1$ and thus a new small scale lambda must be identified if we are to retain the soft scaling $q = O(\lambda^2)$. In this case, $q << m^2/E$ and the conditions for applying Low's original analysis are met.

Recalling the definition of the angular momentum operator, (23), we can rewrite Eq. (148) as the basic CS result, Eqs. (21)-(23), provided we replace the external emission function $\mathcal{V}^{ffG}_{\mu\nu}$ by its tree level expression and consider an on-shell physical graviton. In particular, the CS formula does receive loop corrections even in the low energy regime. Note that for fermions, to obtain the "double $\mathcal{J}$" form at $O(q)$ explicitly, we require a term of the form $q^\rho q^\sigma \sigma^{(i)}_{\rho\mu}\sigma^{(i)}_{\sigma\nu}\mathcal{M}_{el}$ which is both gauge invariant and nonsingular. We have shown that such terms cannot be part of $H_{\mu\nu}$. A simple exercise, however, shows that

$$q^\rho q^\sigma(\sigma^{(i)}_{\rho\mu}\sigma^{(i)}_{\sigma\nu}+\sigma^{(i)}_{\rho\nu}\sigma^{(i)}_{\sigma\mu})=\frac{1}{2}(q_\mu q_\nu - q^2\eta_{\mu\nu})\,, \tag{149}$$

which we will see occurs as a gauge invariant contribution to the external amplitude. This allows us to make contact with the CS result shown in Eqs. (21)-(23).

4.5 External emission

4.5.1 KG decomposition

Having investigated the low energy region and the relation of our results (127) and (136) to the CS formula (21)-(23), we now return to the high energy region. In this section, we will be specifically interested in the structure of graviton emission from the jet functions.

Following Del Duca [14] and drawing inspiration from Grammer and Yennie's decomposition [49], it is possible to separate the radiative jet functions into a gauge invariant piece and a leading part that obeys the off-shell Ward identity (117). For the purpose of analysis, we introduce the notation

$$J^{f,\mu\nu}(p,q)=J^{f,\mu\nu}_L(p,q)+J^{f,\mu\nu}_T(p,q)\,, \tag{150}$$

where for simplicity we have made the replacement $p_i \mapsto p$ and opted to use the leading fermionic jet as an illustrative example. The extension of our analysis to other jets follows the same line of reasoning. The jet functions $J_L^{f,\mu\nu}$ and $J_T^{f,\mu\nu}$ satisfy,

$$\begin{aligned} q_\mu J_L^{f,\mu\nu}(p,q) &= J^f(p)\left(p^\nu - \frac{1}{2}q_\mu \sigma^{\mu\nu}\right) \\ q_\mu J_T^{f,\mu\nu}(p,q) &= 0\,. \end{aligned} \tag{151}$$

Now, in the spirit of Del Duca's analysis [14], we introduce projection operators $K^{\rho\sigma}{}_{\mu\nu}$ and $G^{\rho\sigma}{}_{\mu\nu}$ that isolate $J_L^{\mu\nu}$ and $J_T^{\mu\nu}$. Explicitly, this translates into the requirements

$$\begin{aligned} J^f_{\rho\sigma}(p,q)K^{\rho\sigma}{}_{\mu\nu} &= J^f_{L,\mu\nu}(p,q)\,, \\ J^f_{\rho\sigma}(p,q)G^{\rho\sigma}{}_{\mu\nu} &= J^f_{T,\mu\nu}(p,q)\,. \end{aligned} \tag{152}$$

Of course, this definition is ambiguous as one could always add a transverse piece to $J_L^{f,\mu\nu}$ while maintaining these conditions.

To identify K and G, we first observe that they must add to a product of Kronecker deltas,

$$\delta^\rho_\mu \delta^\sigma_\nu = K^{\rho\sigma}{}_{\mu\nu} + G^{\rho\sigma}{}_{\mu\nu}\,. \tag{153}$$

Drawing inspiration from our work on photons in Sec. 3.3, we define the tensor

$$G^\rho{}_\mu = \delta^\rho_\mu - \frac{q^\rho p_\mu}{p\cdot q}\,, \tag{154}$$

and are led to decompose $\delta^\rho_\mu \delta^\sigma_\nu$ as follows,

$$\begin{aligned} \delta^\rho_\mu \delta^\sigma_\nu &= \left(\frac{q^\rho p_\mu}{p\cdot q} + \left(\delta^\rho_\mu - \frac{q^\rho p_\mu}{p\cdot q}\right)\right) \times \left(\frac{q^\sigma p_\nu}{p\cdot q} + \left(\delta^\sigma_\nu - \frac{q^\sigma p_\nu}{p\cdot q}\right)\right) \\ &= \left(\frac{q^\rho p_\mu}{p\cdot q} + G^\rho{}_\mu\right)\left(\frac{q^\sigma p_\nu}{p\cdot q} + G^\sigma{}_\nu\right)\,. \end{aligned} \tag{155}$$

Expanding the above product invites us to define

$$\begin{aligned} G^{\rho\sigma}{}_{\mu\nu} &= G^\rho{}_\mu G^\sigma{}_\nu\,, \\ K^{\rho\sigma}{}_{\mu\nu} &= \frac{q^\rho p_\mu}{p\cdot q}\frac{q^\sigma p_\nu}{p\cdot q} + \frac{q^\sigma p_\nu}{p\cdot q}G^\rho{}_\mu + \frac{q^\rho p_\mu}{p\cdot q}G^\sigma{}_\nu\,. \end{aligned} \tag{156}$$

Notice that since $q^\mu G^\rho{}_\mu = 0$, we necessarily have that $G^{\rho\sigma}{}_{\mu\nu}$ is transverse to q when contracted with the free indices of $J^f_{T,\mu\nu}$ from Eq. (152). Thus, $G^{\rho\sigma}{}_{\mu\nu}$ has the right property for isolating

a transverse component of the jet function $J^f_{\mu\nu}$. For completeness, we should also verify that $J^f_{\rho\sigma}(p,q)K^{\rho\sigma}{}_{\mu\nu}$ satisfies the off-shell Ward identity (117). We begin with an application of the off-shell Ward identity to rewrite the product $J^f_{\rho\sigma}(p,q)K^{\rho\sigma}{}_{\mu\nu}$ in the form

$$J^f_{\rho\sigma}(p,q)K^{\rho\sigma}{}_{\mu\nu} = J^f(p)\left(p_\mu p_\nu - \frac{1}{2}p_\mu q^\alpha \sigma_{\alpha\nu} - \frac{1}{2}p_\nu q^\alpha \sigma_{\alpha\mu}\right)\frac{1}{p\cdot q}\,, \tag{157}$$

from which it immediately follows that

$$q^\mu J^f_{\rho\sigma}(p,q)K^{\rho\sigma}{}_{\mu\nu} = J^f(p)\left(p_\nu - \frac{1}{2}q^\alpha \sigma_{\alpha\nu}\right)\,. \tag{158}$$

Suppose now that we have another set of tensors $\tilde{K}^{\rho\sigma}{}_{\mu\nu}$ and $\tilde{G}^{\rho\sigma}{}_{\mu\nu}$ that split $J^f_{\mu\nu}(p,q)$ into a piece obeying the off-shell Ward identity and another piece transverse to q^μ. Then we have

$$q^\mu J^f_{\rho\sigma}(p,q)(K^{\rho\sigma}{}_{\mu\nu} - \tilde{K}^{\rho\sigma}{}_{\mu\nu}) = 0\,, \tag{159}$$

and therefore the difference between $K^{\rho\sigma}{}_{\mu\nu}$ and $\tilde{K}^{\rho\sigma}{}_{\mu\nu}$ can be absorbed into $G^{\rho\sigma}{}_{\mu\nu}$. Hence, the tensors $K^{\rho\sigma}{}_{\mu\nu}$ and $G^{\rho\sigma}{}_{\mu\nu}$ are unique up to the addition of a transverse piece to $J_L^{f,\mu\nu}$ and $J_T^{f,\mu\nu}$.

The application of parity to $J^{f,\mu\nu}(p,q)$ shows that the only gamma matrix structures that can be used in its construction are 1, γ^μ, and $\sigma^{\mu\nu}$. The most general expression for the transverse radiative jet function is then

$$\begin{aligned}
J_T^{f,\mu\nu}(p,q) =& \bar{u}(p)\Bigg[F_1(\eta^{\mu\nu}q^2 - q^\mu q^\nu) \\
&+ F_2(\eta^{\mu\nu}q^2 - q^\mu q^\nu)\not{q} \\
&+ F_3\left(p^\mu q^\nu + q^\mu p^\nu - \frac{q^2}{p\cdot q}p^\mu p^\nu - \frac{p\cdot q}{q^2}q^\mu q^\nu\right) \\
&+ F_4\left((p^\mu q^\nu + p^\nu q^\mu - 2\frac{p\cdot q}{q^2}q^\mu q^\nu)\not{q} - (q^2 p^\mu - p\cdot q\, q^\mu)\gamma^\nu - (q^2 p^\nu - p\cdot q\, q^\nu)\gamma^\mu\right) \\
&+ F_5\left(\left(p^\mu p^\nu - \left(\frac{p\cdot q}{q^2}\right)^2 q^\mu q^\nu\right)\not{q} - \frac{p\cdot q}{q^2}(q^2 p^\mu - p\cdot q\, q^\mu)\gamma^\nu - \frac{p\cdot q}{q^2}(q^2 p^\nu - p\cdot q\, q^\nu)\gamma^\mu\right) \\
&+ F_6((q^2 p^\mu - p\cdot q\, q^\mu)q_\alpha \sigma^{\alpha\nu} + (q^2 p^\nu - p\cdot q\, q^\nu)q_\alpha \sigma^{\alpha\mu})\Bigg]\,.
\end{aligned} \tag{160}$$

Each of the coefficients $F_1, \ldots, F_6$ multiplies one of the allowed independent symmetric transverse structures that we can build from $\eta^{\mu\nu}$, p^μ, q^μ, γ^μ, and $\sigma^{\mu\nu}$. Although this is a relatively

long list, we are only interested in those terms that vanish no faster than $O(q)$. The dimensions of the form factors F_i vary from term to term, but, combined with their corresponding tensors, they can have at worst a single algebraic pole, $1/(p \cdot q)$, and no pole in q^2. These restrictions follow immediately from the presence of divergences that are at worst logarithmic for the nonradiative jet functions in the limit of zero masses. Dimensional analysis of the terms in Eq. (160) shows that for $q^2 = 0$, none of these contributions can appear at order q. For the off-shell case, $q^2 \neq 0$, the F_1 term may appear, and we will give a one-loop example of how it occurs below.

It is possible to rewrite the transverse contributions in an interesting way if we contract them with an arbitrary graviton polarization tensor $\tilde{h}^{\mu\nu}$. The result is

$$J^f_{\rho\sigma}(p,q)G^{\rho\sigma}{}_{\mu\nu}\tilde{h}^{\mu\nu} = \frac{p_\mu p_\nu}{(q\cdot p)^2} J^f_{\rho\sigma}(p,q)(q^\mu q^\nu \tilde{h}^{\rho\sigma} - q^\mu q^\sigma \tilde{h}^{\rho\nu} - q^\nu q^\rho \tilde{h}^{\mu\sigma} + q^\rho q^\sigma \tilde{h}^{\mu\nu})\,. \tag{161}$$

We recognize the quantity between brackets on the right hand side as the Riemann curvature tensor (as has also recently been found in [39]) of a plane gravitational wave with polarization vector $\tilde{h}^{\mu\nu}$,

$$R^{\rho\mu\sigma\nu}(\tilde{h},q) \equiv q^\mu q^\nu \tilde{h}^{\rho\sigma} - q^\mu q^\sigma \tilde{h}^{\rho\nu} - q^\nu q^\rho \tilde{h}^{\mu\sigma} + q^\rho q^\sigma \tilde{h}^{\mu\nu}\,. \tag{162}$$

The Riemann tensor term of (161) is unique among high energy power corrections. It is the only high energy correction that is sensitive to the analytic structure of leading jets. The corrections associated with nonleading jets are given by the K projection and factor from the leading jets as in Eq. (147).

Combining Eqs. (136), (157), (161), and (162) enables us to rewrite the soft graviton theorem for fermions, with only leading fermionic jets taken into account, as

$$
\begin{aligned}
&\tilde{h}^{\mu\nu}\mathcal{M}_{\mu\nu} \\
&\quad= \left(\prod_{j=1}^{n} J^f(p_j)\right) \otimes \sum_{i=1}^{n} \frac{\tilde{h}^{\mu\nu}}{p_i\cdot q}\left(p_{i\mu}p_{i\nu} - \frac{1}{2}p_{i\mu}q^\rho\sigma^i_{\rho\nu} - \frac{1}{2}p_{i\nu}q^\rho\sigma^i_{\rho\mu}\right) H(p_1,\ldots,p_i+q,\ldots,p_n) \\
&\qquad+ \left(\prod_{j=1}^{n} J^f(p_j)\right) \otimes \left[\eta_{\mu\nu}\tilde{h}^{\mu\nu}\, H - \frac{1}{2}\tilde{h}^{\mu\nu}\sum_{i=1}^{n}\left(p'_{i\mu}\frac{\partial H}{\partial p'^{\nu}_i} + p'_{i\nu}\frac{\partial H}{\partial p'^{\mu}_i}\right)\right] \\
&\qquad+ \frac{1}{2}\left(\prod_{j=1}^{n} J^f(p_j)\right) \otimes \sum_{i=1}^{n}\tilde{h}^{\mu\nu}\left(p'_i\cdot q\frac{\partial^2 H}{\partial p'^{\mu}_i\partial p'^{\nu}_i} - p'_{i\mu}q^\rho\frac{\partial^2 H}{\partial p'^{\rho}_i\partial p'^{\nu}_i} - p'_{i\nu}q^\rho\frac{\partial^2 H}{\partial p'^{\rho}_i\partial p'^{\mu}_i}\right. \\
&\qquad\qquad\left. + q^\rho\sigma^i_{\rho\mu}\frac{\partial H}{\partial p'^{\nu}_i} + q^\rho\sigma^i_{\rho\nu}\frac{\partial H}{\partial p'^{\mu}_i}\right) \\
&\qquad+ \sum_{i=1}^{n}\left(\prod_{j\neq i} J^f(p_j)\right)\frac{p_{i\mu}p_{i\nu}}{(p_i\cdot q)^2}R^{\rho\mu\sigma\nu}(\tilde{h},q)J^f_{\rho\sigma}(p_i,q)\otimes H(p_1,\ldots,p_i+q,\ldots,p_n) \\
&\qquad+ \left(\prod_{j=1}^{n} J^f(p_j)\right) \otimes \tilde{h}^{\mu\nu}\left[\eta_{\mu\nu}\sum_{i=1}^{n}\xi_i\cdot\frac{\partial H}{\partial p'_i} - \frac{1}{2}\sum_{i,l=1}^{n}\xi_i\cdot\frac{\partial}{\partial p'_i}\left(p'_{l\mu}\frac{\partial H}{\partial p'^{\nu}_l} + p'_{l\nu}\frac{\partial H}{\partial p'^{\mu}_l}\right)\right]. \qquad (163)
\end{aligned}
$$

The first three factorized sums in our result depend only on the nonradiative jet functions and the hard subamplitude. This dependence is completely dictated by the off-shell Ward identity, and is consistent with the CS result, Eqs. (21)-(23) [6]. The fourth sum organizes contributions that are transverse, and do not follow directly from the Ward identities (117). These contributions correspond to the result found by Del Duca for Low's theorem in QED [14]. When the polarization tensor describes the radiation of an external background field by some source, as will be illustrated in the forthcoming example, these contributions couple the scattering process to the Riemann tensor of the background field. Note that the q and ξ_i dependence have been left implicit in the external amplitudes. At low energies, the Riemann tensor correction remains and couples to the fully dressed graviton-fermion external vertex.

4.5.2 Example of off-shell emission

We begin with a few remarks about the case of a physical on-shell graviton. The polarization tensor of the external graviton takes the form $\tilde{h}^{\rho\sigma} = \epsilon^\rho\epsilon^\sigma$, giving

$$
R^{\rho\mu\sigma\nu} = (q^\rho\epsilon^\mu - q^\mu\epsilon^\rho)(q^\sigma\epsilon^\nu - q^\nu\epsilon^\sigma)\,. \qquad (164)
$$

In the case of scalar theory, the jet function $J^f_{\rho\sigma}$ can only be built from $p_{i\rho}$, q_ρ, and $\eta_{\rho\sigma}$, all of which are annihilated when contracted with $R^{\rho\mu\sigma\nu}p_{i\mu}p_{i\nu}$ – this critically depends on the graviton being on-shell. Therefore, we conclude that transverse loop corrections are not present in the case of gravity coupled to scalars when emitting an on-shell graviton.

In the case of Yukawa theories, if the outgoing particle is a scalar, then our previous argument for scalar theories still holds. If the outgoing particle is a fermion, then we can decompose the jet function appearing in the product $p_{i\mu}p_{i\nu}J^f_{\rho\sigma}R^{\rho\mu\sigma\nu}$ into the components $J^f_{L,\rho\sigma}$ and $J^f_{T,\rho\sigma}$ from Eq. (151). The component $J^f_{L,\rho\sigma}$ is shown in Eq. (157), while the transverse piece $J^f_{T,\rho\sigma}$ can be decomposed as in equation (160). Once again, the product $R^{\rho\mu\sigma\nu}p_{i\mu}p_{i\nu}$ annihilates all terms contributing to $J^f_{\rho\sigma}(p,q)$ and there are no transverse corrections to the soft theorem.

One wonders if we can find instances where loop corrections are not annihilated by the Riemann tensor of linearized gravity. From our discussion we know that, at least for Yukawa and scalar theories, we have to consider an off-shell emitted graviton to find such an occurence. This study is the object of the rest of this section.

The most natural setting for the study of off-shell graviton emission is in the scenario where a scattering amplitude takes place in the viscinity of a strong classical source of background gravitational field. We imagine that this source influences the scattering process by exchanging a single soft graviton, as classical fields are made up of highly occupied soft radiation modes. The emission amplitude of a soft graviton by this classical source is denoted $S^{\rho\sigma}$. We further imagine that this classical source is very heavy and graviton emission from it is thus described by the following amplitude, which is really just the stress tensor of a very heavy object whose recoil we neglect,

$$S^{\alpha\beta}_{\text{HEAVY}} = M^2\delta^\alpha_0\delta^\beta_0\,. \tag{165}$$

The classical source is coupled to the scattering amplitude through an intermediate propagator

$$\mathcal{P}^{\mu\nu}{}_{\alpha\beta} = \frac{i}{2}\frac{\delta^\mu_\alpha\delta^\nu_\beta + \delta^\mu_\beta\delta^\nu_\alpha - \eta^{\mu\nu}\eta_{\alpha\beta}}{q^2}\,. \tag{166}$$

The gravitational field polarization tensor $\tilde{h}^{\mu\nu}$ from which we built the Riemann tensor then takes the form

$$\tilde{h}^{\mu\nu} \equiv \mathcal{P}^{\mu\nu}{}_{\alpha\beta}S^{\alpha\beta}_{\text{HEAVY}}\,. \tag{167}$$

The result of our KG decomposition instructs us to use the above polarization tensor as input for the Riemann tensor which appears in our formula for the transverse loop corrections to

external graviton emission (161). For concreteness, we focus on the amplitude where a scalar jet exchanges a single graviton with the heavy classical source,

$$\mathcal{M}_{ex} \equiv J^s_{\rho\sigma}(p,q) G^{\rho\sigma}{}_{\mu\nu} \tilde{h}^{\mu\nu} = \frac{p_\mu p_\nu}{(p\cdot q)^2} J^s_{\rho\sigma}(p,q) R^{\rho\mu\sigma\nu} \,, \tag{168}$$

and simply ignore the hard part and other jets since they play no role in this discussion. The right hand side completely separates information about the scattered particle contained in $\frac{p_\mu p_\nu}{(p\cdot q)^2} J^s_{\rho\sigma}(p,q)$ from the external gravitational field. It will be convenient to introduce a scalar mass m_s, which may be thought of as being $O(\lambda^2)$ in the high energy limit, but is otherwise of arbitrary size. Note that in the high energy region, this choice does not alter our power counting rules listed in Table 1.

To illustrate how transverse corrections to external emission can be nonvanishing for off-shell gravitons, we will calculate the contribution to $\mathcal{M}_{ex}$ from the diagram shown in Fig. 34. The amplitude for graviton emission from the jet function in this specific example is found to be

$$J^{s,\rho\sigma}(p,q) = (\eta^{\rho\sigma} q^2 - q^\rho q^\sigma)\Theta(p,q) \,, \tag{169}$$

with

$$\Theta(p,q) = \frac{i g' \mu^{-2\epsilon} \kappa}{(4\pi)^{2-\epsilon}} \Gamma(\epsilon) \int_0^1 dx\, x(1-x) \left(\frac{m_s^2}{\mu^2} - x(1-x)\frac{q^2}{\mu^2} \right)^{-\epsilon} \frac{i}{2p\cdot q + q^2} \,, \tag{170}$$

and where we have opted to carry out the calculation in $D = 4 - 2\epsilon$ spacetime dimensions. The constant g' is the coupling of ϕ^4 theory.

We can then couple this loop correction to the massive object in (165), as illustrated in Fig. 34. This results in the following expression for the single graviton exchange amplitude,

$$\mathcal{M}_{ex} = \frac{iM^2}{2q^2} [(3-D)q^2 - 2(q_0)^2] \Theta(p,q) \,, \tag{171}$$

which is nonvanishing in general.

Consider first the region where Low's analysis is applicable, $q \ll m_s$. Working with the integral representation of the jet function (170) provides a more transparent analysis of this region. The integrand can be expanded in powers of q^2 using the binomial theorem since $q^2 \ll m_s^2$, yielding

$$\Theta(p,q) = \frac{i g' \mu^{-2\epsilon} \kappa}{(4\pi)^{2-\epsilon}} \left(\frac{m_s^2}{\mu^2} \right)^{-\epsilon} \Gamma(\epsilon) \left[\frac{1}{6} + \frac{\epsilon}{30} \frac{q^2}{m_s^2} + O(q^4) \right] \frac{i}{2p\cdot q + q^2} \,. \tag{172}$$

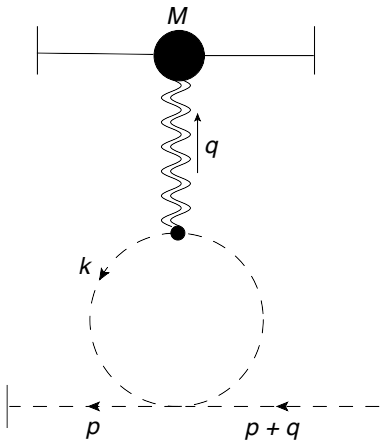

Figure 34: The soft graviton is absorbed by a very massive object whose recoil we neglect. This allows us to identify a lowest order correction to the soft graviton theorem in the case of an off-shell soft graviton.

In an on-shell renormalization scheme, one removes the full correction at $q^2 = 0$. Implementing this scheme leaves us with the following contribution to the jet function,

$$\Theta_R(p,q) = \frac{ig'\kappa}{(4\pi)^2}\left[\frac{1}{30}\frac{q^2}{m_s^2} + O(q^4)\right]\frac{i}{2p\cdot q + q^2}\,. \tag{173}$$

We thus obtain a correction of order q/m_s^2.

If we return to the region $q = O(m_s)$, then we resort to fully evaluating the integral in (170), obtaining the result

$$\begin{aligned}\Theta(p,q) = \frac{ig'\mu^{-2\epsilon}\kappa}{(4\pi)^{2-\epsilon}}\Bigg[&\frac{1}{6\epsilon} - \frac{\gamma}{6} + \frac{2}{3}\frac{m_s^2}{q^2} - \frac{1}{6}\log\left(\frac{m_s^2}{\mu^2}\right)\\ &+\frac{1}{6}\left(1+\frac{2m_s^2}{q^2}\right)\sqrt{1-\frac{4m_s^2}{q^2}}\log\left(\frac{\sqrt{1-4m_s^2/q^2}-1}{\sqrt{1-4m_s^2/q^2}+1}\right) + \frac{10}{36}\Bigg]\frac{i}{2p\cdot q + q^2}\,,\end{aligned} \tag{174}$$

where we have expanded in ϵ before performing the integral while avoiding any expansion in q. Proceeding with an on-shell renormalization scheme as we did before, we expand the counterterm in powers of ϵ, thereby obtaining

$$c.t. = \frac{ig'\mu^{-2\epsilon}\kappa}{(4\pi)^{2-\epsilon}}\left(\frac{1}{6\epsilon} - \frac{\gamma}{6} - \frac{1}{6}\log\left(\frac{m_s^2}{\mu^2}\right)\right)\frac{i}{2p\cdot q + q^2}\,. \tag{175}$$

Subtracting this counterterm from (174) results in the correction,

$$\Theta_R(p,q) = \frac{ig'\kappa}{(4\pi)^2}\left[\frac{2}{3}\frac{m_s^2}{q^2} + \frac{1}{6}\left(1+\frac{2m_s^2}{q^2}\right)\sqrt{1-\frac{4m_s^2}{q^2}}\log\left(\frac{\sqrt{1-4m_s^2/q^2}-1}{\sqrt{1-4m_s^2/q^2}+1}\right) + \frac{10}{36}\right]\frac{i}{2p\cdot q+q^2}\,. \tag{176}$$

The leading term of this expression is of order $O(q^{-1})$. It is worth noting that all of the apparent poles in this expression cancel.

It is also interesting to take the limit $q \gg m_s$ so that the graviton momentum is no longer soft. Retaining the leading term only, we obtain

$$\Theta_R(p,q) = \frac{ig'\kappa}{(4\pi)^2}\frac{1}{6}\log\left(\frac{m_s^2}{-q^2}\right)\frac{i}{2p\cdot q+q^2}\,. \tag{177}$$

In this case, the soft graviton theorem receives a logarithmic correction from the external jet functions. In all cases, we find that the Riemann tensor is coupled to nonvanishing loop corrections from the jet, whether we are in the high or low energy regime. We conclude by mentioning that the Riemann tensor corrections we have identified can be viewed as quantum corrections to the Newtonian potential [67, 74–78].

5 Conclusion

Inspired by the renewed interest in soft theorems, we have set out to investigate the role of loop corrections in soft radiation theorems. In the context of Low's theorem, work on this subject had already been carried out by del Duca [14] who showed that in the limit of high center of mass energy E, Low's argument only applies in the vanishingly small region $q \ll m^2/E$, where q is the soft momentum. In the regime where $q \sim m^2/E$, del Duca identified loop corrections that take the form of universal infrared sensitive matrix elements, the jet functions. To identify these loop corrections, he needed to adapt Low's analysis by factorizing the elastic amplitude into jet functions and a hard part, and then to consider separately photon emission from each factor. More recently, an analysis of soft theorems in effective field theory has been given in [18].

Following Refs. [12,13], we have applied power counting techniques to derive an extension of soft radiation theorems to Yukawa and scalar theories at all loop orders in both the high energy and low energy regions. Our strategy at high energies is to apply Low's original analysis [1] to a radiative amplitude factorized into jets, a soft cloud, and a hard part. This factorization is a solution to the obstacle arising when, in the high energy region, invariants built with the soft photon or graviton momentum become of the same order of magnitude as the other invariants in denominators of the loop integral. This phenomenon occurs in the vicinity of pinch surfaces and prevents us from expanding the elastic amplitude in powers of q, as is typically done in an argument à la Low. Factorizing the amplitude isolates these nonanalytic contributions and encapsulates them into the jet functions and the soft cloud. The hard parts, on the other hand, get their leading contribution from hard exchanges and can legitimately be expanded in powers of q.

In the high energy region, the total center of mass energy E is very large compared to the mass m of the fermions. This led us to identify the parameter $\lambda \equiv m/E$ as a small quantity suitable for expressing the orders of magnitude of the various quantities in the problem. In particular, soft radiation theorems were recast as expansions in λ rather than q. We have designed, in Refs. [12,13], a power counting technique that allows us to determine the order of magnitude of any factorized contribution corresponding to a given reduced diagram. As we have reviewed in Sec. 2.2.1, singular regions of loop space are classified according to their degree of divergence γ, which indicates an overall scaling of λ^γ. Del Duca's analysis considers attaching a soft photon to the pinch surface with minimal γ. However, in the region $q \sim \lambda^2 E$, the soft photon theorem is an expansion going from order λ^{-2} to λ^0. Since attaching a soft photon to a collinear fermion line reduces the degree of divergence of a nonradiative diagram by 2, it is clear that to obtain all contributions to the radiative amplitude up to $O(\lambda^0)$, one needs to attach the soft photons to nonradiative diagrams with a scaling up to λ^2. Del Duca was concerned with QED, and therefore, we may not directly compare our results with his.

However, it is natural to suspect that, compared to Ref. [14], additional terms may occur from matrix elements with $\gamma = -1$ and $\gamma = 0$ in certain amplitudes in gauge as well as Yukawa theories [18].

We showed that reduced diagrams contributing to soft theorems are in one-to-one correspondence with the reduced diagrams of the elastic amplitude of orders ranging from $O(\lambda^0)$ to $O(\lambda^2)$ for photons, and up to $O(\lambda^4)$ for gravitons. This allowed us to determine all factorized contributions to the radiative amplitude from an analysis of the pinch surfaces of the elastic amplitude. The reduced diagrams resulting from this analysis are shown in Figs. 9 to 19. The jet functions identified using power counting are reminiscent of the higher dimension operators of the SCET approach to soft theorems [18]. The jets are also analogous to final state wave functions in bound state scattering [62–64]. The hard parts, on the other hand, play a role similar to the matching coefficients of effective field theory. A systematic algorithm for computing them would involve a series of nested subtractions similar to the "garden and tulip" construction of [56]. This is also closely related to the nested subtractions of [57].

New terms in the soft photon theorem originate from the nonleading fs, fss, and fff-jets. As we have seen, there are also contributions from diagrams with soft two-point functions, which is qualitatively new. The reduced diagrams corresponding to the new sources of terms in the soft photon theorem were shown in Figs. 17 and 18. We emphasize that our treatment takes into account all infrared sensitive behavior of the radiative amplitude at all loop orders in the region $q \sim m^2/E$. In particular, we do not restrict ourselves to the massless case, although our results are easily adapted to this limit. The full list of contributions to the soft photon theorem from nonleading jets is generated by attaching a photon to the diagrams of Figs. 17 and 18. Factorizing the radiative amplitude into emission from all components identified in such a list gives rise to the formula shown in Eq. (146).

Having derived the proper factorization of the radiative amplitude, we obtained the final form of our extension of Low's theorem by applying del Duca's technique. This involves the application of the jet Ward identities (85) to derive the radiative hard part, followed by an application of the KG decomposition to isolate the leading term from subleading corrections. The end result of this procedure is given in formulas (97), (98), (99), and (100). Of course, the leading term retains its form as in Low's classic result.

In gravity, we have found that, as in electromagnetism, the soft expansion is altered by jet functions, both leading and nonleading. Further, at $O(\lambda^2)$, graviton emission from the soft cloud is also significant, which makes contact with the problem of gluon emission in gauge theories. The jet functions give rise to separately transverse contributions to the external amplitude, as shown in (100). In gravity, we found that jet functions supply loop corrections to the soft graviton theorem that are coupled to a Riemann curvature tensor for linearized gravity at low and high energies. In low energy scattering, the Riemann tensor contribution

is the only correction to the CS tree level theorem.

Although we have not touched upon the problems of double photon or graviton emission, and virtual corrections, these can be addressed using our methods. Our results in Yukawa and scalar theories are interesting in their own right because of their potential applications to nonlinear sigma models and pion scattering. However, they can also be viewed as a testing ground for gauge theories. One theory of particular interest to us is of course QCD. Work in this direction has already been undertaken in Refs. [18, 28–30, 46, 47].

References

[1] F. E. Low, "Bremsstrahlung of very low-energy quanta in elementary particle collisions," *Phys. Rev.*, vol. 110, pp. 974–977, 1958.

[2] T. H. Burnett and N. M. Kroll, "Extension of the low soft photon theorem," *Phys. Rev. Lett.*, vol. 20, p. 86, 1968.

[3] S. Weinberg, "Infrared photons and gravitons," *Phys. Rev.*, vol. 140, pp. B516–B524, 1965.

[4] T. He, V. Lysov, P. Mitra, and A. Strominger, "BMS supertranslations and Weinbergs soft graviton theorem," *JHEP*, vol. 05, p. 151, 2015.

[5] A. Strominger, "On BMS Invariance of Gravitational Scattering," *JHEP*, vol. 07, p. 152, 2014.

[6] F. Cachazo and A. Strominger, "Evidence for a New Soft Graviton Theorem," 2014.

[7] R. Britto, F. Cachazo, and B. Feng, "New recursion relations for tree amplitudes of gluons," *Nucl. Phys.*, vol. B715, pp. 499–522, 2005.

[8] R. Britto, F. Cachazo, B. Feng, and E. Witten, "Direct proof of tree-level recursion relation in Yang-Mills theory," *Phys. Rev. Lett.*, vol. 94, p. 181602, 2005.

[9] S. Weinberg, "Photons and Gravitons in s Matrix Theory: Derivation of Charge Conservation and Equality of Gravitational and Inertial Mass," *Phys. Rev.*, vol. 135, pp. B1049–B1056, 1964.

[10] Z. Bern, S. Davies, P. Di Vecchia, and J. Nohle, "Low-Energy Behavior of Gluons and Gravitons from Gauge Invariance," *Phys. Rev.*, vol. D90, no. 8, p. 084035, 2014.

[11] J. Broedel, M. de Leeuw, J. Plefka, and M. Rosso, "Constraining subleading soft gluon and graviton theorems," *Phys. Rev.*, vol. D90, no. 6, p. 065024, 2014.

[12] H. Gervais, "Soft Photon Theorem for High Energy Amplitudes in Yukawa and Scalar Theories," *Phys. Rev.*, vol. D95, no. 12, p. 125009, 2017.

[13] H. Gervais, "Soft Graviton Emission at High and Low Energies in Yukawa and Scalar Theories," 2017.

[14] V. Del Duca, "High-energy Bremsstrahlung Theorems for Soft Photons," *Nucl. Phys.*, vol. B345, pp. 369–388, 1990.

[15] Z. Bern, S. Davies, and J. Nohle, "On Loop Corrections to Subleading Soft Behavior of Gluons and Gravitons," *Phys. Rev.*, vol. D90, no. 8, p. 085015, 2014.

[16] S. He, Y.-t. Huang, and C. Wen, "Loop Corrections to Soft Theorems in Gauge Theories and Gravity," *JHEP*, vol. 12, p. 115, 2014.

[17] F. Cachazo and E. Y. Yuan, "Are Soft Theorems Renormalized?," 2014.

[18] A. J. Larkoski, D. Neill, and I. W. Stewart, "Soft Theorems from Effective Field Theory," *JHEP*, vol. 06, p. 077, 2015.

[19] G. F. Sterman, "Summation of Large Corrections to Short Distance Hadronic Cross-Sections," *Nucl. Phys.*, vol. B281, pp. 310–364, 1987.

[20] S. Catani and L. Trentadue, "Resummation of the QCD Perturbative Series for Hard Processes," *Nucl. Phys.*, vol. B327, pp. 323–352, 1989.

[21] G. P. Korchemsky and G. Marchesini, "Resummation of large infrared corrections using Wilson loops," *Phys. Lett.*, vol. B313, pp. 433–440, 1993.

[22] G. P. Korchemsky and G. Marchesini, "Structure function for large x and renormalization of Wilson loop," *Nucl. Phys.*, vol. B406, pp. 225–258, 1993.

[23] S. Forte and G. Ridolfi, "Renormalization group approach to soft gluon resummation," *Nucl. Phys.*, vol. B650, pp. 229–270, 2003.

[24] H. Contopanagos, E. Laenen, and G. F. Sterman, "Sudakov factorization and resummation," *Nucl. Phys.*, vol. B484, pp. 303–330, 1997.

[25] A. Banfi, G. P. Salam, and G. Zanderighi, "Principles of general final-state resummation and automated implementation," *JHEP*, vol. 03, p. 073, 2005.

[26] T. Becher and M. Neubert, "Threshold resummation in momentum space from effective field theory," *Phys. Rev. Lett.*, vol. 97, p. 082001, 2006.

[27] G. Luisoni and S. Marzani, "QCD resummation for hadronic final states," *J. Phys.*, vol. G42, no. 10, p. 103101, 2015.

[28] D. Bonocore, E. Laenen, L. Magnea, S. Melville, L. Vernazza, and C. D. White, "A factorization approach to next-to-leading-power threshold logarithms," *JHEP*, vol. 06, p. 008, 2015.

[29] D. Bonocore, E. Laenen, L. Magnea, L. Vernazza, and C. D. White, "Non-abelian factorisation for next-to-leading-power threshold logarithms," 2016.

[30] V. Del Duca, E. Laenen, L. Magnea, L. Vernazza, and C. D. White, "Universality of next-to-leading power threshold effects for colourless final states in hadronic collisions," 2017.

[31] F. Cachazo, S. He, and E. Y. Yuan, "Scattering of Massless Particles in Arbitrary Dimensions," *Phys. Rev. Lett.*, vol. 113, no. 17, p. 171601, 2014.

[32] F. Cachazo, S. He, and E. Y. Yuan, "Scattering of Massless Particles: Scalars, Gluons and Gravitons," *JHEP*, vol. 07, p. 033, 2014.

[33] B. U. W. Schwab and A. Volovich, "Subleading Soft Theorem in Arbitrary Dimensions from Scattering Equations," *Phys. Rev. Lett.*, vol. 113, no. 10, p. 101601, 2014.

[34] Y. Geyer, A. E. Lipstein, and L. Mason, "Ambitwistor strings at null infinity and (subleading) soft limits," *Class. Quant. Grav.*, vol. 32, no. 5, p. 055003, 2015.

[35] B. U. W. Schwab, "Subleading Soft Factor for String Disk Amplitudes," *JHEP*, vol. 08, p. 062, 2014.

[36] M. Bianchi, S. He, Y.-t. Huang, and C. Wen, "More on Soft Theorems: Trees, Loops and Strings," *Phys. Rev.*, vol. D92, no. 6, p. 065022, 2015.

[37] A. Sen, "Soft Theorems in Superstring Theory," 2017.

[38] A. Sen, "Subleading Soft Graviton Theorem for Loop Amplitudes," 2017.

[39] A. Laddha and A. Sen, "Sub-subleading Soft Graviton Theorem in Generic Theories of Quantum Gravity," 2017.

[40] C. D. White, "Path Integral Methods for Soft Gluon Resummation," in *Proceedings, 17th International Workshop on Deep-Inelastic Scattering and Related Subjects (DIS 2009): Madrid, Spain, April 26-30, 2009*, 2009.

[41] C. D. White, "New Results in Soft Gluon Physics," in *Proceedings, 46th Rencontres de Moriond on QCD and High Energy Interactions: La Thuile, Italy, March 20-27, 2011*, pp. 195–198, 2011.

[42] C. D. White, "Factorization Properties of Soft Graviton Amplitudes," *JHEP*, vol. 05, p. 060, 2011.

[43] C. D. White, "New insights into soft gluons and gravitons," *PoS*, vol. ICHEP2012, p. 288, 2013.

[44] C. D. White, "Diagrammatic insights into next-to-soft corrections," *Phys. Lett.*, vol. B737, pp. 216–222, 2014.

[45] E. Laenen, G. Stavenga, and C. D. White, "Path integral approach to eikonal and next-to-eikonal exponentiation," *JHEP*, vol. 03, p. 054, 2009.

[46] E. Laenen, L. Magnea, G. Stavenga, and C. D. White, "Next-to-eikonal corrections to soft gluon radiation: a diagrammatic approach," *JHEP*, vol. 01, p. 141, 2011.

[47] A. Luna, S. Melville, S. G. Naculich, and C. D. White, "Next-to-soft corrections to high energy scattering in QCD and gravity," *JHEP*, vol. 01, p. 052, 2017.

[48] J. C. Collins, D. E. Soper, and G. F. Sterman, "Factorization of Hard Processes in QCD," *Adv. Ser. Direct. High Energy Phys.*, vol. 5, pp. 1–91, 1989.

[49] G. Grammer, Jr. and D. R. Yennie, "Improved treatment for the infrared divergence problem in quantum electrodynamics," *Phys. Rev.*, vol. D8, pp. 4332–4344, 1973.

[50] L. D. Landau, "On analytic properties of vertex parts in quantum field theory," *Nucl. Phys.*, vol. 13, pp. 181–192, 1959.

[51] S. Coleman and R. E. Norton, "Singularities in the physical region," *Nuovo Cim.*, vol. 38, pp. 438–442, 1965.

[52] S. B. Libby and G. F. Sterman, "Jet and Lepton Pair Production in High-Energy Lepton-Hadron and Hadron-Hadron Scattering," *Phys. Rev.*, vol. D18, p. 3252, 1978.

[53] G. F. Sterman, "Partons, factorization and resummation, TASI 95," in *QCD and beyond. Proceedings, Theoretical Advanced Study Institute in Elementary Particle Physics, TASI-95, Boulder, USA, June 4-30, 1995*, pp. 327–408, 1995.

[54] G. F. Sterman, *An Introduction to quantum field theory*. Cambridge University Press, 1993.

[55] J. Collins, *Foundations of perturbative QCD*. Cambridge University Press, 2013.

[56] J. C. Collins and D. E. Soper, "Back-To-Back Jets in QCD," *Nucl. Phys.*, vol. B193, p. 381, 1981. [Erratum: Nucl. Phys.B213,545(1983)].

[57] O. Erdoğan and G. Sterman, "Ultraviolet divergences and factorization for coordinate-space amplitudes," *Phys. Rev.*, vol. D91, no. 6, p. 065033, 2015.

[58] R. Akhoury, "Mass Divergences of Wide Angle Scattering Amplitudes," *Phys. Rev.*, vol. D19, p. 1250, 1979.

[59] A. Sen, "Asymptotic Behavior of the Wide Angle On-Shell Quark Scattering Amplitudes in Nonabelian Gauge Theories," *Phys. Rev.*, vol. D28, p. 860, 1983.

[60] G. F. Sterman, "Mass Divergences in Annihilation Processes. 1. Origin and Nature of Divergences in Cut Vacuum Polarization Diagrams," *Phys. Rev.*, vol. D17, p. 2773, 1978.

[61] G. F. Sterman, "Mass Divergences in Annihilation Processes. 2. Cancellation of Divergences in Cut Vacuum Polarization Diagrams," *Phys. Rev.*, vol. D17, p. 2789, 1978.

[62] A. V. Efremov and A. V. Radyushkin, "Factorization and Asymptotical Behavior of Pion Form-Factor in QCD," *Phys. Lett.*, vol. 94B, pp. 245–250, 1980.

[63] G. P. Lepage and S. J. Brodsky, "Exclusive Processes in Quantum Chromodynamics: Evolution Equations for Hadronic Wave Functions and the Form-Factors of Mesons," *Phys. Lett.*, vol. B87, pp. 359–365, 1979.

[64] G. P. Lepage and S. J. Brodsky, "Exclusive Processes in Perturbative Quantum Chromodynamics," *Phys. Rev.*, vol. D22, p. 2157, 1980.

[65] Z.-B. Kang, J.-W. Qiu, and G. Sterman, "Heavy quarkonium production and polarization," *Phys. Rev. Lett.*, vol. 108, p. 102002, 2012.

[66] Z.-B. Kang, Y.-Q. Ma, J.-W. Qiu, and G. Sterman, "Heavy Quarkonium Production at Collider Energies: Factorization and Evolution," *Phys. Rev.*, vol. D90, no. 3, p. 034006, 2014.

[67] N. E. Bjerrum-Bohr, *Quantum gravity, effective fields and string theory.* PhD thesis, Bohr Inst., 2004.

[68] M. J. G. Veltman, "Quantum Theory of Gravitation," *Conf. Proc.*, vol. C7507281, pp. 265–327, 1975.

[69] G. 't Hooft, "Renormalization of Massless Yang-Mills Fields," *Nucl. Phys.*, vol. B33, pp. 173–199, 1971.

[70] R. Brout and F. Englert, "Gravitational Ward Identity and the Principle of Equivalence," *Phys. Rev.*, vol. 141, no. 4, pp. 1231–1232, 1966.

[71] L. Bessler, T. Muta, and H. Umezawa, "Nucleon mass and the gravitational ward-takahashi identity," *Phys. Rev.*, vol. 180, pp. 1604–1605, 1969.

[72] C. Coriano, L. Delle Rose, and M. Serino, "Gravity and the Neutral Currents: Effective Interactions from the Trace Anomaly," *Phys. Rev.*, vol. D83, p. 125028, 2011.

[73] C. Coriano, L. Delle Rose, E. Gabrielli, and L. Trentadue, "One loop Standard Model corrections to flavor diagonal fermion-graviton vertices," *Phys. Rev.*, vol. D87, no. 5, p. 054020, 2013.

[74] N. E. J. Bjerrum-Bohr, "Leading quantum gravitational corrections to scalar QED," *Phys. Rev.*, vol. D66, p. 084023, 2002.

[75] N. E. J. Bjerrum-Bohr, J. F. Donoghue, and B. R. Holstein, "Quantum corrections to the Schwarzschild and Kerr metrics," *Phys. Rev.*, vol. D68, p. 084005, 2003. [Erratum: Phys. Rev.D71,069904(2005)].

[76] N. E. J. Bjerrum-Bohr, J. F. Donoghue, and B. R. Holstein, "Quantum gravitational corrections to the nonrelativistic scattering potential of two masses," *Phys. Rev.*, vol. D67, p. 084033, 2003. [Erratum: Phys. Rev.D71,069903(2005)].

[77] B. R. Holstein and J. F. Donoghue, "Classical physics and quantum loops," *Phys. Rev. Lett.*, vol. 93, p. 201602, 2004.

[78] N. E. J. Bjerrum-Bohr, J. F. Donoghue, B. R. Holstein, L. Plante, and P. Vanhove, "Light-like Scattering in Quantum Gravity," *JHEP*, vol. 11, p. 117, 2016.